NASA/TM–2025–0001451

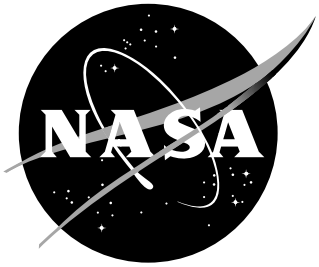

Apollo Heat-Shield Half Body Laminar Computational Fluid Dynamics Database

A. J. Hyatt
NASA Johnson Space Center

August 2025

NASA STI Program . . . in Profile

Since its founding, NASA has been dedicated to the advancement of aeronautics and space science. The NASA scientific and technical information (STI) program plays a key part in helping NASA maintain this important role.

The NASA STI Program operates under the auspices of the Agency Chief Information Officer. It collects, organizes, provides for archiving, and disseminates NASA's STI. The NASA STI Program provides access to the NASA Aeronautics and Space Database and its public interface, the NASA Technical Report Server, thus providing one of the largest collection of aeronautical and space science STI in the world. Results are published in both non-NASA channels and by NASA in the NASA STI Report Series, which includes the following report types:

- TECHNICAL PUBLICATION. Reports of completed research or a major significant phase of research that present the results of NASA programs and include extensive data or theoretical analysis. Includes compilations of significant scientific and technical data and information deemed to be of continuing reference value. NASA counterpart of peer-reviewed formal professional papers, but having less stringent limitations on manuscript length and extent of graphic presentations.
- TECHNICAL MEMORANDUM. Scientific and technical findings that are preliminary or of specialized interest, e.g., quick release reports, working papers, and bibliographies that contain minimal annotation. Does not contain extensive analysis.
- CONTRACTOR REPORT. Scientific and technical findings by NASA-sponsored contractors and grantees.
- CONFERENCE PUBLICATION. Collected papers from scientific and technical conferences, symposia, seminars, or other meetings sponsored or co-sponsored by NASA.
- SPECIAL PUBLICATION. Scientific, technical, or historical information from NASA programs, projects, and missions, often concerned with subjects having substantial public interest.
- TECHNICAL TRANSLATION. English-language translations of foreign scientific and technical material pertinent to NASA's mission.

Specialized services also include creating custom thesauri, building customized databases, and organizing and publishing research results.

For more information about the NASA STI Program, see the following:

- Access the NASA STI program home page at ***http://www.sti.nasa.gov***
- E-mail your question via the Internet to help@sti.nasa.gov
- Fax your question to the NASA STI Help Desk at 443-757-5803
- Phone the NASA STI Help Desk at 443-757-5802
- Write to:
  NASA STI Help Desk
  NASA Center for AeroSpace Information
  7115 Standard Drive
  Hanover, MD 21076–1320

NASA/TM–2025–0001451

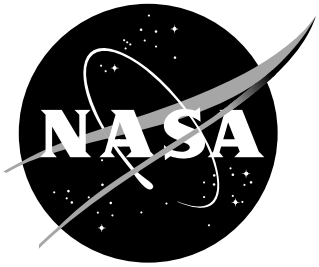

Apollo Heat-Shield Half Body Laminar Computational Fluid Dynamics Database

A. J. Hyatt
NASA Johnson Space Center

National Aeronautics and
Space Administration

Johnson Space Center
Houston, TX

August 2025

Available from:

NASA Center for AeroSpace Information
7115 Standard Drive
Hanover, MD 21076-1320
443-757-5802

Abstract

A series of Computational Fluid Dynamics solutions have been computed on the Apollo heat-shield geometry for the evaluation of different interpolation approaches within the database of solutions. In addition, given the rise of Artificial Intelligence, this dataset could also be used to develop or evalate the application of Artifical Intelligence methods for the estimation of aerodynamic and aerothermodynamic environments during atmospheric entry. Each of the 185 heat-shield only (no backshell) half body solutions have been computed using standard best practice with NASA's Data Parallel Line Relaxation solver and post processed to calculate quantities of interest at both the surface and boundary layer edge.

1 Introduction

The prediction of aerodynamic and aerothermodynamic environments on a spacecraft during atmospheric entry generally starts with computing a number of Computation Fluid Dynamics (CFD) solutions on the specific geometry and at relevant flight conditions. These discrete solutions are then used to estimate the environment along an entire trajectory(s) of interest. Several approaches exist including, 1) performing the CFD along a trajectory of interest and then fitting the computed environments with a functional form or simply spline fitting, 2) performing the CFD around a design flight corridor and then interpolating from those solutions to a trajectory of interest.

This dataset was created to facilitate the development of best practices for using CFD solutions as the basis for predicting flight environments and for testing the application of Artificial Intelligence / Machine Learning (AI/ML) approaches for similar applications. The Apollo geometry was used to avoid any release restrictions associated with current NASA spacecraft. A total of 185 solutions have been computed surrounding the Apollo 4 trajectory.

2 Background

The Apollo geometry was selected for this investigation due to the relevance to many current NASA and commercial spacecraft while avoiding proprietary and export concerns. The Apollo re-entry capsule had a spherical heatshield, 3.912 meters in diameter, shown in Figure 1. Similarly, the Orion, SpaceX Dragon, and Boeing Starliner re-entry capsules are all blunt bodies with spherical heatshields, ranging in size from 4 to 5 meters. The Apollo 4 trajectory was particularly relevant for Orion since it re-entered at lunar return velocity, which drove the CFD solutions computed for this investigation to envelope that trajectory.

Apollo 4 was an uncrewed flight test of the Saturn V launch vehicle and the Command Module (CM) that eventually took astronauts to the Moon. The mission launched from the Kennedy Space Center on November 9, 1967 and splashed down in the Pacific Ocean later that same day. The re-entry trajectory is shown in Figure 2. The spacecraft starts on the top right of the figure at entry interface (velocity of roughly 11 km/s and altitude of 120 km) and decelerates until it reaches splashdown on the bottom left of the figure.

2.1 Grid

The grid used for the CFD solutions is shown in Figure 3. The grid terminated at the shoulder because this investigation focused on the heatshield and did not include the conic backshell. The grid was composed of four point matched blocks, outlined in magenta, and included 25,088 surface cells. The surface grid was then extruded 128 steps to generate a volume grid of 3,211,264 cells. Figure 3a shows only the surface grid and Figure 3b includes the surface along with the pitch plane and the exit plane of the extruded volume grid prior to grid adaptation.

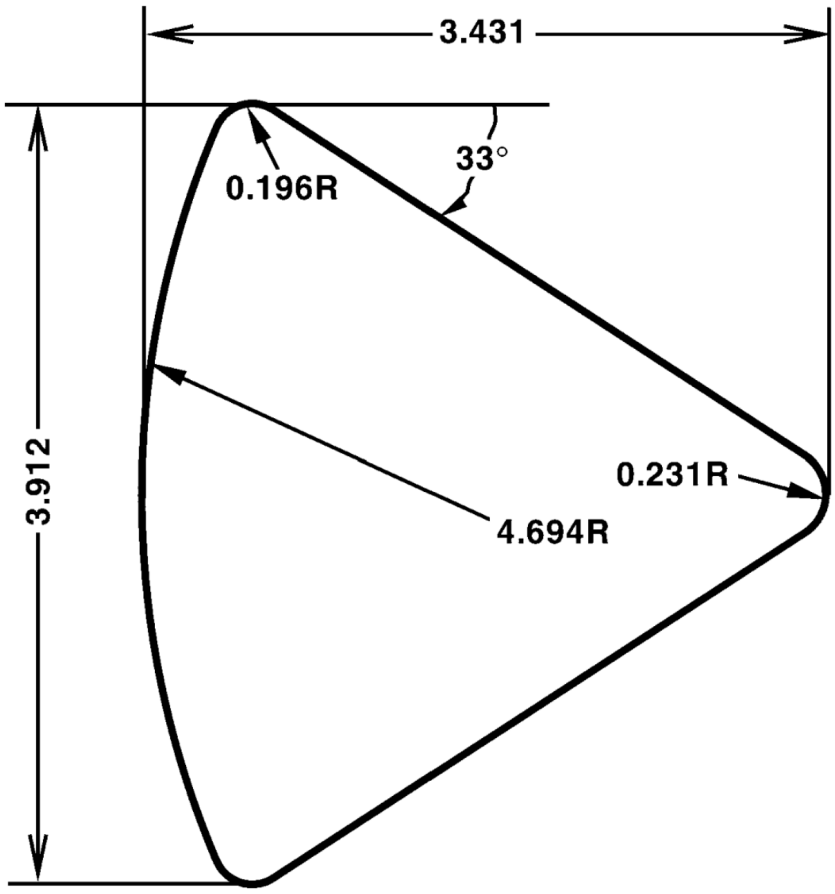

Figure 1. Schematic of the Apollo Command Module [1]. All dimensions are in units of meters.

2.2 CFD

The Data Parallel Line Relaxation (DPLR) [2] code was used to generate each of the CFD solutions. DPLR uses a finite volume approach to solve the Navier-Stokes equations and includes both thermal and chemical non-equilibrium, allowing it to accurately predict aerothermodynamic environments on spacecraft at Low Earth Orbit (LEO), lunar, and interplanetary entry velocities. It also leverages Message Passing Interface (MPI) to run in parallel and scales efficiently on modern CPU compute clusters.

All of the solutions used the same set of physical models. This initial investigation only considered laminar solutions and each used the 11-species Park 90 [3] chemistry model. The solutions assumed vibrational non-equilibrium by including a second temperature (T_v) [4] which was decoupled from the translational temperature (T_t). The rotational (T_r) temperature was coupled with the translational temperature. The surface was assumed to be fully catalytic and in radiative equilibrium with an emissivity (ϵ) of 0.85. The diffusion was modeled with Self-Consistent Effective Binary Diffusion (SCEBD) [5].

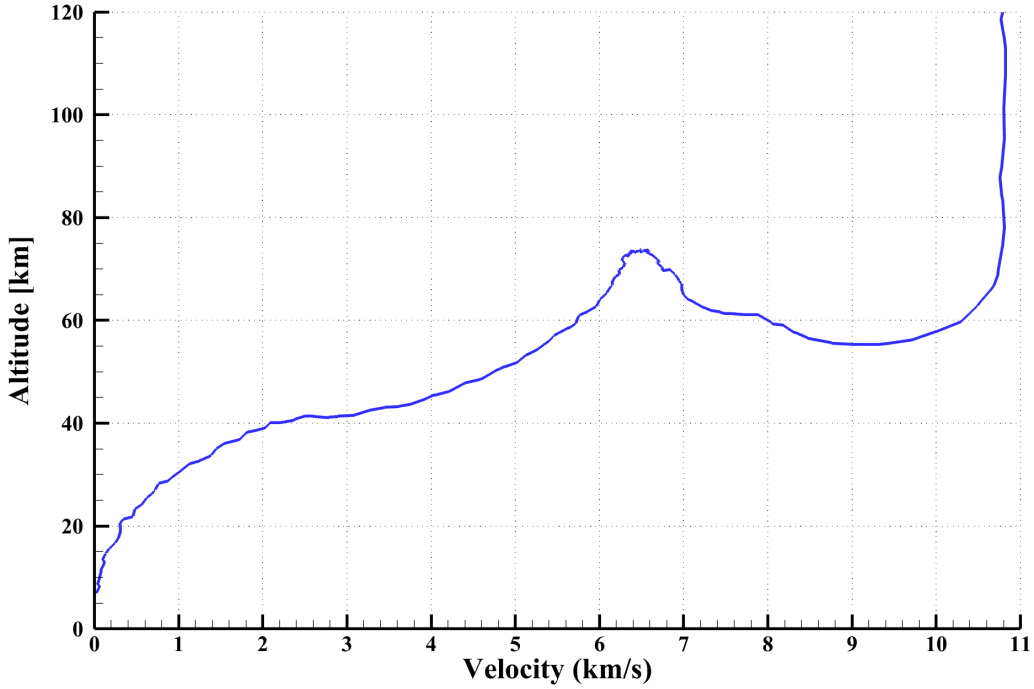

Figure 2. Apollo 4 re-entry trajectory.

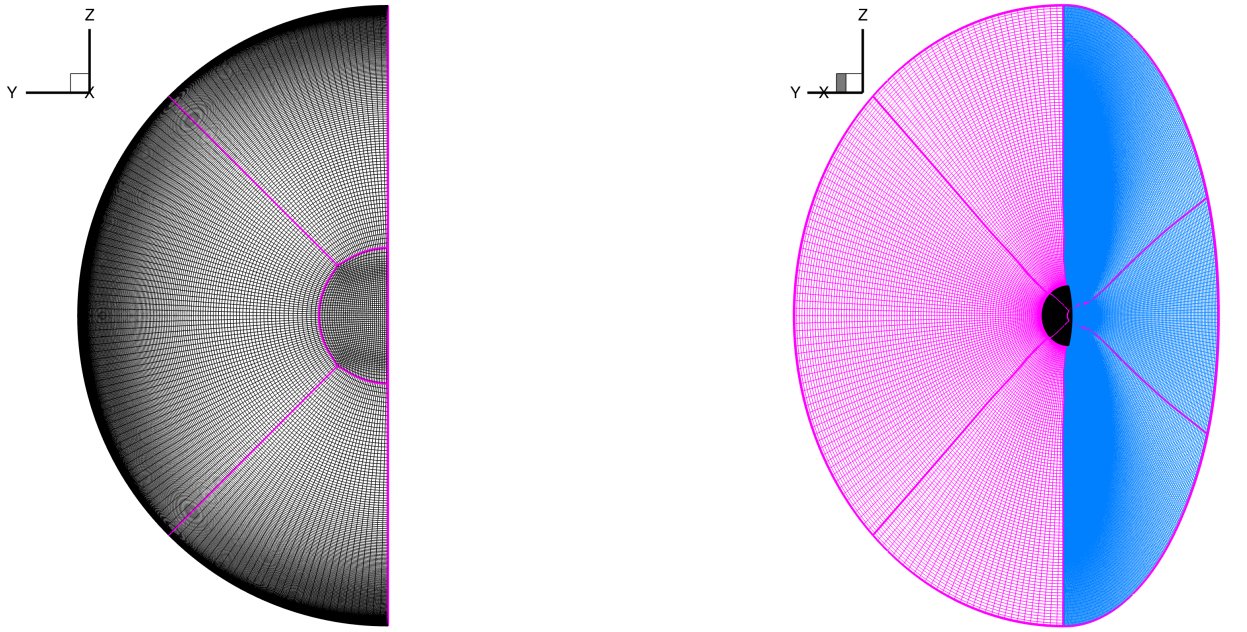

(a) Surface grid

(b) Surface grid with pitch plane (blue) and exit plane (magenta) at the heatshield shoulder

Figure 3. Initial CFD grid prior to shock tailoring. The mesh is composed of four point matched blocks, which are outlined in magenta.

3 Results

A total of 185 solutions have been computed around the Apollo 4 trajectory, between 3 km/s and 11 km/s at increments of 0.5 km/s. Three or four densities were assumed at each velocity, corresponding to altitudes in round kilometers. The 1976 standard atmosphere [6] was assumed to calculate the air density and temperature that correspond to each altitude. Finally, at each velocity and density combination, three or four angles-of-attack were assumed, leading to the 185 unique CFD solutions. The angle-of-attack was calculated from the capsule body axis and the coordinate system was pilot-centric, as shown in Figure 4, which led to angles-of-attack between 152 and 158 degrees. A sample CFD solution is shown in Figure 5. The heat flux (q_w) contours are shown on the surface and Mach contours are shown on the pitch plane. Note the solution domain has been reduced to a region starting just outside the bow shock, as compared to the original volume grid shown in Figure 3b.

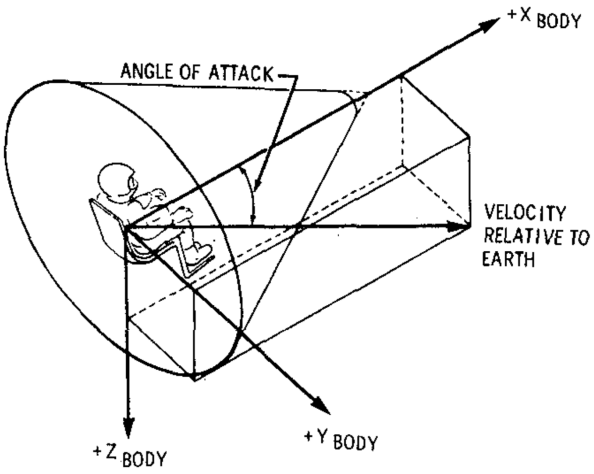

Figure 4. Apollo body-axis system showing relationship of total angle-of-attack [7].

While each solution was computed using the same initial grid, DPLR requires a shock aligned grid, so computing each solution included several grid tailoring steps to achieve a suitable grid for each condition. The grid tailoring adjusts the outer boundary of the grid to align with the shock and then redistributes the grid between the surface and the outer boundary along the off body grid lines, generally the K dimension. Figure 6 shows the pitch plane of the grid both before and after the shock tailoring process, as well as the Mach contours in the pitch plane to illustrate how the tailored grid is aligned with the strong bow shock.

The same initial grid was used for each solution but it was shock aligned or tailored until the heat flux (q_w) distribution had the expected pattern for a spherical geometry with laminar flow. The solutions were then converged as far as possible, generally between 9 and 13 orders of magnitude. The solutions are depicted in flight space in Figure 7 along with the Apollo 4 trajectory. In addition, Table 1 provides the specific flight condition for each CFD solution, all 185 of them. Finally, Figure 8 shows sample surface contours of the pressure and heat flux (q_w). Pressure is the primary surface quantity of interest for aerodynamics and heat flux (q_w) is one of the primary surface quantities of interest for aerothermodynamics.

Table 1: CFD solution conditions

Velocity (km/s)	Altitude (km)	Density (kg/m^3)	Angle-of-Attack (degrees)
3.0	35.0	8.214×10^{-3}	152.0
3.0	35.0	8.214×10^{-3}	154.0
3.0	35.0	8.214×10^{-3}	156.0
3.0	40.0	3.851×10^{-3}	152.0
3.0	40.0	3.851×10^{-3}	154.0
3.0	40.0	3.851×10^{-3}	156.0
3.0	45.0	1.881×10^{-3}	152.0

Table 1: CFD solution conditions

Velocity (km/s)	Altitude (km)	Density (kg/m^3)	Angle-of-Attack (degrees)
3.0	45.0	1.881×10^{-3}	154.0
3.0	45.0	1.881×10^{-3}	156.0
3.5	35.0	8.214×10^{-3}	152.0
3.5	35.0	8.214×10^{-3}	154.0
3.5	35.0	8.214×10^{-3}	156.0
3.5	40.0	3.851×10^{-3}	152.0
3.5	40.0	3.851×10^{-3}	154.0
3.5	40.0	3.851×10^{-3}	156.0
3.5	45.0	1.881×10^{-3}	152.0
3.5	45.0	1.881×10^{-3}	154.0
3.5	45.0	1.881×10^{-3}	156.0
4.0	40.0	3.851×10^{-3}	152.0
4.0	40.0	3.851×10^{-3}	154.0
4.0	45.0	1.881×10^{-3}	152.0
4.0	45.0	1.881×10^{-3}	154.0
4.0	45.0	1.881×10^{-3}	156.0
4.0	50.0	9.775×10^{-4}	152.0
4.0	50.0	9.775×10^{-4}	154.0
4.0	50.0	9.775×10^{-4}	156.0
4.5	40.0	3.851×10^{-3}	152.0
4.5	40.0	3.851×10^{-3}	154.0
4.5	40.0	3.851×10^{-3}	156.0
4.5	45.0	1.881×10^{-3}	152.0
4.5	45.0	1.881×10^{-3}	154.0
4.5	45.0	1.881×10^{-3}	156.0
4.5	50.0	9.775×10^{-4}	152.0
4.5	50.0	9.775×10^{-4}	154.0
4.5	50.0	9.775×10^{-4}	156.0
5.0	45.0	1.881×10^{-3}	152.0
5.0	45.0	1.881×10^{-3}	154.0
5.0	45.0	1.881×10^{-3}	156.0
5.0	50.0	9.775×10^{-4}	152.0
5.0	50.0	9.775×10^{-4}	154.0
5.0	50.0	9.775×10^{-4}	156.0
5.0	55.0	5.367×10^{-4}	152.0
5.0	55.0	5.367×10^{-4}	154.0
5.0	55.0	5.367×10^{-4}	156.0
5.5	50.0	9.775×10^{-4}	152.0
5.5	50.0	9.775×10^{-4}	154.0
5.5	50.0	9.775×10^{-4}	156.0
5.5	55.0	5.367×10^{-4}	152.0
5.5	55.0	5.367×10^{-4}	154.0
5.5	55.0	5.367×10^{-4}	156.0
5.5	55.0	5.367×10^{-4}	158.0
5.5	60.0	2.883×10^{-4}	152.0

Table 1: CFD solution conditions

Velocity (km/s)	Altitude (km)	Density (kg/m^3)	Angle-of-Attack (degrees)
5.5	60.0	2.883×10^{-4}	154.0
5.5	60.0	2.883×10^{-4}	156.0
5.5	60.0	2.883×10^{-4}	158.0
6.0	55.0	5.367×10^{-4}	152.0
6.0	55.0	5.367×10^{-4}	154.0
6.0	55.0	5.367×10^{-4}	156.0
6.0	55.0	5.367×10^{-4}	158.0
6.0	60.0	2.883×10^{-4}	152.0
6.0	60.0	2.883×10^{-4}	154.0
6.0	60.0	2.883×10^{-4}	156.0
6.0	60.0	2.883×10^{-4}	158.0
6.0	65.0	1.493×10^{-4}	152.0
6.0	65.0	1.493×10^{-4}	154.0
6.0	65.0	1.493×10^{-4}	156.0
6.0	65.0	1.493×10^{-4}	158.0
6.0	70.0	7.424×10^{-5}	152.0
6.0	70.0	7.424×10^{-5}	154.0
6.0	70.0	7.424×10^{-5}	156.0
6.0	70.0	7.424×10^{-5}	158.0
6.5	65.0	1.493×10^{-4}	152.0
6.5	65.0	1.493×10^{-4}	154.0
6.5	65.0	1.493×10^{-4}	156.0
6.5	65.0	1.493×10^{-4}	158.0
6.5	70.0	7.424×10^{-5}	152.0
6.5	70.0	7.424×10^{-5}	154.0
6.5	70.0	7.424×10^{-5}	156.0
6.5	70.0	7.424×10^{-5}	158.0
6.5	75.0	3.486×10^{-5}	152.0
6.5	75.0	3.486×10^{-5}	154.0
6.5	75.0	3.486×10^{-5}	156.0
6.5	75.0	3.486×10^{-5}	158.0
6.5	80.0	1.570×10^{-5}	152.0
6.5	80.0	1.570×10^{-5}	154.0
6.5	80.0	1.570×10^{-5}	156.0
6.5	80.0	1.570×10^{-5}	158.0
7.0	60.0	2.883×10^{-4}	152.0
7.0	60.0	2.883×10^{-4}	154.0
7.0	60.0	2.883×10^{-4}	156.0
7.0	60.0	2.883×10^{-4}	158.0
7.0	65.0	1.493×10^{-4}	152.0
7.0	65.0	1.493×10^{-4}	154.0
7.0	65.0	1.493×10^{-4}	156.0
7.0	65.0	1.493×10^{-4}	158.0
7.0	70.0	7.424×10^{-5}	152.0
7.0	70.0	7.424×10^{-5}	154.0

Table 1: CFD solution conditions

Velocity (km/s)	Altitude (km)	Density (kg/m^3)	Angle-of-Attack (degrees)
7.0	70.0	7.424×10^{-5}	156.0
7.0	70.0	7.424×10^{-5}	158.0
7.0	75.0	3.486×10^{-5}	152.0
7.0	75.0	3.486×10^{-5}	154.0
7.0	75.0	3.486×10^{-5}	156.0
7.0	75.0	3.486×10^{-5}	158.0
7.5	55.0	5.367×10^{-4}	152.0
7.5	55.0	5.367×10^{-4}	154.0
7.5	55.0	5.367×10^{-4}	156.0
7.5	55.0	5.367×10^{-4}	158.0
7.5	60.0	2.883×10^{-4}	152.0
7.5	60.0	2.883×10^{-4}	154.0
7.5	60.0	2.883×10^{-4}	156.0
7.5	60.0	2.883×10^{-4}	158.0
7.5	65.0	1.493×10^{-4}	152.0
7.5	65.0	1.493×10^{-4}	154.0
7.5	65.0	1.493×10^{-4}	156.0
7.5	65.0	1.493×10^{-4}	158.0
8.0	55.0	5.367×10^{-4}	152.0
8.0	55.0	5.367×10^{-4}	154.0
8.0	55.0	5.367×10^{-4}	156.0
8.0	55.0	5.367×10^{-4}	158.0
8.0	60.0	2.883×10^{-4}	152.0
8.0	60.0	2.883×10^{-4}	154.0
8.0	60.0	2.883×10^{-4}	156.0
8.0	60.0	2.883×10^{-4}	158.0
8.0	65.0	1.493×10^{-4}	152.0
8.0	65.0	1.493×10^{-4}	154.0
8.0	65.0	1.493×10^{-4}	156.0
8.0	65.0	1.493×10^{-4}	158.0
8.5	50.0	9.775×10^{-4}	152.0
8.5	50.0	9.775×10^{-4}	154.0
8.5	50.0	9.775×10^{-4}	156.0
8.5	50.0	9.775×10^{-4}	158.0
8.5	55.0	5.367×10^{-4}	152.0
8.5	55.0	5.367×10^{-4}	154.0
8.5	55.0	5.367×10^{-4}	156.0
8.5	55.0	5.367×10^{-4}	158.0
8.5	60.0	2.883×10^{-4}	152.0
8.5	60.0	2.883×10^{-4}	154.0
8.5	60.0	2.883×10^{-4}	156.0
8.5	60.0	2.883×10^{-4}	158.0
9.0	50.0	9.775×10^{-4}	152.0
9.0	50.0	9.775×10^{-4}	154.0
9.0	50.0	9.775×10^{-4}	156.0

Table 1: CFD solution conditions

Velocity (km/s)	Altitude (km)	Density (kg/m^3)	Angle-of-Attack (degrees)
9.0	55.0	5.367×10^{-4}	152.0
9.0	55.0	5.367×10^{-4}	154.0
9.0	55.0	5.367×10^{-4}	156.0
9.0	60.0	2.883×10^{-4}	152.0
9.0	60.0	2.883×10^{-4}	154.0
9.0	60.0	2.883×10^{-4}	156.0
9.5	50.0	9.775×10^{-4}	152.0
9.5	50.0	9.775×10^{-4}	154.0
9.5	50.0	9.775×10^{-4}	156.0
9.5	55.0	5.367×10^{-4}	152.0
9.5	55.0	5.367×10^{-4}	154.0
9.5	60.0	2.883×10^{-4}	152.0
9.5	60.0	2.883×10^{-4}	154.0
9.5	60.0	2.883×10^{-4}	156.0
10.0	55.0	5.367×10^{-4}	152.0
10.0	55.0	5.367×10^{-4}	154.0
10.0	55.0	5.367×10^{-4}	156.0
10.0	60.0	2.883×10^{-4}	152.0
10.0	60.0	2.883×10^{-4}	154.0
10.0	60.0	2.883×10^{-4}	156.0
10.0	65.0	1.493×10^{-4}	152.0
10.0	65.0	1.493×10^{-4}	154.0
10.0	65.0	1.493×10^{-4}	156.0
10.5	55.0	5.367×10^{-4}	152.0
10.5	55.0	5.367×10^{-4}	154.0
10.5	60.0	2.883×10^{-4}	152.0
10.5	60.0	2.883×10^{-4}	154.0
10.5	60.0	2.883×10^{-4}	156.0
10.5	65.0	1.493×10^{-4}	152.0
10.5	65.0	1.493×10^{-4}	154.0
10.5	65.0	1.493×10^{-4}	156.0
10.5	70.0	7.424×10^{-5}	152.0
10.5	70.0	7.424×10^{-5}	154.0
10.5	70.0	7.424×10^{-5}	156.0
11.0	70.0	7.424×10^{-5}	152.0
11.0	70.0	7.424×10^{-5}	154.0
11.0	70.0	7.424×10^{-5}	156.0
11.0	75.0	3.486×10^{-5}	152.0
11.0	75.0	3.486×10^{-5}	154.0
11.0	75.0	3.486×10^{-5}	156.0
11.0	80.0	1.570×10^{-5}	152.0
11.0	80.0	1.570×10^{-5}	154.0
11.0	80.0	1.570×10^{-5}	156.0

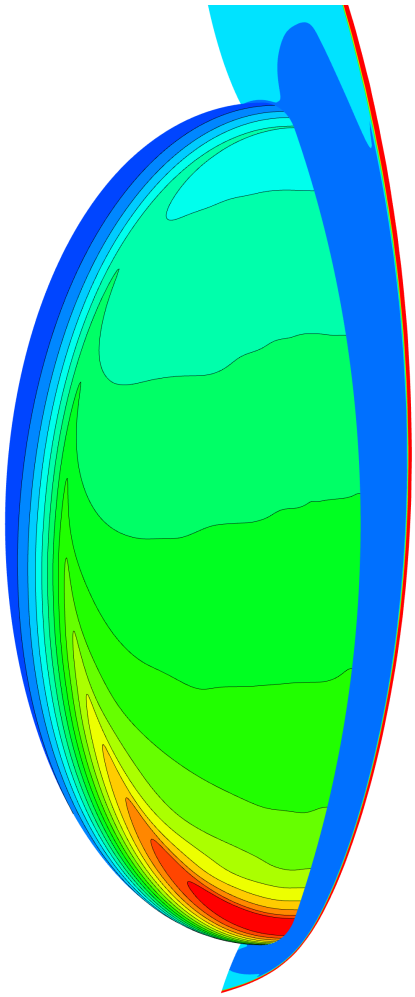

Figure 5. Sample CFD solution at a velocity of 6.5 km/s, 65 km altitude, and 154 degrees angle-of-attack. The surface contours show the heat flux and the pitch plane shows Mach contours.

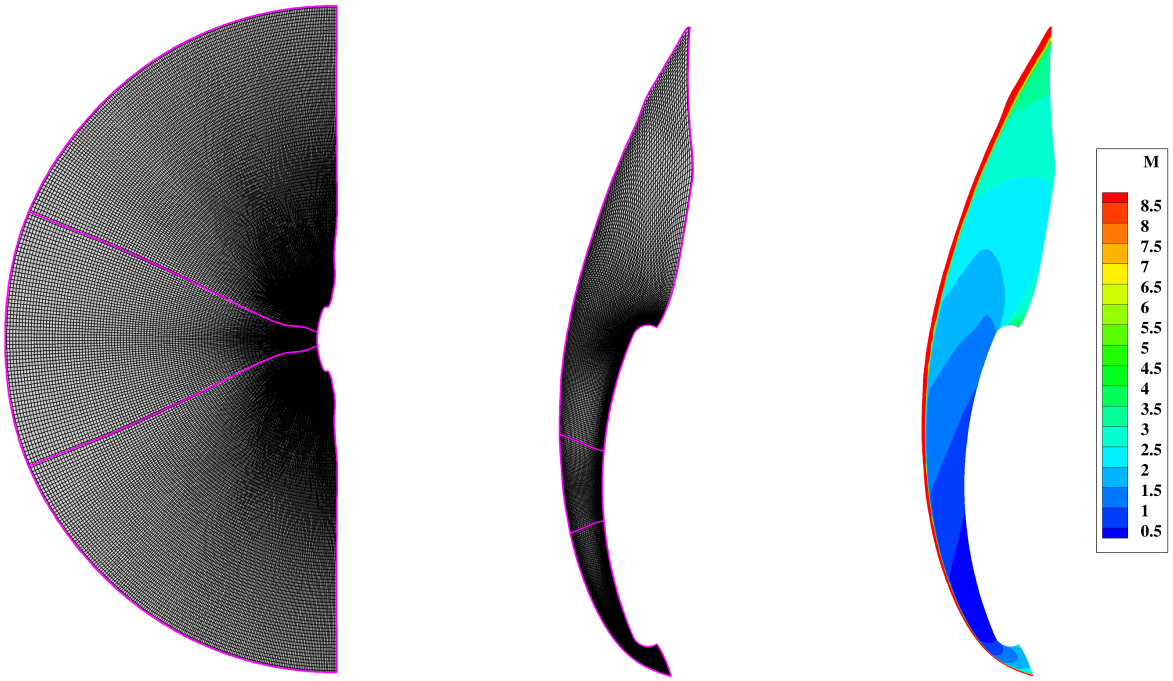

(a) Initial Grid (b) Shock Aligned Grid (c) Pitch Plane Mach Contours

Figure 6. Example of the shock alignment impact to the grid. The first image shows the initial grid prior to performing any shock alignment steps. The second image shows the grid after the last shock alignment. And the final images shows the Mach contours at velocity 3.0 km/s, altitude 35.0 km, and 152 degrees angle-of-attack. The high speed freestream flow is only present in the last couple cells outside the shock, and the majority of the grid is now within the shock with tight clustering near the surface.

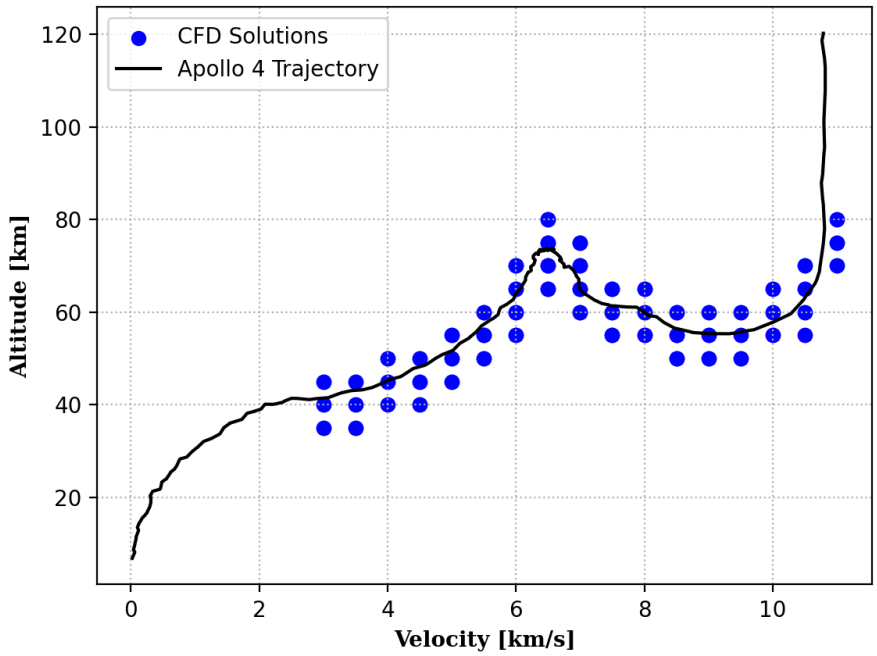

(a) CFD solutions in altitude versus velocity space

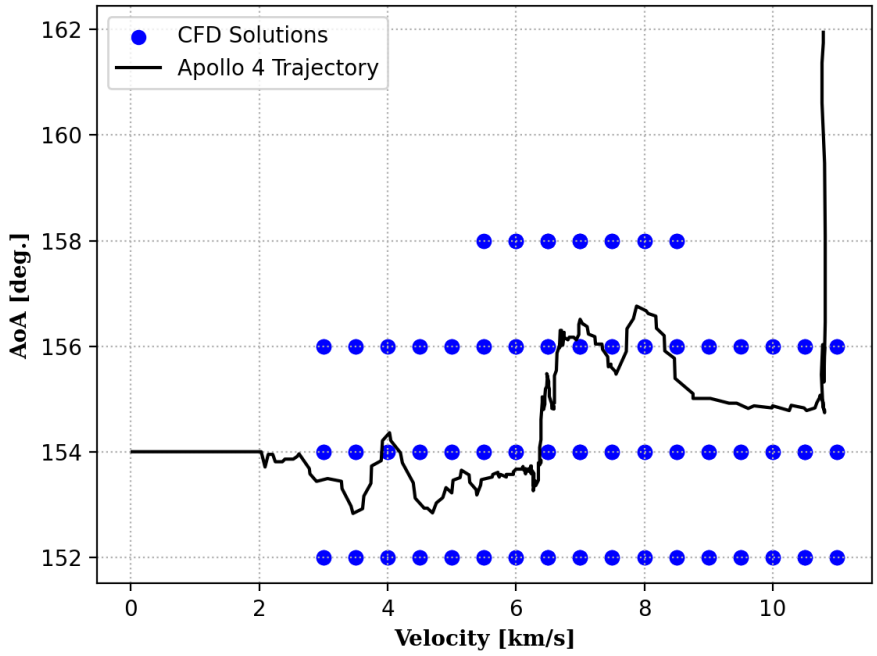

(b) CFD solutions in angle-of-attack versus velocity space

Figure 7. Discrete CFD solutions shown as blue freckles with the Apollo 4 trajectory included in black.

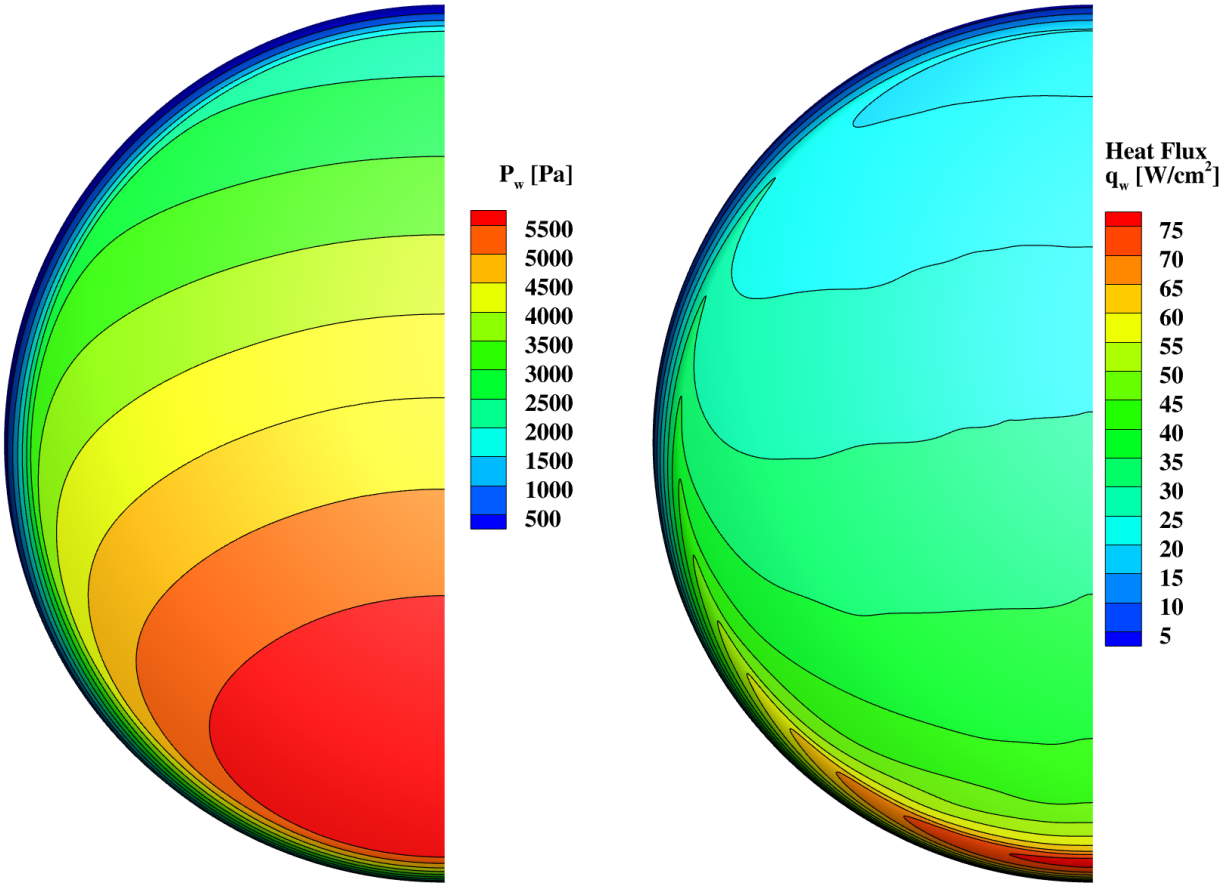

(a) Pressure

(b) Heat Flux

Figure 8. Sample surface property contours at velocity 6.5 km/s, altitude 65 km, and angle-of-attack 154 degrees.

3.1 Post Processing

Each CFD solution was post-processed using the BLAYER tool [8] to estimate the edge of the boundary layer and several coresponding flow quantities at the boundary layer edge. BLAYER uses the total enthalpy profile from the surface to the outer boundary along grid lines in the off body direction to identify the edge of the boundary layer. Ultimately, a Tecplot formatted file with the BLAYER results was generated for each CFD solution. These files contain the following quantities at each grid point on the surface (the file only contains the surface but includes both surface and edge quantities of interest on the surface). The following quantities are included:

- Surface Quantities
  - Density (kg/m^3)
  - Pressure (Pa)
  - Temperature (K)
  - Temperature, vibrational (K)
  - Total Enthalpy (J/kg)
  - Viscosity (Pa $\times$ s)
  - Species Densities [N2, O2, NO, NO+, N2+, O2+, N, O, N+, O+, e] (kg/m^3)
  - Heat Flux (W/m^2)
  - Heat Flux, vibrational (W/m^2)
  - Shear, x-component (Pa)
  - Shear, y-component (Pa)
  - Shear, z-component (Pa)
  - Thermal Conductivity (W/m $\times$ K)
- Edge Quantities
  - Density (kg/m^3)
  - Pressure (Pa)
  - Temperature (K)
  - Temperature, vibrational (K)
  - Total Enthalpy (J/kg)
  - Velocity, x-component (m/s)
  - Velocity, y-component (m/s)
  - Velocity, z-component (m/s)
  - Mach number (M$_e$)
  - Viscosity (Pa $\times$ s)
  - Species Densities [N2, O2, NO, NO+, N2+, O2+, N, O, N+, O+, e] (kg/m^3)
  - Boundary Layer Thickness (m)
  - Displacement Thickness (m)
  - Momentum Thickness (m)
  - Reynolds number (1/m)
  - Film Coefficient (kg/m$^2\times$ s)
  - Thermal Conductivity (W/m $\times$ K)

4 Conclusion

A series (database) of 185 laminar CFD solutions have been generated on the Apollo spacecraft geometry. These solutions were generated with NASA's DPLR CFD solver using standard best practices for aerothermodynamic solutions. This database is intended to be used for developing standard best practice for generating environments on a desired trajectory from a discrete set of CFD solutions, but could also be used to evaluate the application of Artificial Intelligence methods to generate environments.

References

1. Wright, M., Prabhu, D., and Martinez, E., *Analysis of Apollo Command Module Afterbody Heating Part I: AS-202*, Journal of Thermophysics and Heat Transfer, 2006

2. Wright, Michael, *Data Parallel Line Relaxation Code*, Journal of Thermophysics and Heat Transfer, 2001

3. Park, C., *Chemical Kinetics for Air*, Journal of Thermophysics and Heat Transfer, 1990

4. Park, C., *Nonequilibrium Hypersonic Aerothermodynamics*, Wiley, 1990.

5. Ramshaw, J. *Self-Consistent Effective Binary Diffusion in Multicomponent Gas Mixtures*, Journal of Non-Equilibrium Thermodynamics, 15,295. 1990.

6. NOAA, *U. S. Standard Atmosphere, 1976*, 1976

7. Hillje, E. R. and Savage, R., *Status of the aerodynamic characteristics of the Apollo entry configuration*, Entry Vehicle Systems and Technology Meeting, Williamsburg, VA, 1968

8. Private communication, Saunders, D. AMA Incorporated

Appendix A

CFD Solution Plots

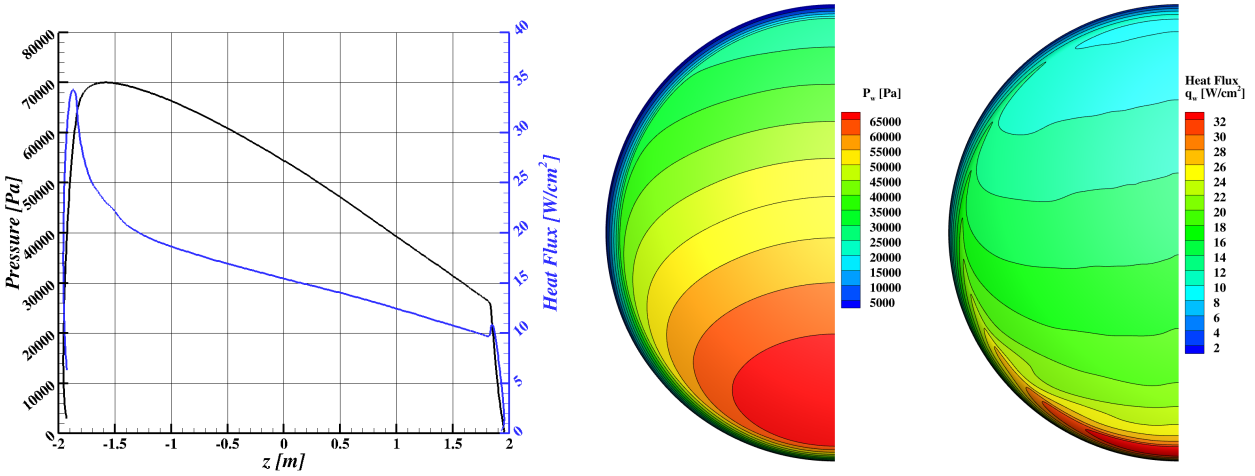

(a) Pitch plane pressure and heat flux (b) Pressure (c) Heat flux

Figure A9. Pressure and heat flux at velocity 3.0 km/s, altitude 35.0 km, and angle-of-attack 152.0 degrees.

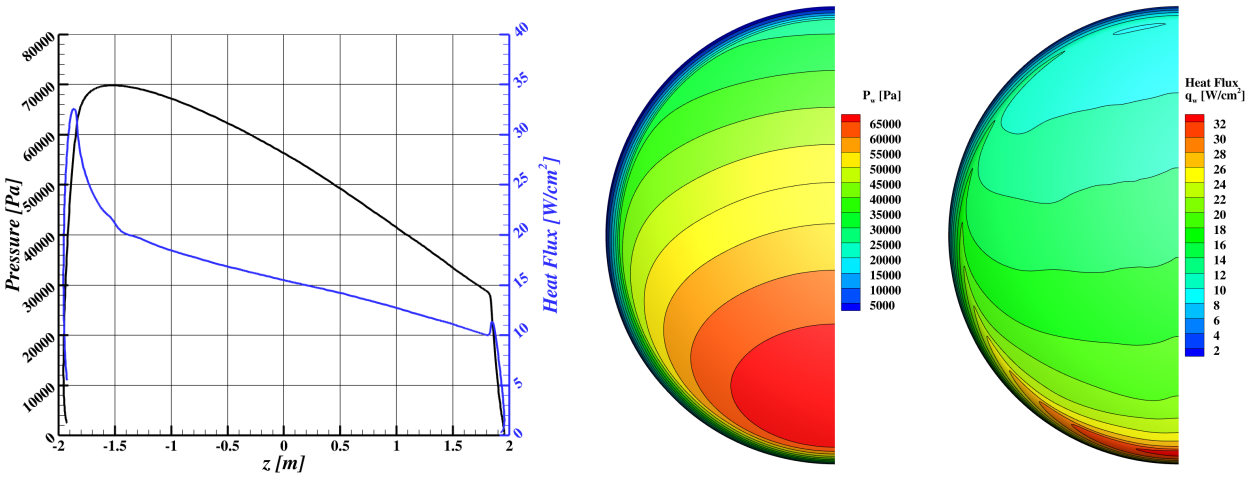

(a) Pitch plane pressure and heat flux (b) Pressure (c) Heat flux

Figure A10. Pressure and heat flux at velocity 3.0 km/s, altitude 35.0 km, and angle-of-attack 154.0 degrees.

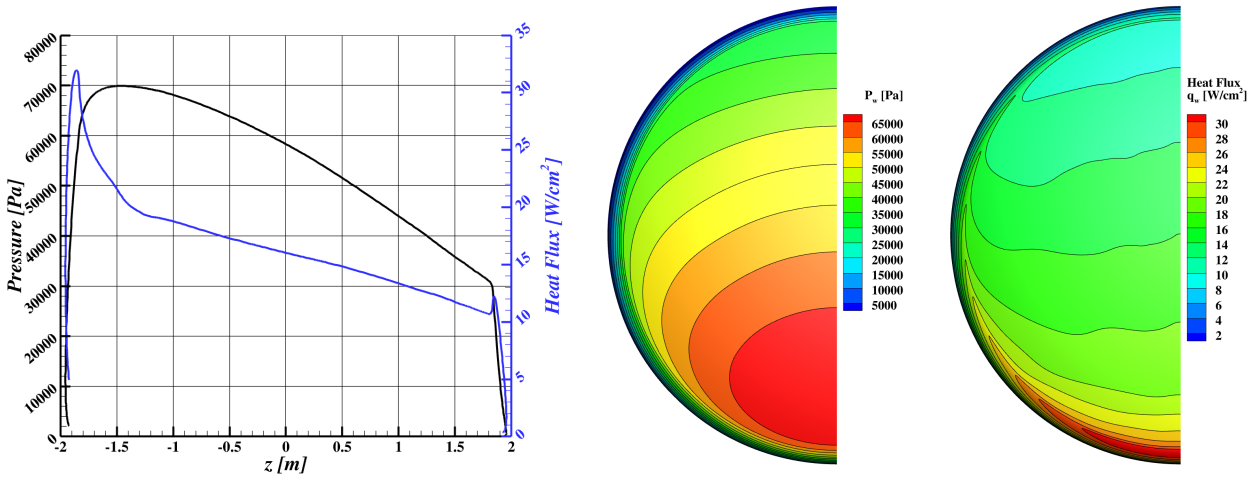

(a) Pitch plane pressure and heat flux (b) Pressure (c) Heat flux

Figure A11. Pressure and heat flux at velocity 3.0 km/s, altitude 35.0 km, and angle-of-attack 156.0 degrees.

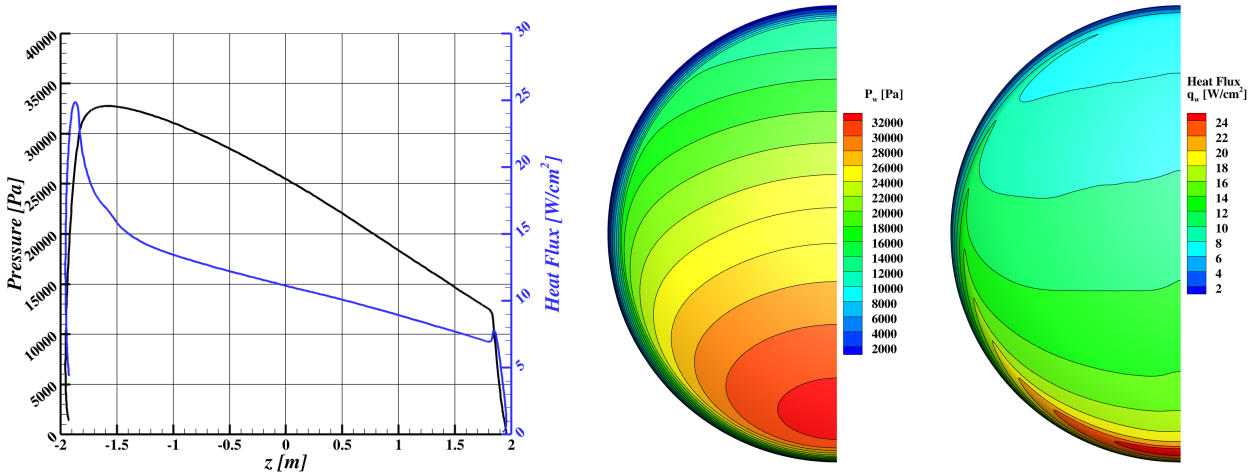

(a) Pitch plane pressure and heat flux (b) Pressure (c) Heat flux

Figure A12. Pressure and heat flux at velocity 3.0 km/s, altitude 40.0 km, and angle-of-attack 152.0 degrees.

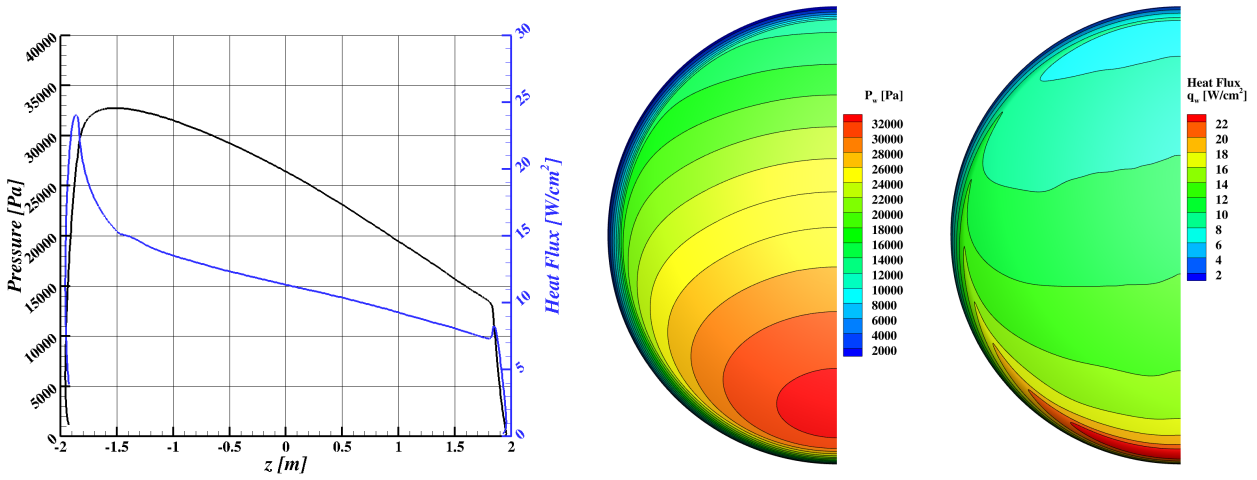

(a) Pitch plane pressure and heat flux (b) Pressure (c) Heat flux

Figure A13. Pressure and heat flux at velocity 3.0 km/s, altitude 40.0 km, and angle-of-attack 154.0 degrees.

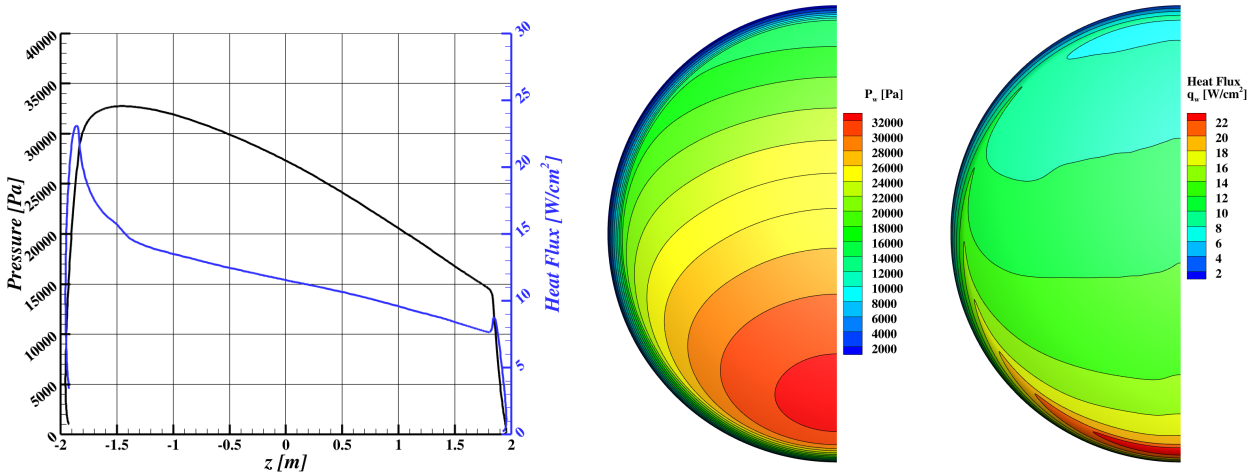

(a) Pitch plane pressure and heat flux (b) Pressure (c) Heat flux

Figure A14. Pressure and heat flux at velocity 3.0 km/s, altitude 40.0 km, and angle-of-attack 156.0 degrees.

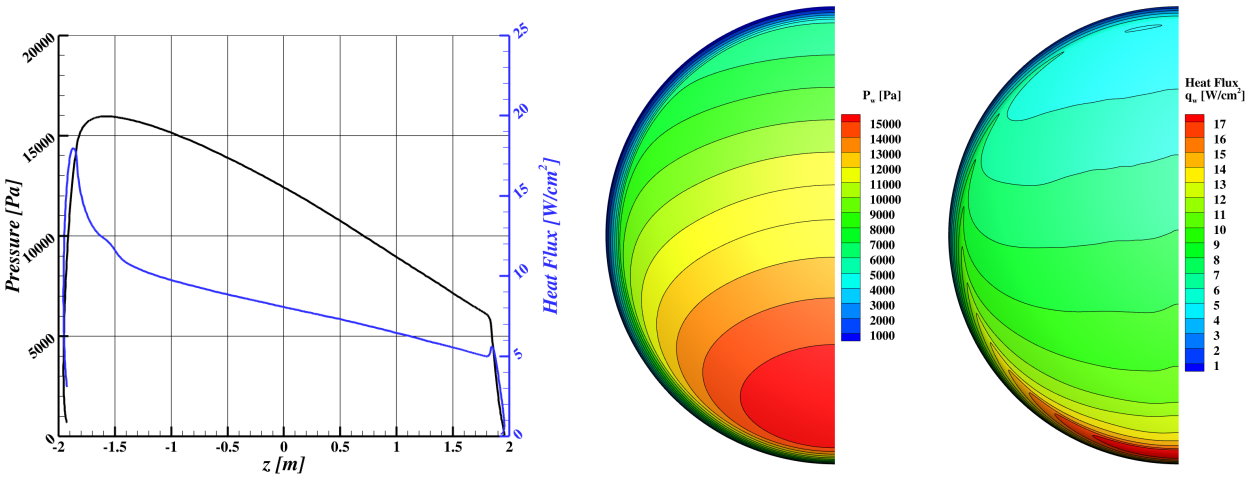

(a) Pitch plane pressure and heat flux (b) Pressure (c) Heat flux

Figure A15. Pressure and heat flux at velocity 3.0 km/s, altitude 45.0 km, and angle-of-attack 152.0 degrees.

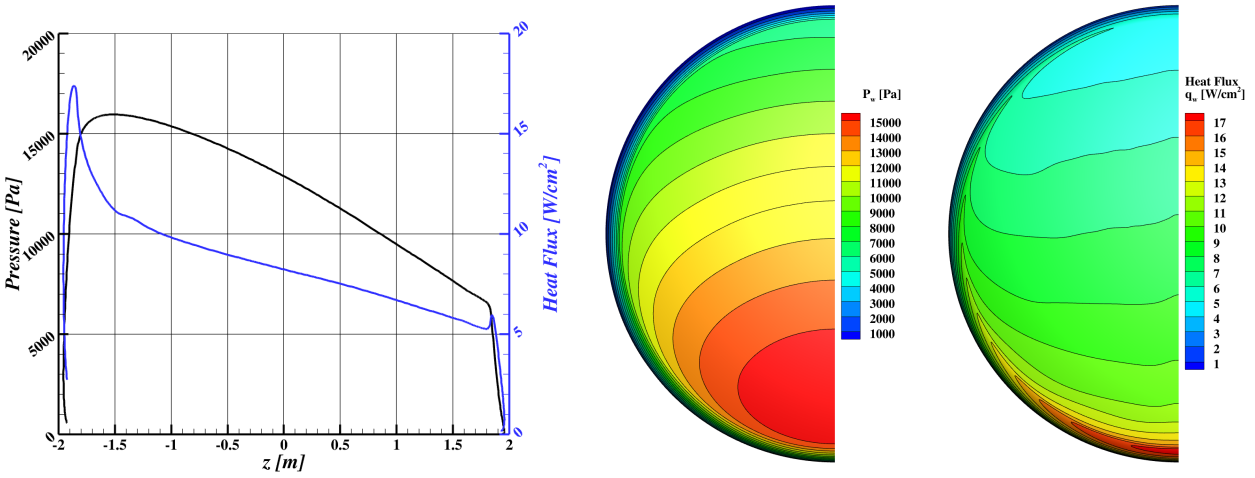

(a) Pitch plane pressure and heat flux (b) Pressure (c) Heat flux

Figure A16. Pressure and heat flux at velocity 3.0 km/s, altitude 45.0 km, and angle-of-attack 154.0 degrees.

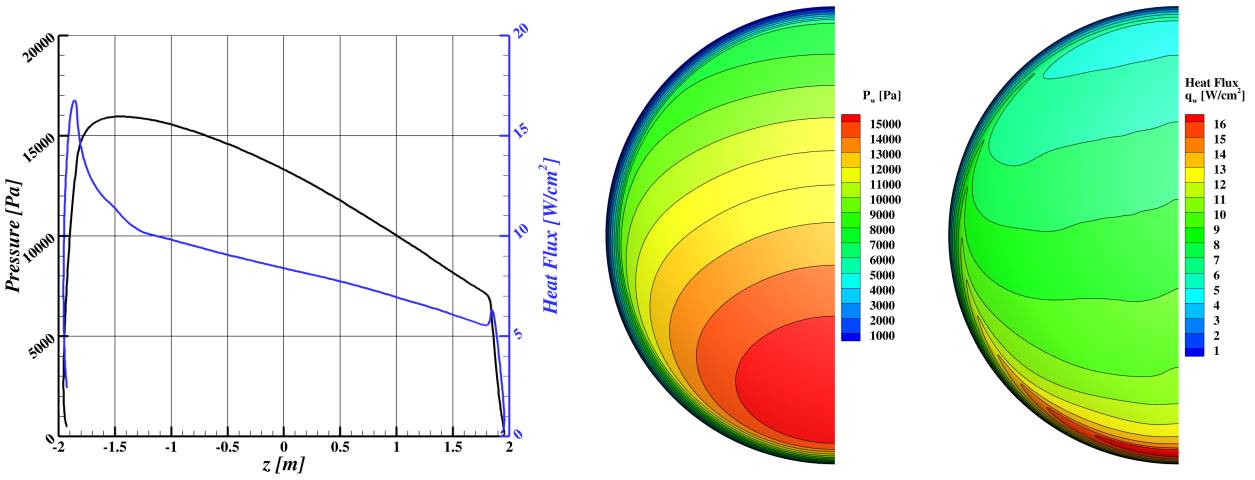

(a) Pitch plane pressure and heat flux (b) Pressure (c) Heat flux

Figure A17. Pressure and heat flux at velocity 3.0 km/s, altitude 45.0 km, and angle-of-attack 156.0 degrees.

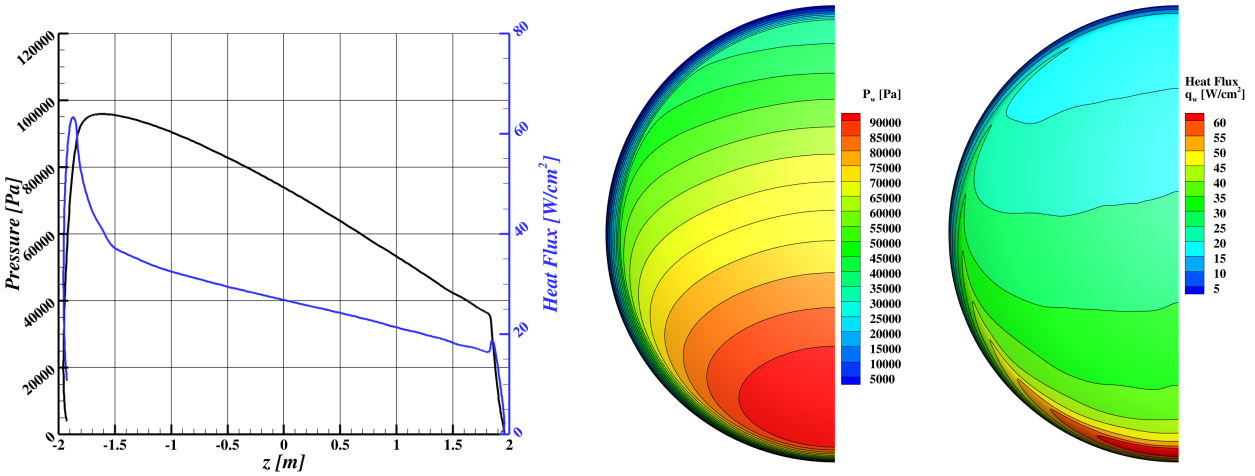

(a) Pitch plane pressure and heat flux (b) Pressure (c) Heat flux

Figure A18. Pressure and heat flux at velocity 3.5 km/s, altitude 35.0 km, and angle-of-attack 152.0 degrees.

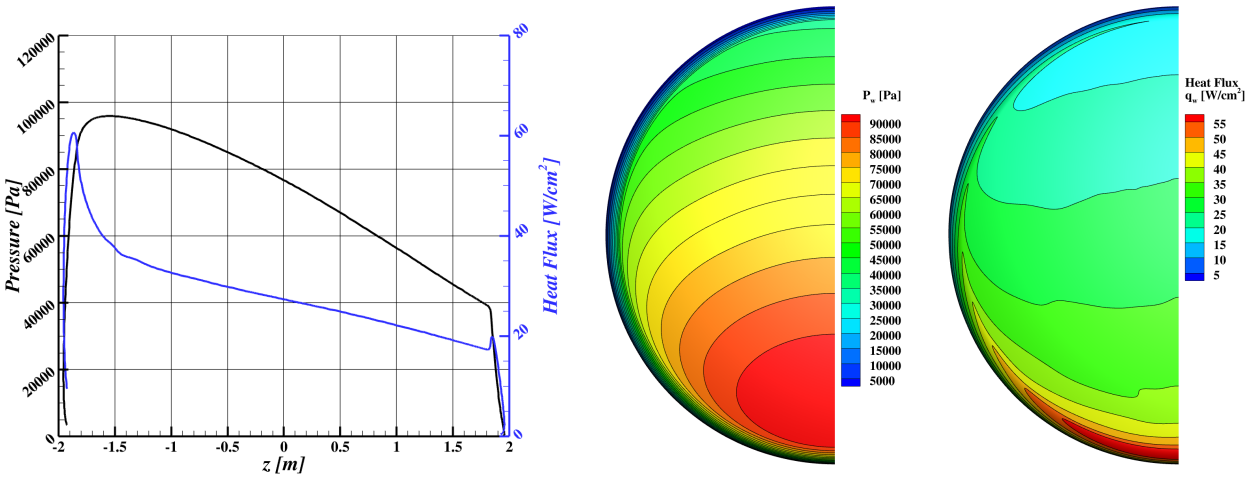

(a) Pitch plane pressure and heat flux (b) Pressure (c) Heat flux

Figure A19. Pressure and heat flux at velocity 3.5 km/s, altitude 35.0 km, and angle-of-attack 154.0 degrees.

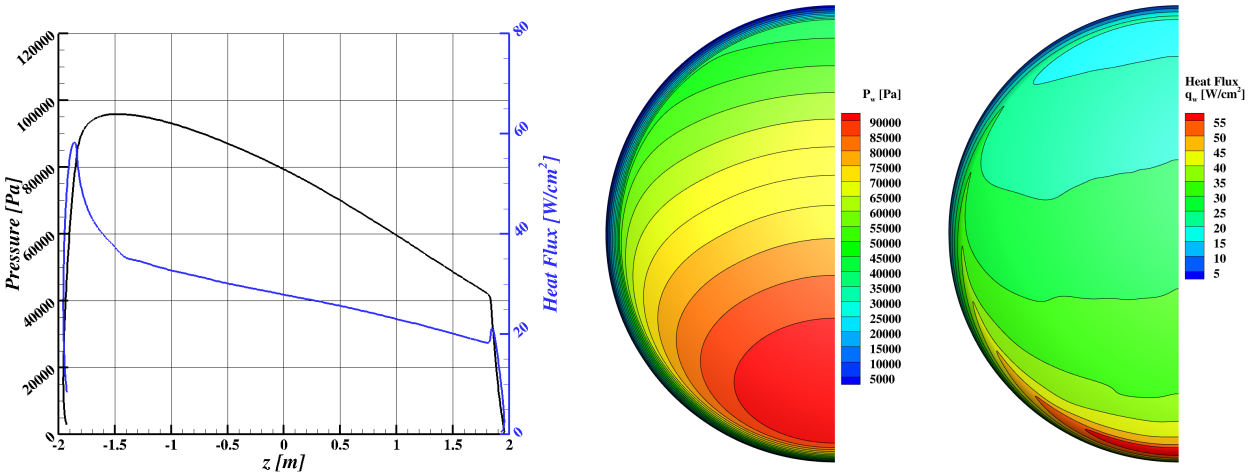

(a) Pitch plane pressure and heat flux (b) Pressure (c) Heat flux

Figure A20. Pressure and heat flux at velocity 3.5 km/s, altitude 35.0 km, and angle-of-attack 156.0 degrees.

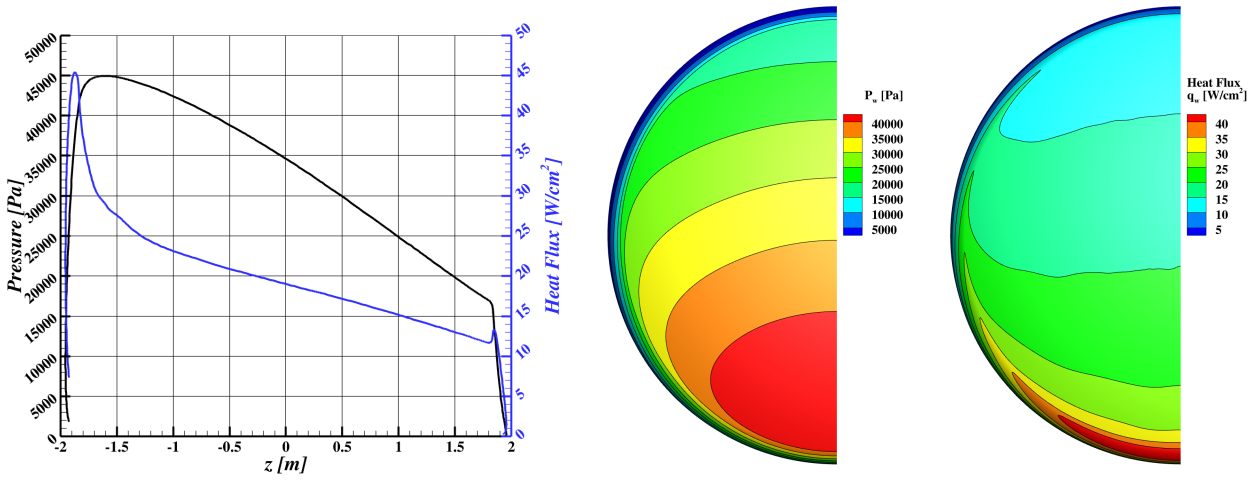

(a) Pitch plane pressure and heat flux (b) Pressure (c) Heat flux

Figure A21. Pressure and heat flux at velocity 3.5 km/s, altitude 40.0 km, and angle-of-attack 152.0 degrees.

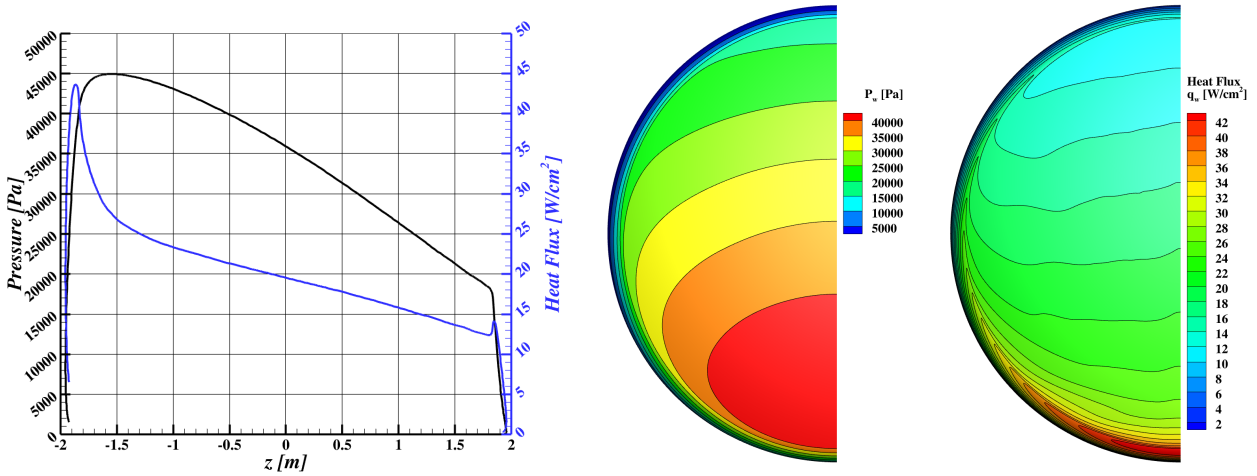

(a) Pitch plane pressure and heat flux (b) Pressure (c) Heat flux

Figure A22. Pressure and heat flux at velocity 3.5 km/s, altitude 40.0 km, and angle-of-attack 154.0 degrees.

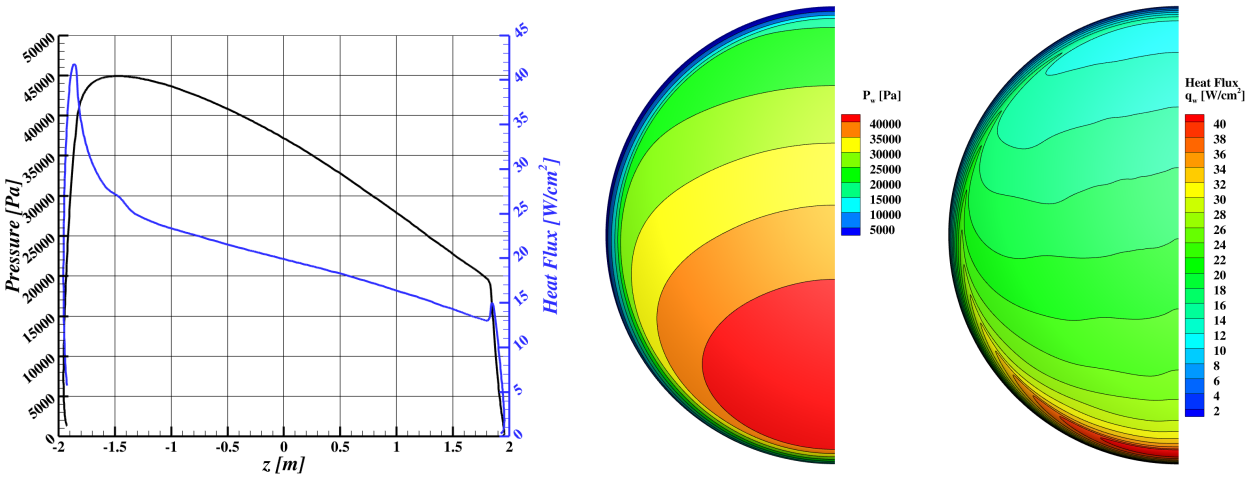

(a) Pitch plane pressure and heat flux (b) Pressure (c) Heat flux

Figure A23. Pressure and heat flux at velocity 3.5 km/s, altitude 40.0 km, and angle-of-attack 156.0 degrees.

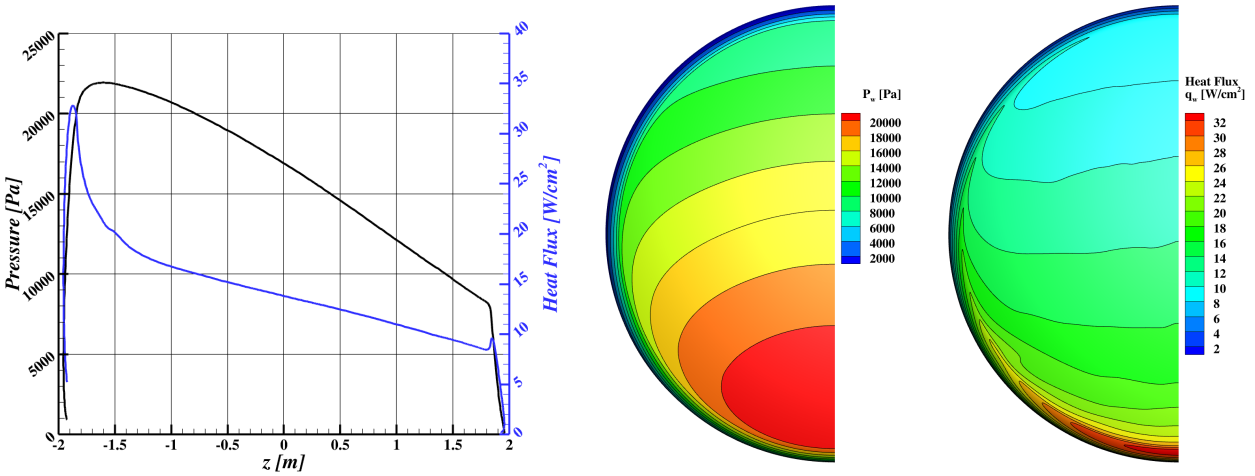

(a) Pitch plane pressure and heat flux (b) Pressure (c) Heat flux

Figure A24. Pressure and heat flux at velocity 3.5 km/s, altitude 45.0 km, and angle-of-attack 152.0 degrees.

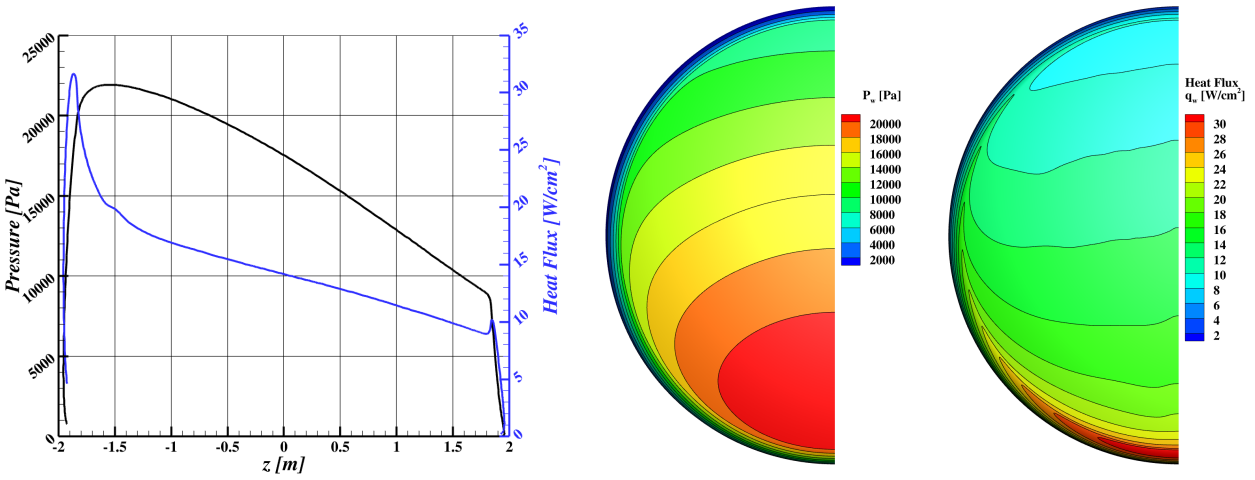

(a) Pitch plane pressure and heat flux (b) Pressure (c) Heat flux

Figure A25. Pressure and heat flux at velocity 3.5 km/s, altitude 45.0 km, and angle-of-attack 154.0 degrees.

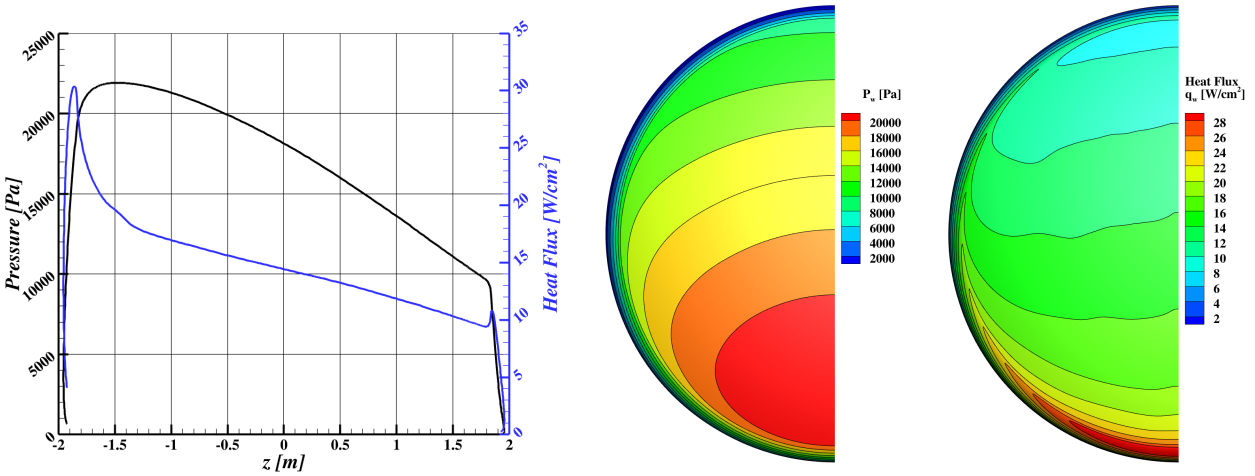

(a) Pitch plane pressure and heat flux (b) Pressure (c) Heat flux

Figure A26. Pressure and heat flux at velocity 3.5 km/s, altitude 45.0 km, and angle-of-attack 156.0 degrees.

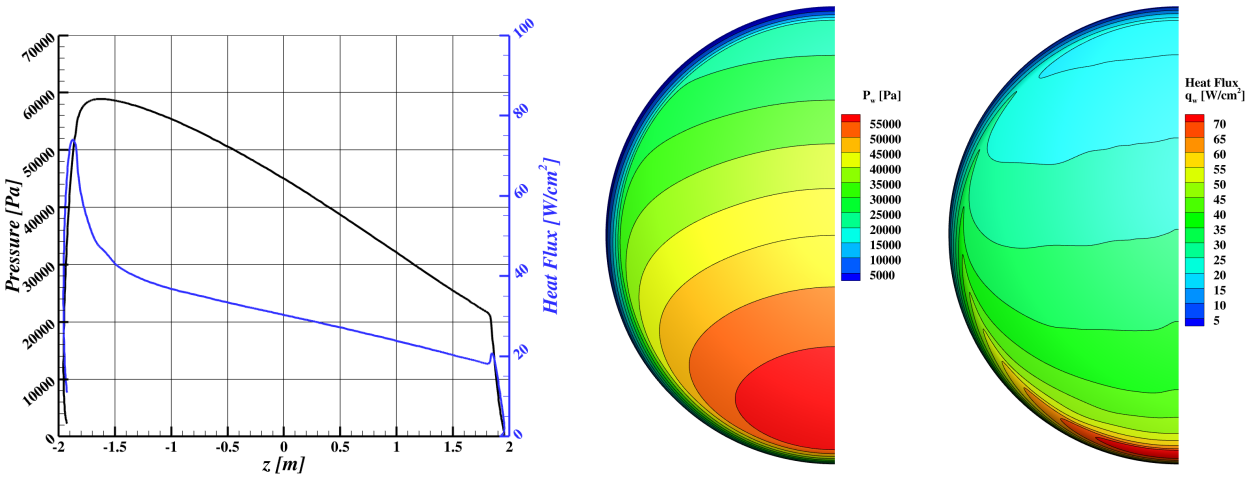

(a) Pitch plane pressure and heat flux (b) Pressure (c) Heat flux

Figure A27. Pressure and heat flux at velocity 4.0 km/s, altitude 40.0 km, and angle-of-attack 152.0 degrees.

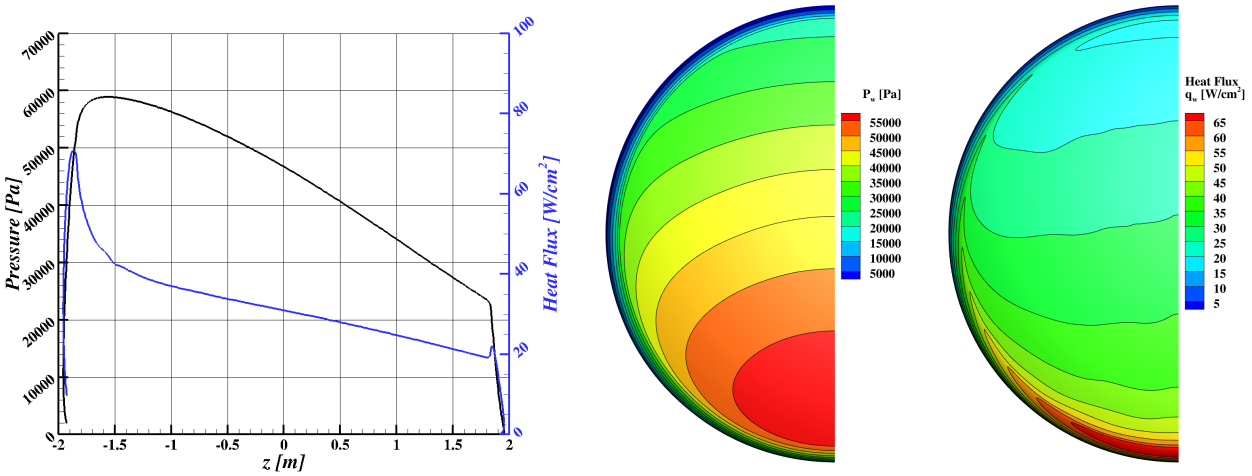

(a) Pitch plane pressure and heat flux (b) Pressure (c) Heat flux

Figure A28. Pressure and heat flux at velocity 4.0 km/s, altitude 40.0 km, and angle-of-attack 154.0 degrees.

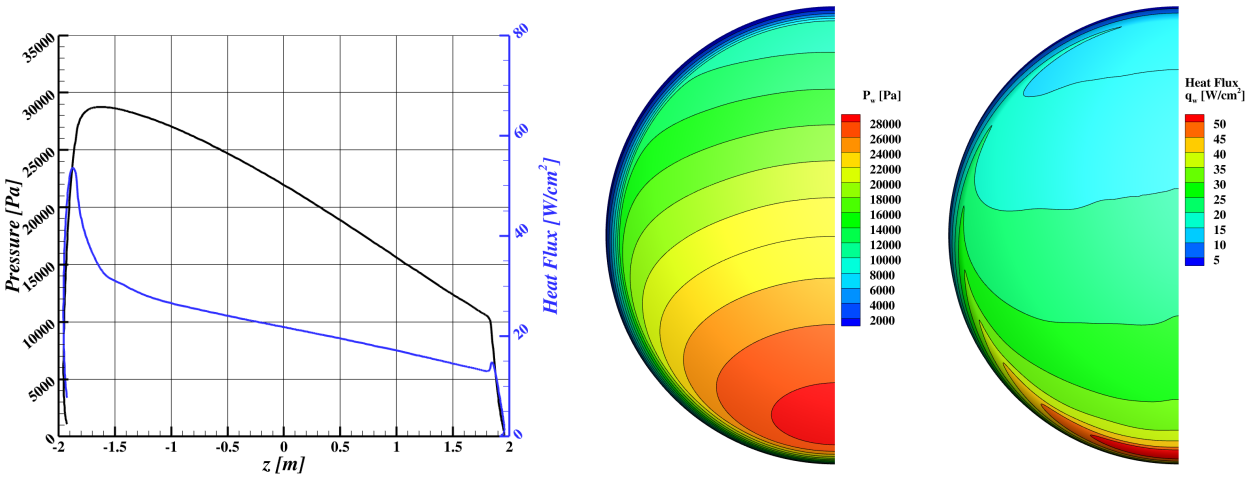

(a) Pitch plane pressure and heat flux (b) Pressure (c) Heat flux

Figure A29. Pressure and heat flux at velocity 4.0 km/s, altitude 45.0 km, and angle-of-attack 152.0 degrees.

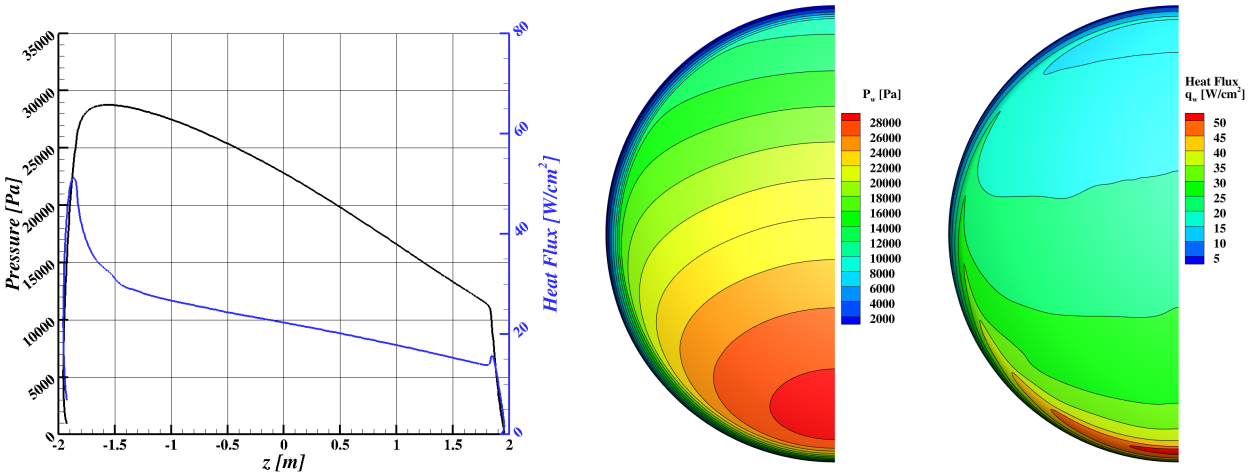

(a) Pitch plane pressure and heat flux (b) Pressure (c) Heat flux

Figure A30. Pressure and heat flux at velocity 4.0 km/s, altitude 45.0 km, and angle-of-attack 154.0 degrees.

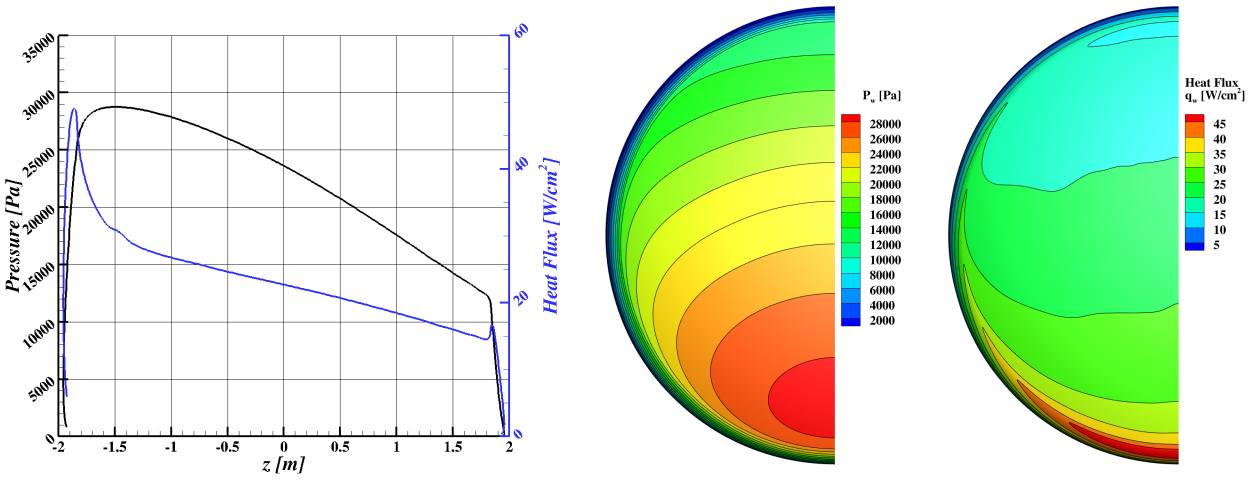

(a) Pitch plane pressure and heat flux (b) Pressure (c) Heat flux

Figure A31. Pressure and heat flux at velocity 4.0 km/s, altitude 45.0 km, and angle-of-attack 156.0 degrees.

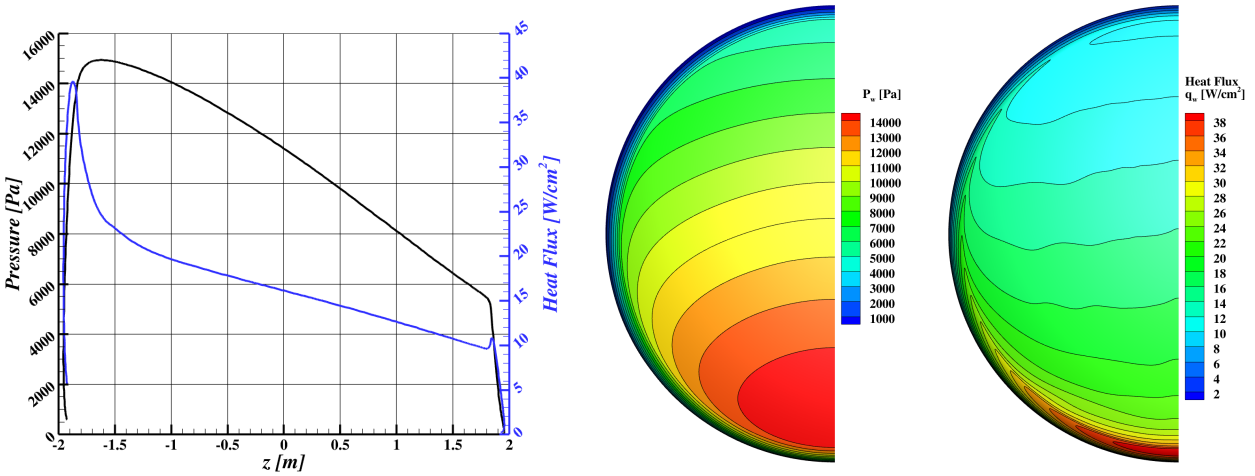

(a) Pitch plane pressure and heat flux (b) Pressure (c) Heat flux

Figure A32. Pressure and heat flux at velocity 4.0 km/s, altitude 50.0 km, and angle-of-attack 152.0 degrees.

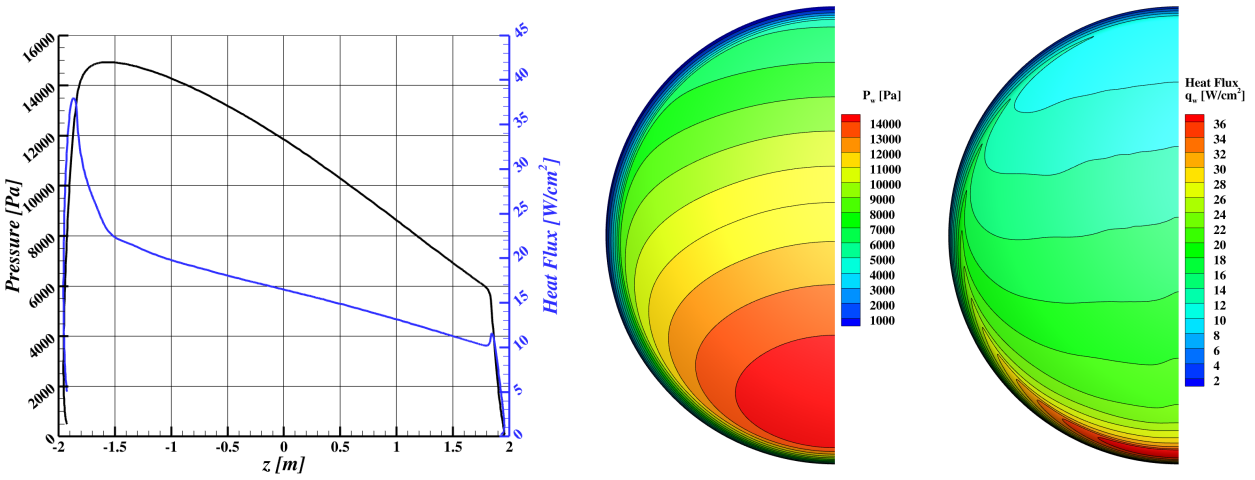

(a) Pitch plane pressure and heat flux (b) Pressure (c) Heat flux

Figure A33. Pressure and heat flux at velocity 4.0 km/s, altitude 50.0 km, and angle-of-attack 154.0 degrees.

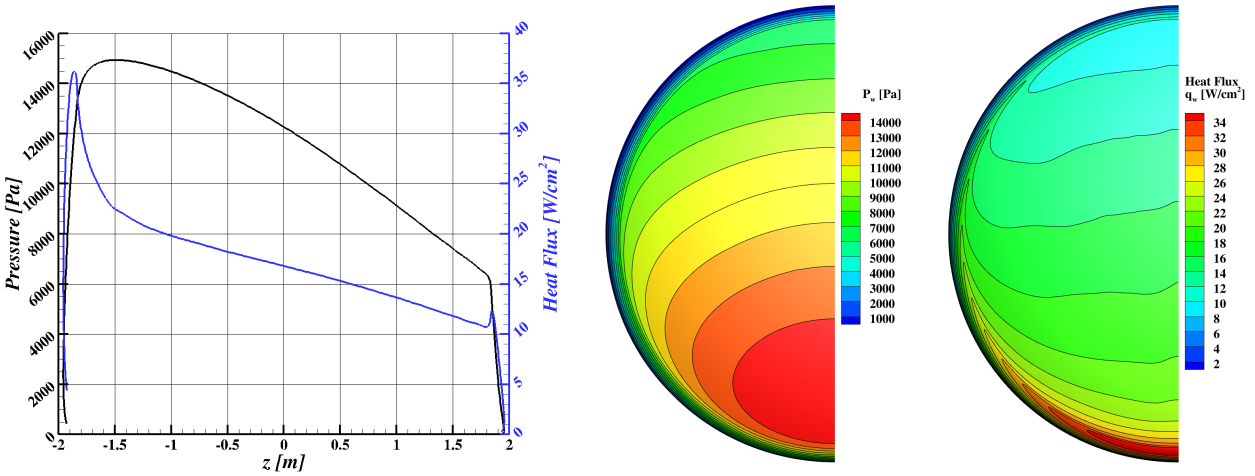

(a) Pitch plane pressure and heat flux (b) Pressure (c) Heat flux

Figure A34. Pressure and heat flux at velocity 4.0 km/s, altitude 50.0 km, and angle-of-attack 156.0 degrees.

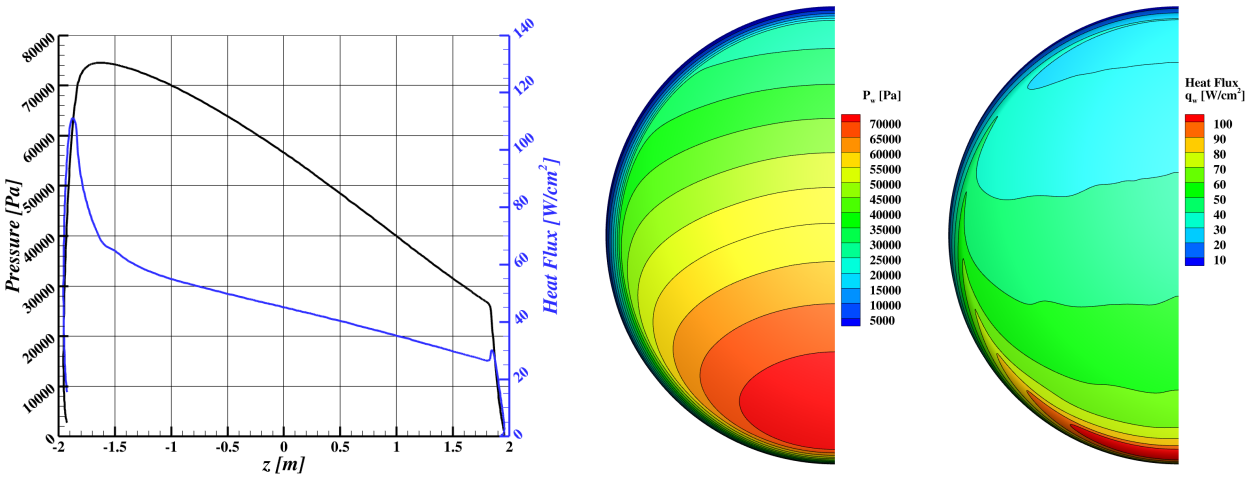

(a) Pitch plane pressure and heat flux (b) Pressure (c) Heat flux

Figure A35. Pressure and heat flux at velocity 4.5 km/s, altitude 40.0 km, and angle-of-attack 152.0 degrees.

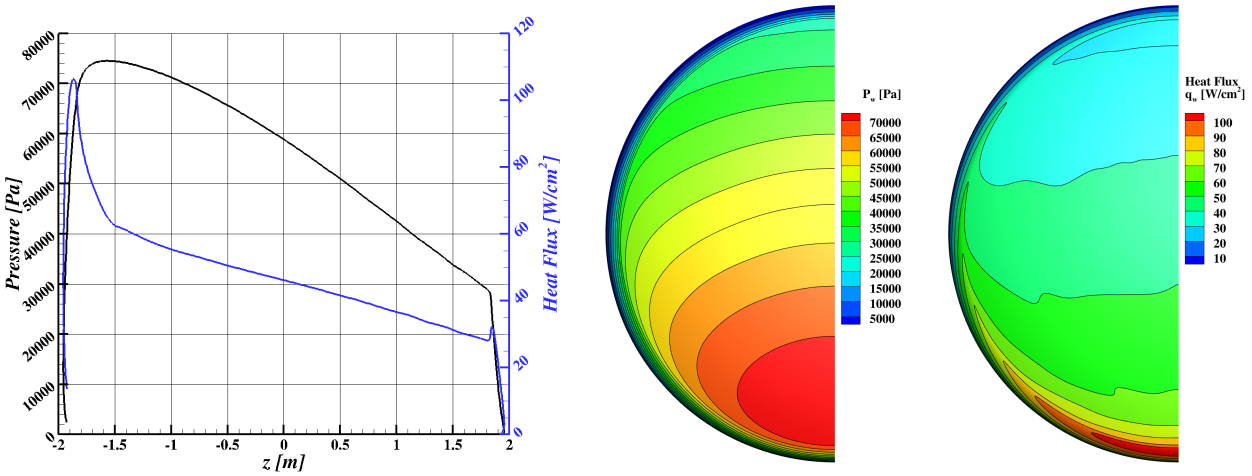

(a) Pitch plane pressure and heat flux (b) Pressure (c) Heat flux

Figure A36. Pressure and heat flux at velocity 4.5 km/s, altitude 40.0 km, and angle-of-attack 154.0 degrees.

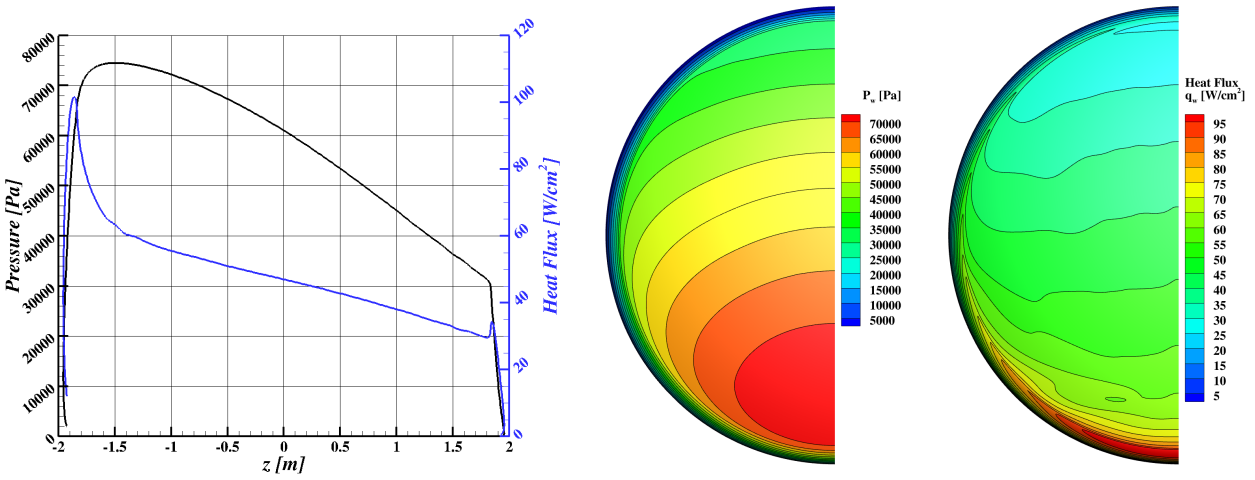

(a) Pitch plane pressure and heat flux (b) Pressure (c) Heat flux

Figure A37. Pressure and heat flux at velocity 4.5 km/s, altitude 40.0 km, and angle-of-attack 156.0 degrees.

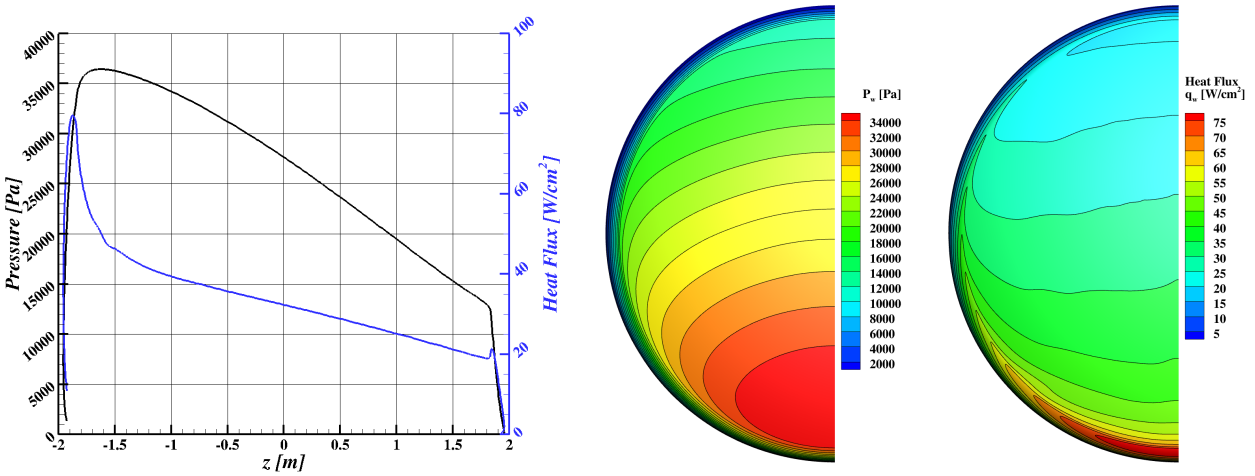

(a) Pitch plane pressure and heat flux (b) Pressure (c) Heat flux

Figure A38. Pressure and heat flux at velocity 4.5 km/s, altitude 45.0 km, and angle-of-attack 152.0 degrees.

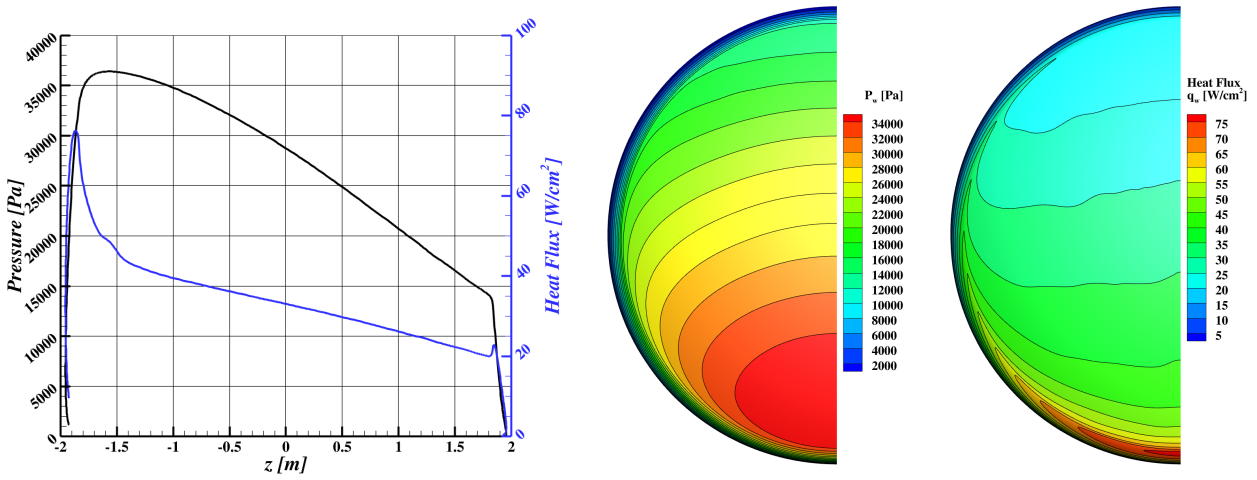

(a) Pitch plane pressure and heat flux (b) Pressure (c) Heat flux

Figure A39. Pressure and heat flux at velocity 4.5 km/s, altitude 45.0 km, and angle-of-attack 154.0 degrees.

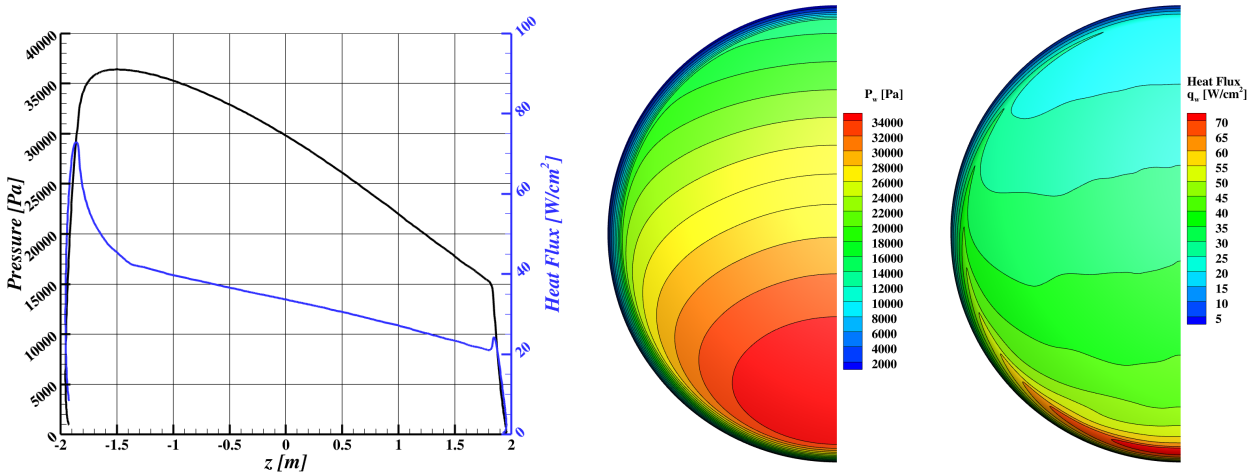

(a) Pitch plane pressure and heat flux (b) Pressure (c) Heat flux

Figure A40. Pressure and heat flux at velocity 4.5 km/s, altitude 45.0 km, and angle-of-attack 156.0 degrees.

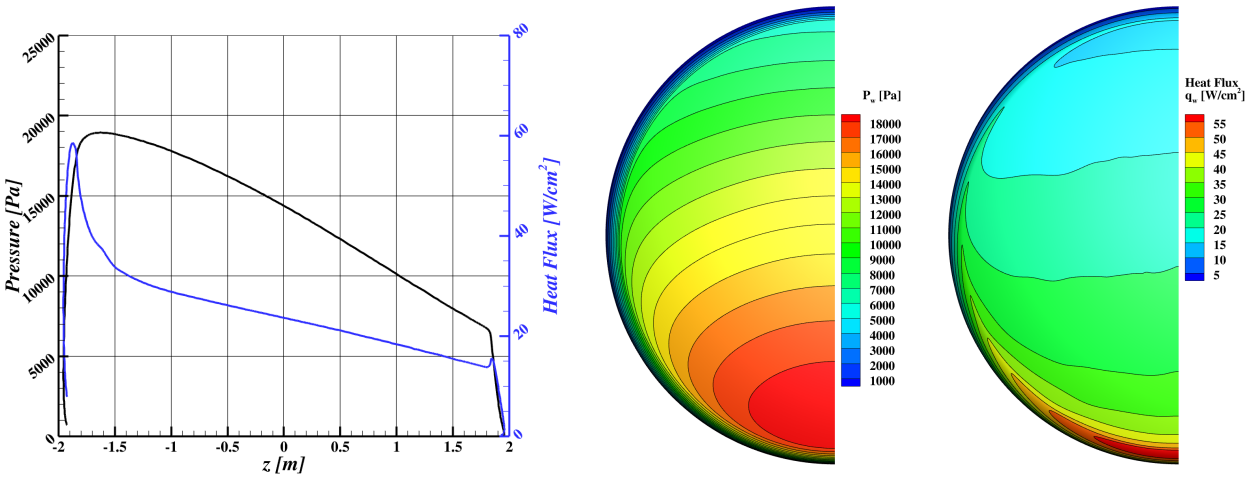

(a) Pitch plane pressure and heat flux (b) Pressure (c) Heat flux

Figure A41. Pressure and heat flux at velocity 4.5 km/s, altitude 50.0 km, and angle-of-attack 152.0 degrees.

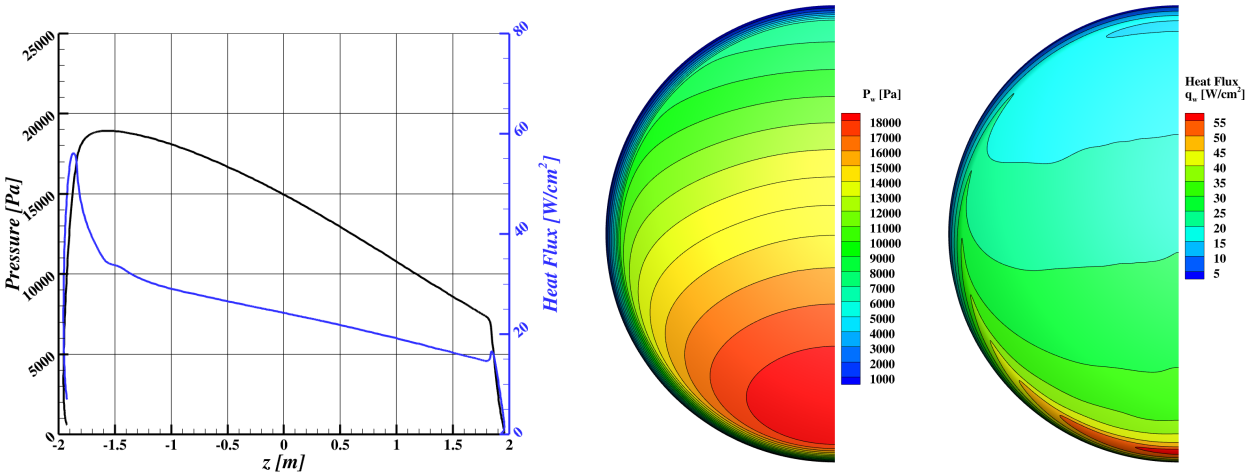

(a) Pitch plane pressure and heat flux (b) Pressure (c) Heat flux

Figure A42. Pressure and heat flux at velocity 4.5 km/s, altitude 50.0 km, and angle-of-attack 154.0 degrees.

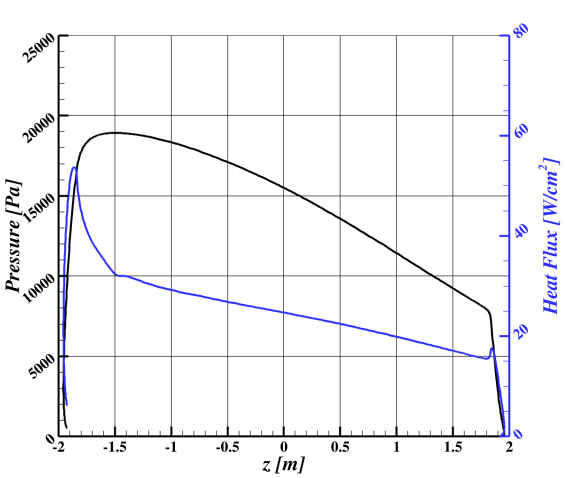

(a) Pitch plane pressure and heat flux

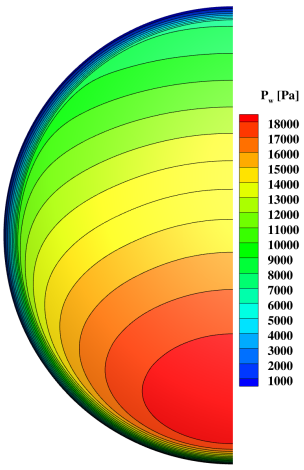

(b) Pressure

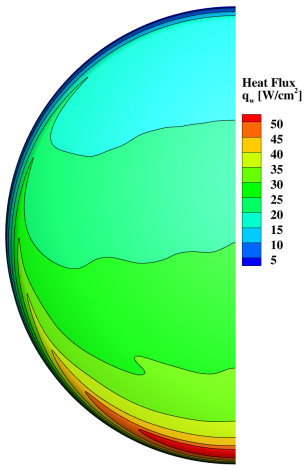

(c) Heat flux

Figure A43. Pressure and heat flux at velocity 4.5 km/s, altitude 50.0 km, and angle-of-attack 156.0 degrees.

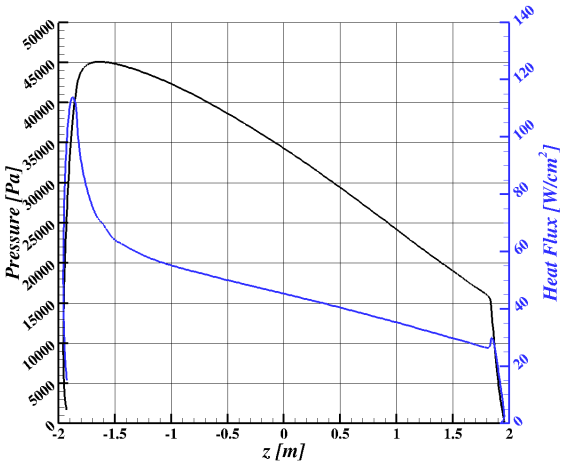

(a) Pitch plane pressure and heat flux

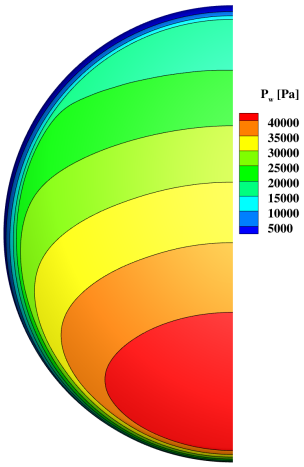

(b) Pressure

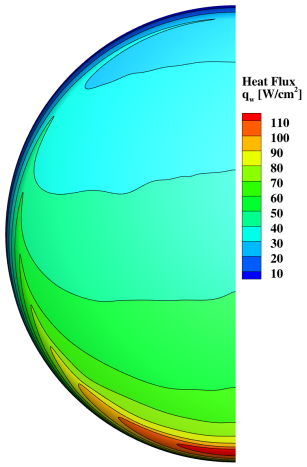

(c) Heat flux

Figure A44. Pressure and heat flux at velocity 5.0 km/s, altitude 45.0 km, and angle-of-attack 152.0 degrees.

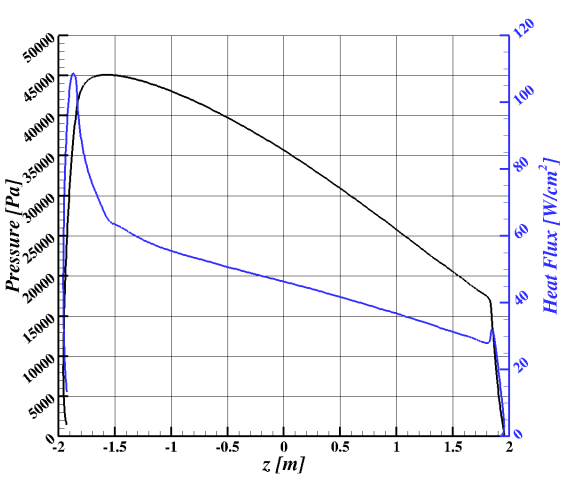

(a) Pitch plane pressure and heat flux

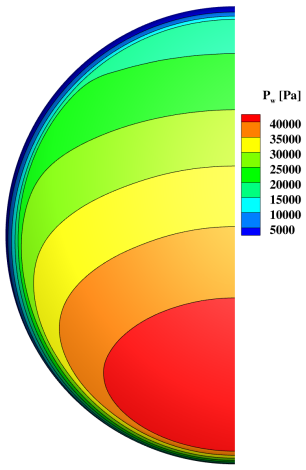

(b) Pressure

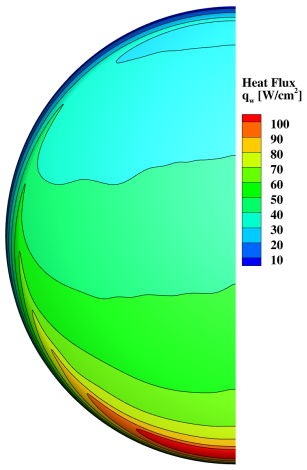

(c) Heat flux

Figure A45. Pressure and heat flux at velocity 5.0 km/s, altitude 45.0 km, and angle-of-attack 154.0 degrees.

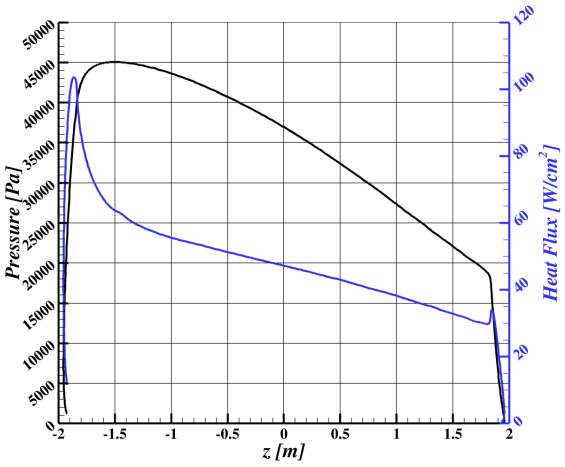

(a) Pitch plane pressure and heat flux

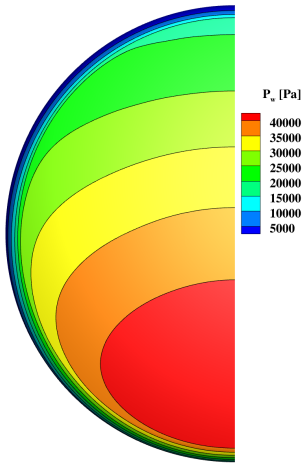

(b) Pressure

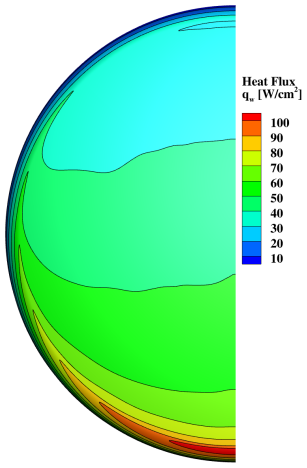

(c) Heat flux

Figure A46. Pressure and heat flux at velocity 5.0 km/s, altitude 45.0 km, and angle-of-attack 156.0 degrees.

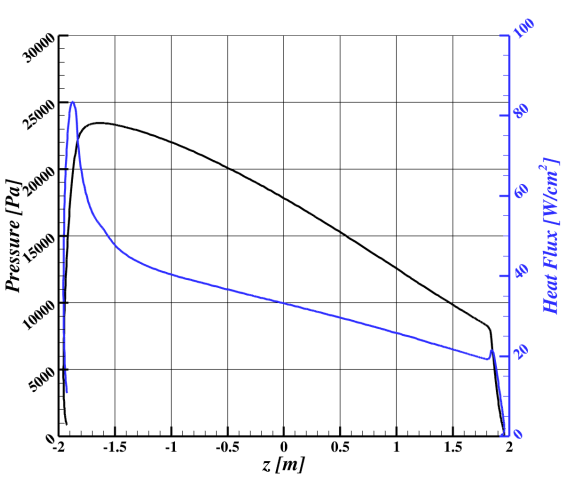

(a) Pitch plane pressure and heat flux

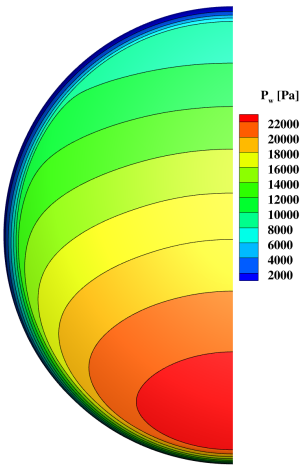

(b) Pressure

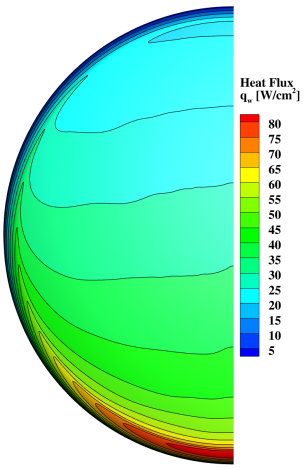

(c) Heat flux

Figure A47. Pressure and heat flux at velocity 5.0 km/s, altitude 50.0 km, and angle-of-attack 152.0 degrees.

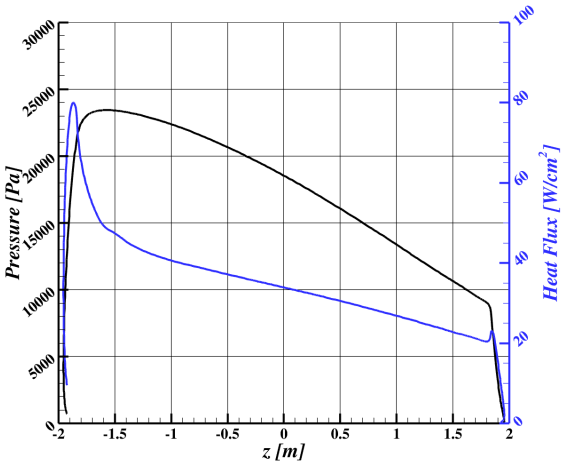

(a) Pitch plane pressure and heat flux

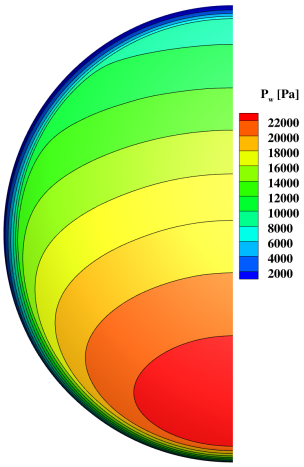

(b) Pressure

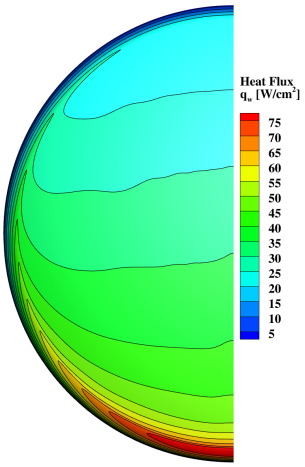

(c) Heat flux

Figure A48. Pressure and heat flux at velocity 5.0 km/s, altitude 50.0 km, and angle-of-attack 154.0 degrees.

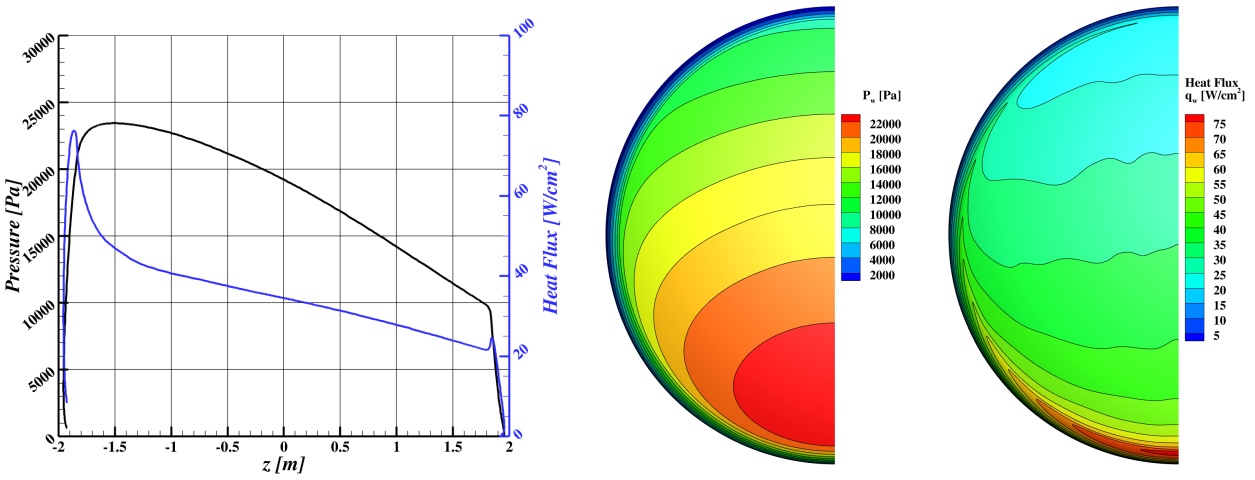

(a) Pitch plane pressure and heat flux (b) Pressure (c) Heat flux

Figure A49. Pressure and heat flux at velocity 5.0 km/s, altitude 50.0 km, and angle-of-attack 156.0 degrees.

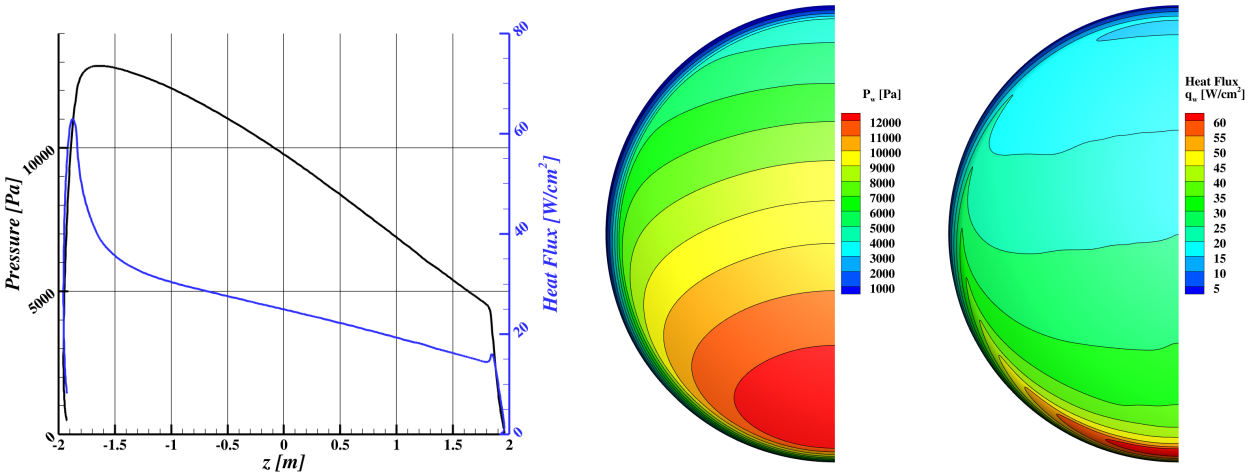

(a) Pitch plane pressure and heat flux (b) Pressure (c) Heat flux

Figure A50. Pressure and heat flux at velocity 5.0 km/s, altitude 55.0 km, and angle-of-attack 152.0 degrees.

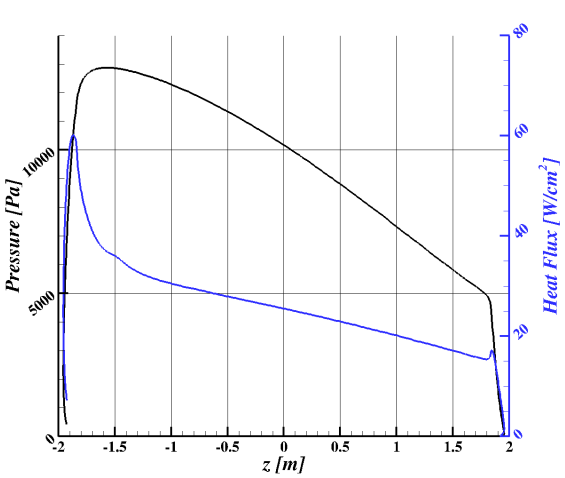

(a) Pitch plane pressure and heat flux

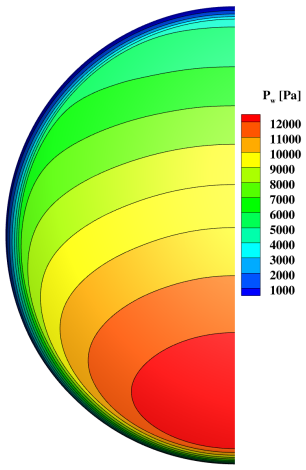

(b) Pressure

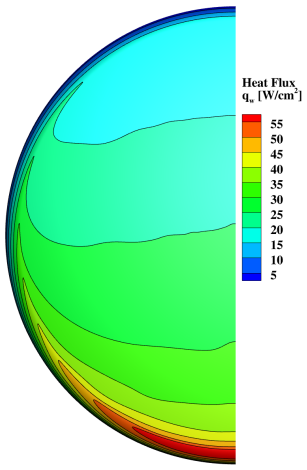

(c) Heat flux

Figure A51. Pressure and heat flux at velocity 5.0 km/s, altitude 55.0 km, and angle-of-attack 154.0 degrees.

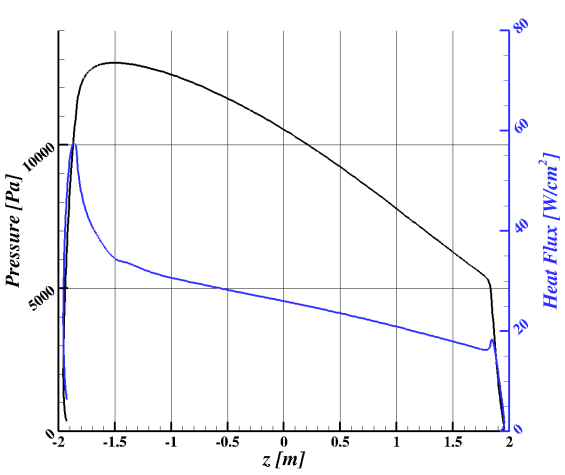

(a) Pitch plane pressure and heat flux

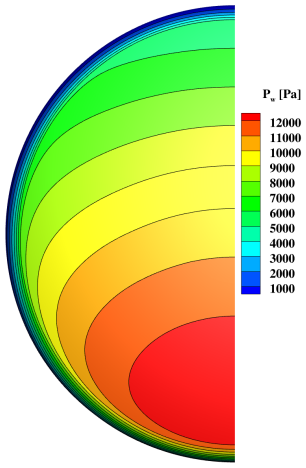

(b) Pressure

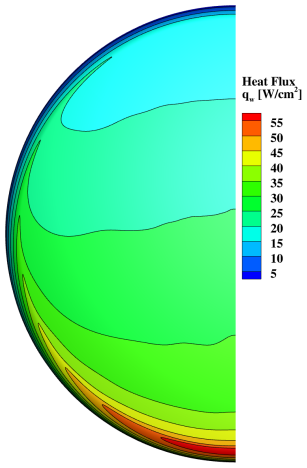

(c) Heat flux

Figure A52. Pressure and heat flux at velocity 5.0 km/s, altitude 55.0 km, and angle-of-attack 156.0 degrees.

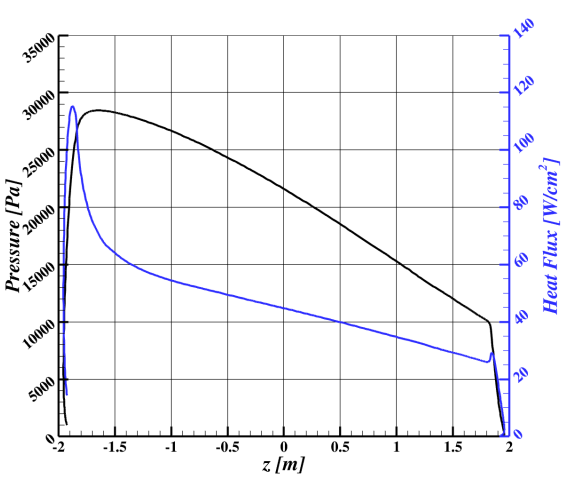

(a) Pitch plane pressure and heat flux

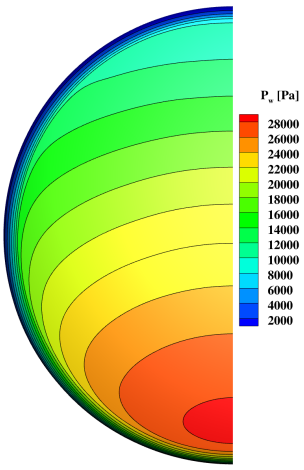

(b) Pressure

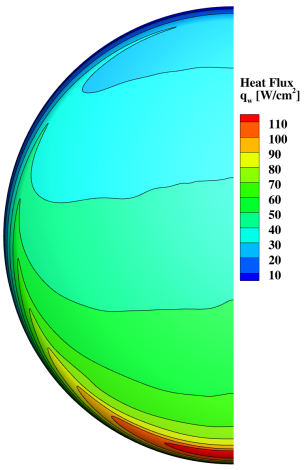

(c) Heat flux

Figure A53. Pressure and heat flux at velocity 5.5 km/s, altitude 50.0 km, and angle-of-attack 152.0 degrees.

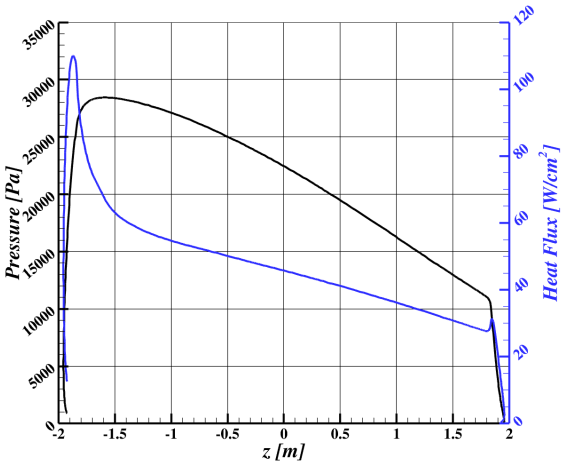

(a) Pitch plane pressure and heat flux

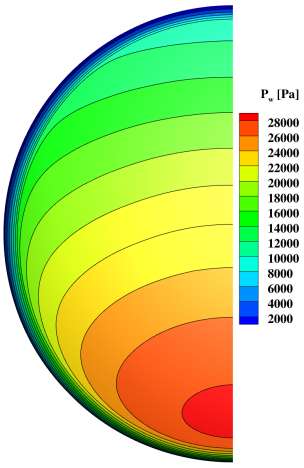

(b) Pressure

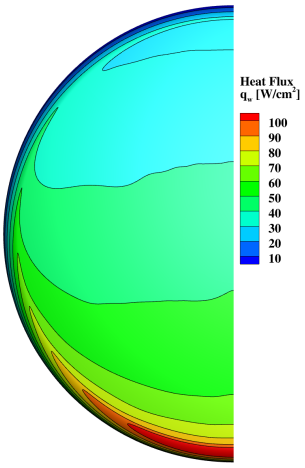

(c) Heat flux

Figure A54. Pressure and heat flux at velocity 5.5 km/s, altitude 50.0 km, and angle-of-attack 154.0 degrees.

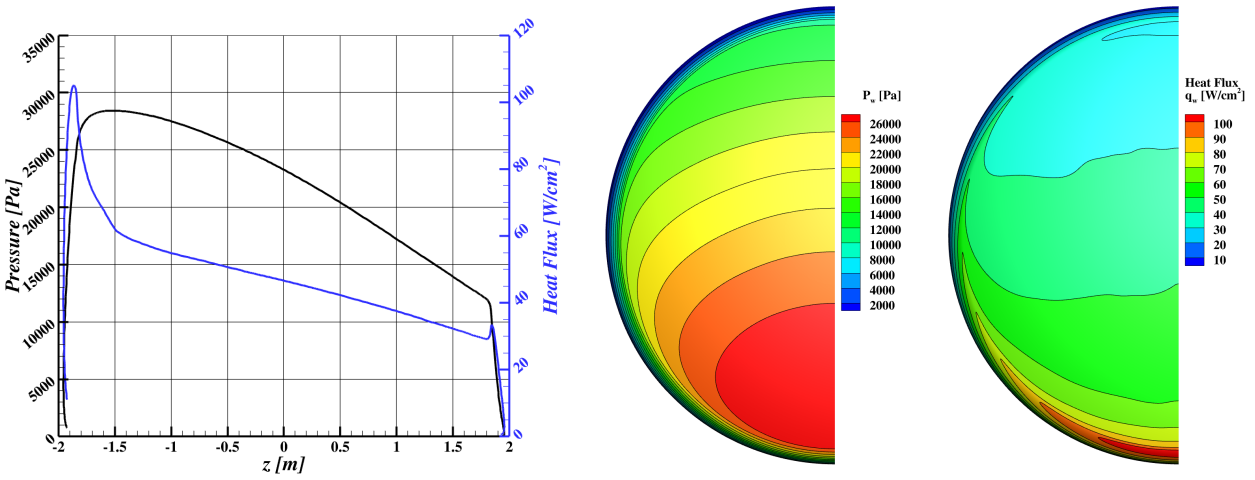

(a) Pitch plane pressure and heat flux (b) Pressure (c) Heat flux

Figure A55. Pressure and heat flux at velocity 5.5 km/s, altitude 50.0 km, and angle-of-attack 156.0 degrees.

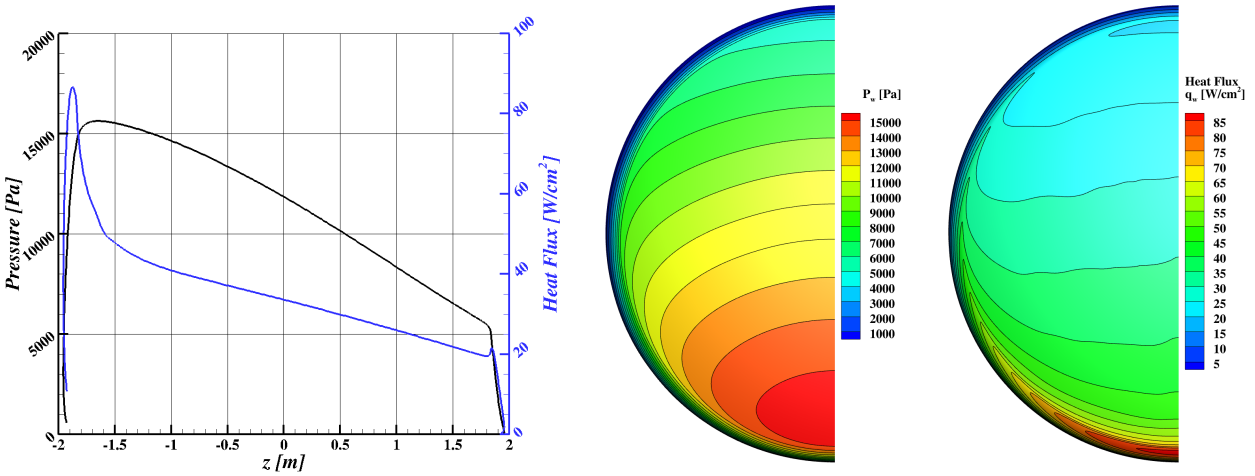

(a) Pitch plane pressure and heat flux (b) Pressure (c) Heat flux

Figure A56. Pressure and heat flux at velocity 5.5 km/s, altitude 55.0 km, and angle-of-attack 152.0 degrees.

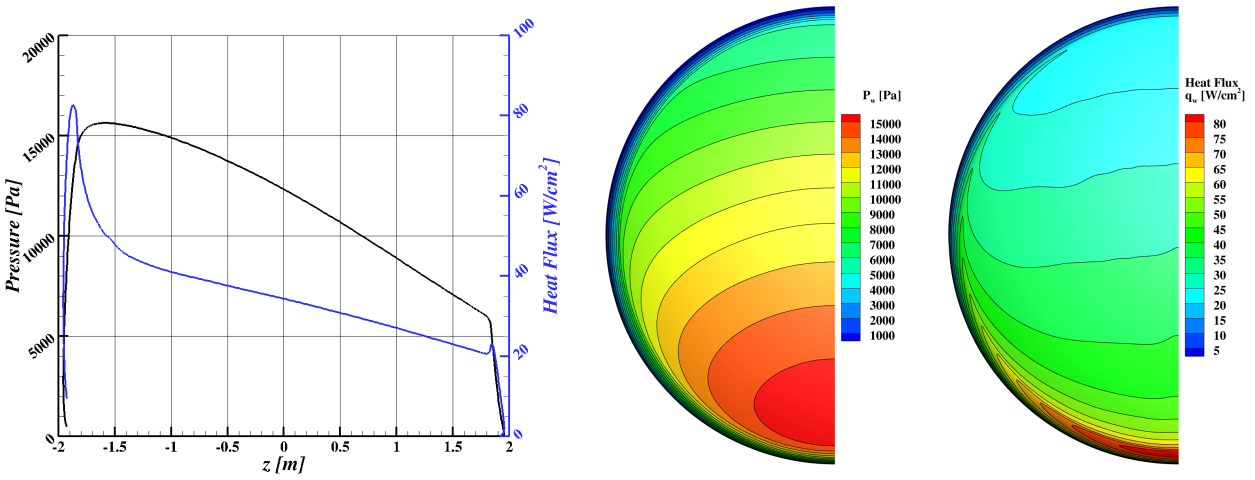

(a) Pitch plane pressure and heat flux (b) Pressure (c) Heat flux

Figure A57. Pressure and heat flux at velocity 5.5 km/s, altitude 55.0 km, and angle-of-attack 154.0 degrees.

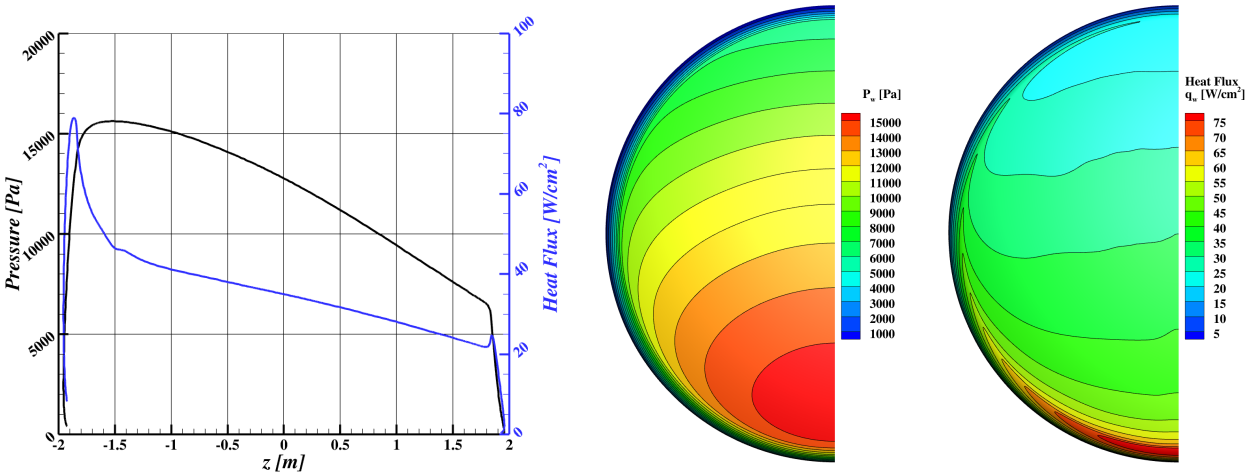

(a) Pitch plane pressure and heat flux (b) Pressure (c) Heat flux

Figure A58. Pressure and heat flux at velocity 5.5 km/s, altitude 55.0 km, and angle-of-attack 156.0 degrees.

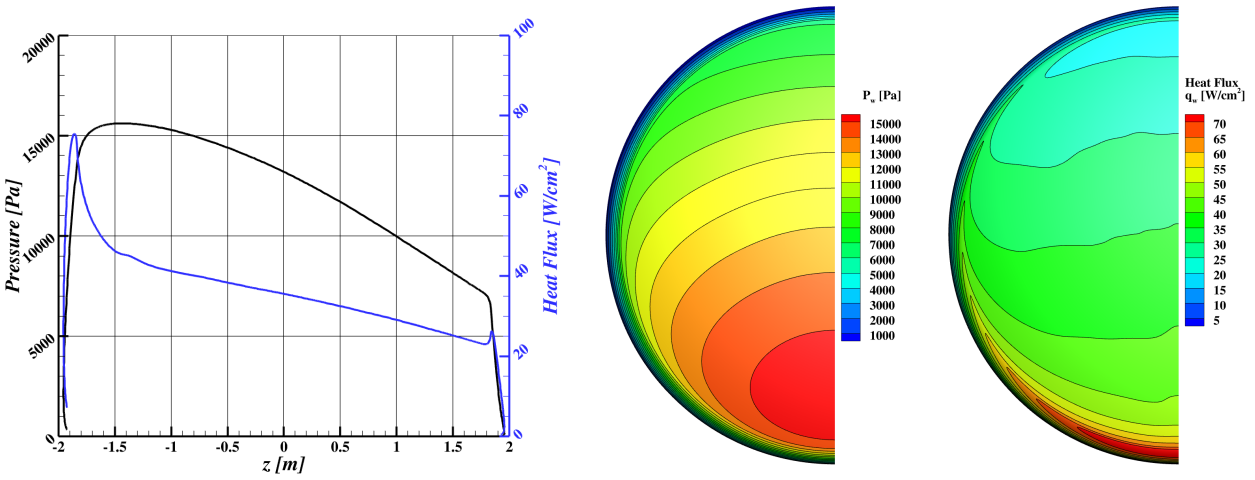

(a) Pitch plane pressure and heat flux (b) Pressure (c) Heat flux

Figure A59. Pressure and heat flux at velocity 5.5 km/s, altitude 55.0 km, and angle-of-attack 158.0 degrees.

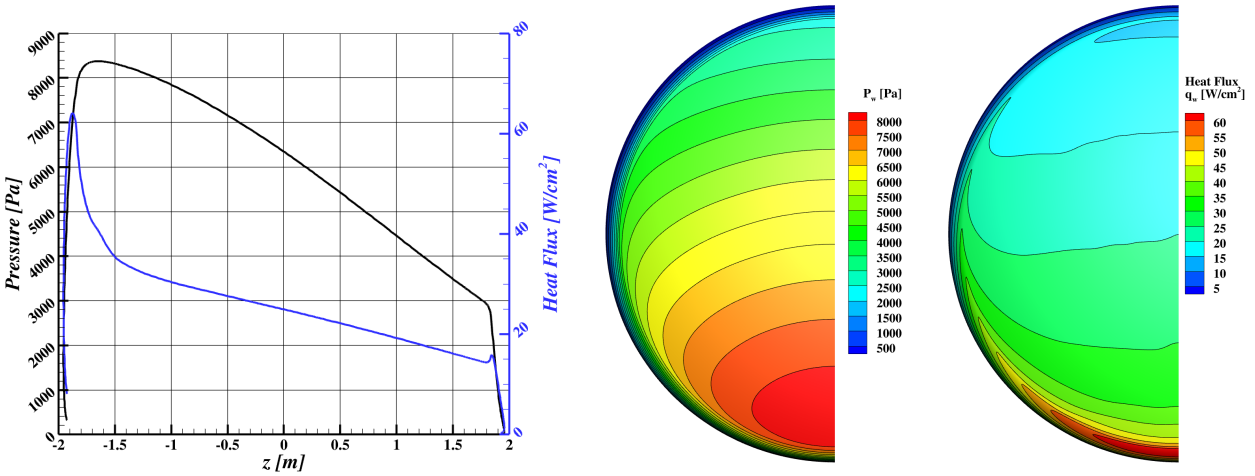

(a) Pitch plane pressure and heat flux (b) Pressure (c) Heat flux

Figure A60. Pressure and heat flux at velocity 5.5 km/s, altitude 60.0 km, and angle-of-attack 152.0 degrees.

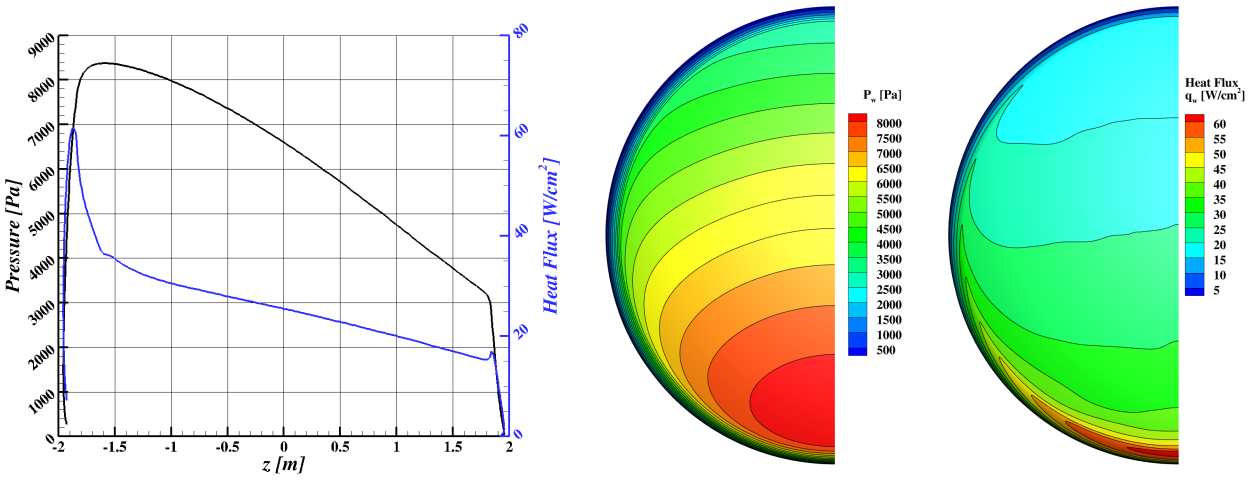

(a) Pitch plane pressure and heat flux (b) Pressure (c) Heat flux

Figure A61. Pressure and heat flux at velocity 5.5 km/s, altitude 60.0 km, and angle-of-attack 154.0 degrees.

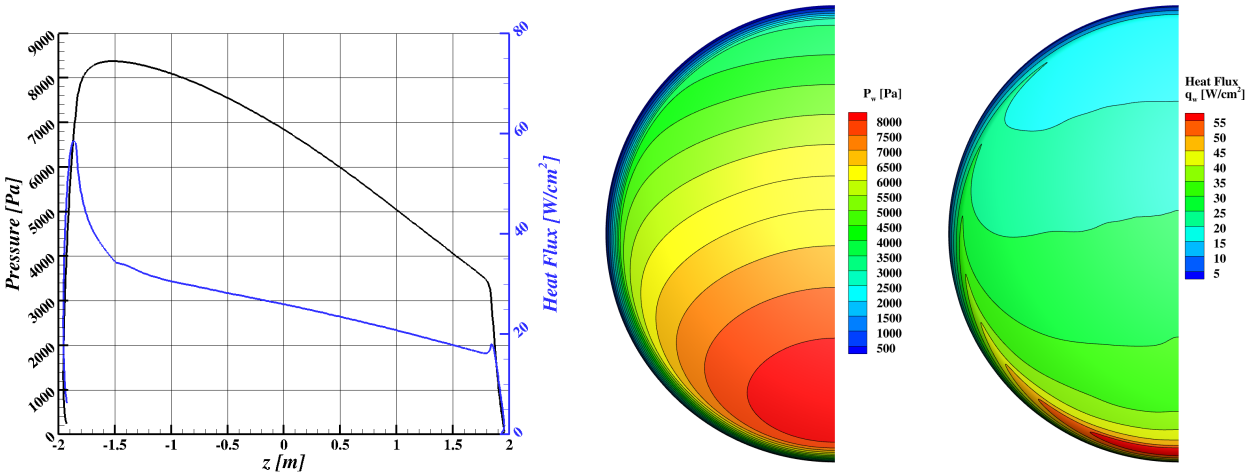

(a) Pitch plane pressure and heat flux (b) Pressure (c) Heat flux

Figure A62. Pressure and heat flux at velocity 5.5 km/s, altitude 60.0 km, and angle-of-attack 156.0 degrees.

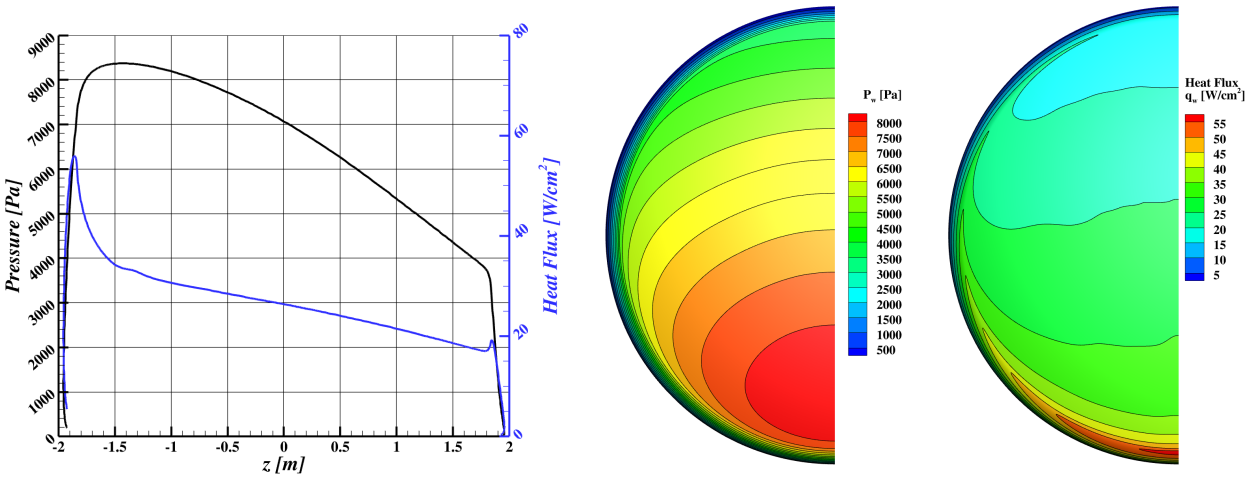

(a) Pitch plane pressure and heat flux (b) Pressure (c) Heat flux

Figure A63. Pressure and heat flux at velocity 5.5 km/s, altitude 60.0 km, and angle-of-attack 158.0 degrees.

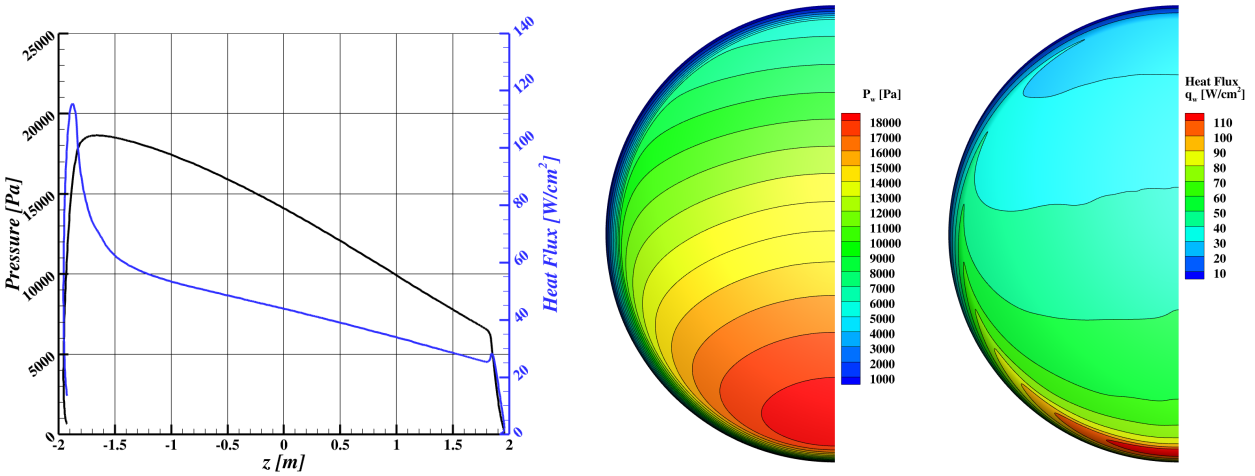

(a) Pitch plane pressure and heat flux (b) Pressure (c) Heat flux

Figure A64. Pressure and heat flux at velocity 6.0 km/s, altitude 55.0 km, and angle-of-attack 152.0 degrees.

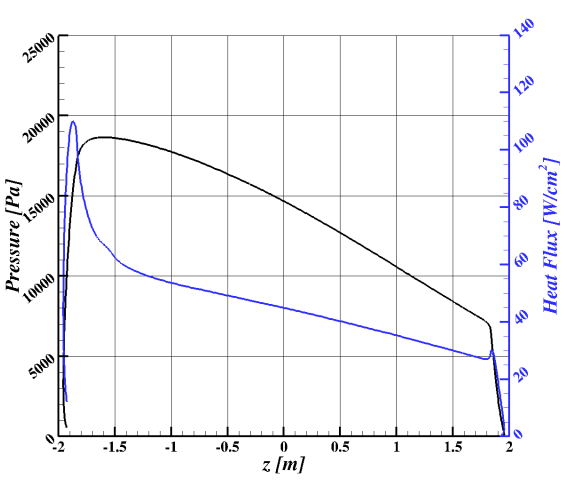

(a) Pitch plane pressure and heat flux

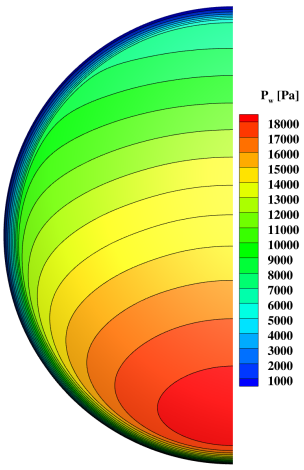

(b) Pressure

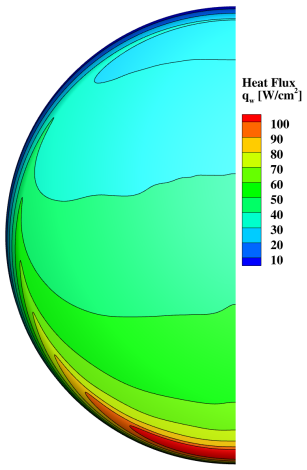

(c) Heat flux

Figure A65. Pressure and heat flux at velocity 6.0 km/s, altitude 55.0 km, and angle-of-attack 154.0 degrees.

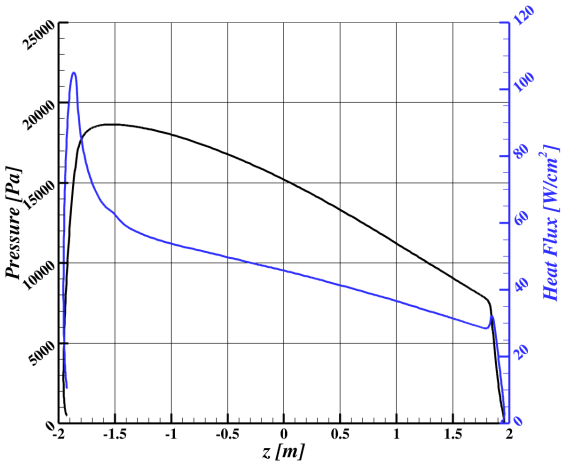

(a) Pitch plane pressure and heat flux

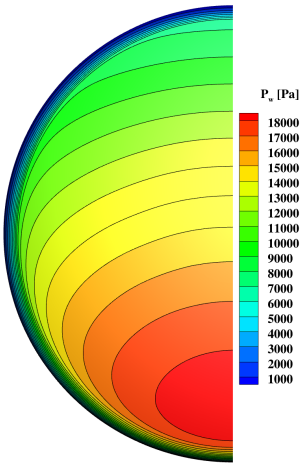

(b) Pressure

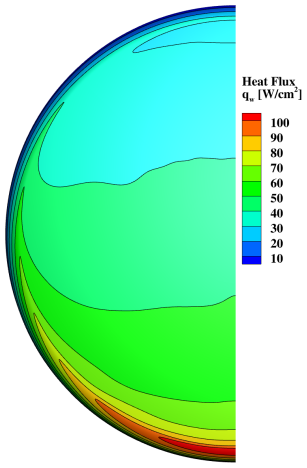

(c) Heat flux

Figure A66. Pressure and heat flux at velocity 6.0 km/s, altitude 55.0 km, and angle-of-attack 156.0 degrees.

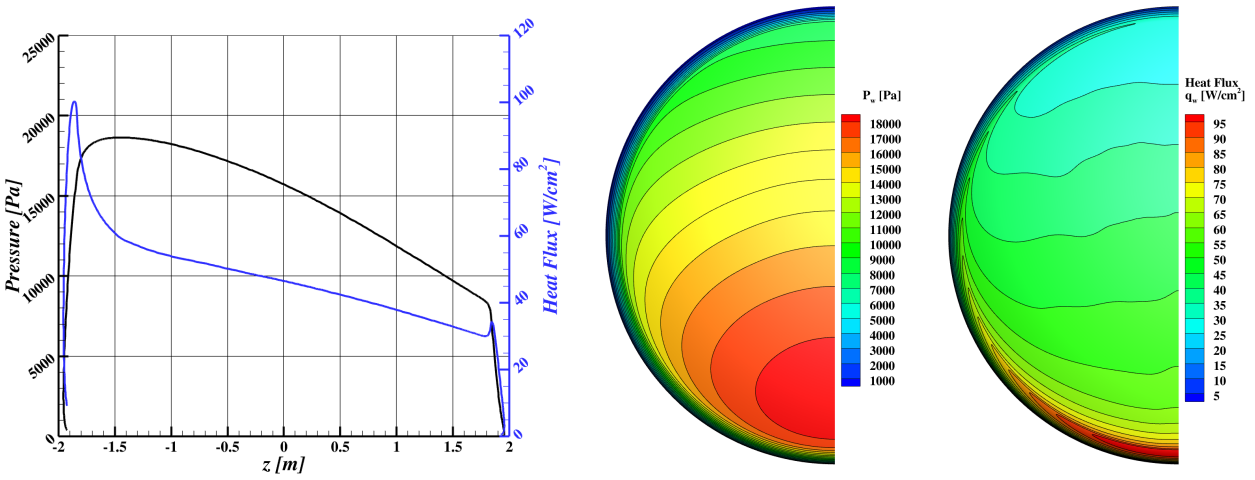

(a) Pitch plane pressure and heat flux (b) Pressure (c) Heat flux

Figure A67. Pressure and heat flux at velocity 6.0 km/s, altitude 55.0 km, and angle-of-attack 158.0 degrees.

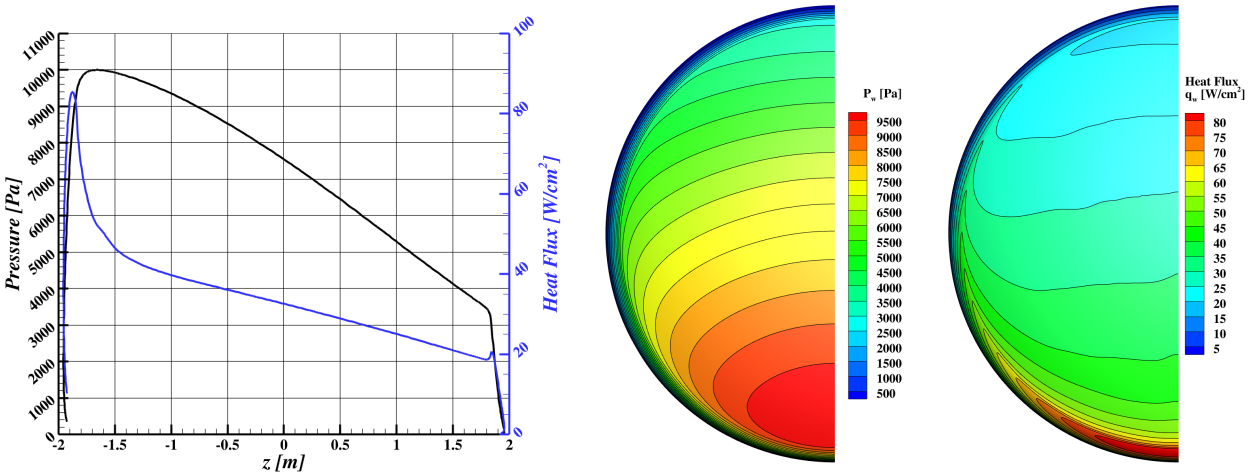

(a) Pitch plane pressure and heat flux (b) Pressure (c) Heat flux

Figure A68. Pressure and heat flux at velocity 6.0 km/s, altitude 60.0 km, and angle-of-attack 152.0 degrees.

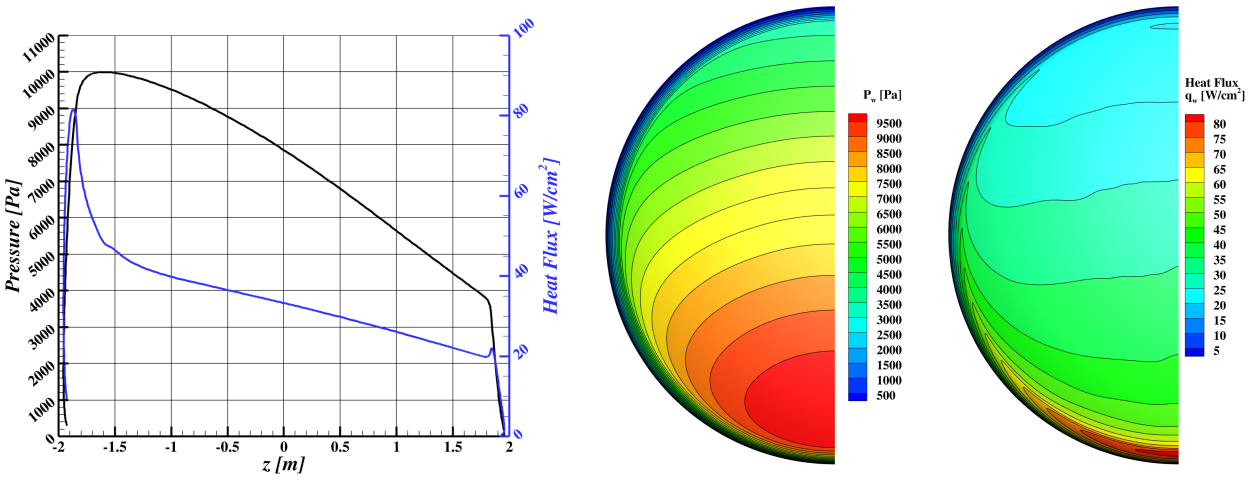

(a) Pitch plane pressure and heat flux (b) Pressure (c) Heat flux

Figure A69. Pressure and heat flux at velocity 6.0 km/s, altitude 60.0 km, and angle-of-attack 154.0 degrees.

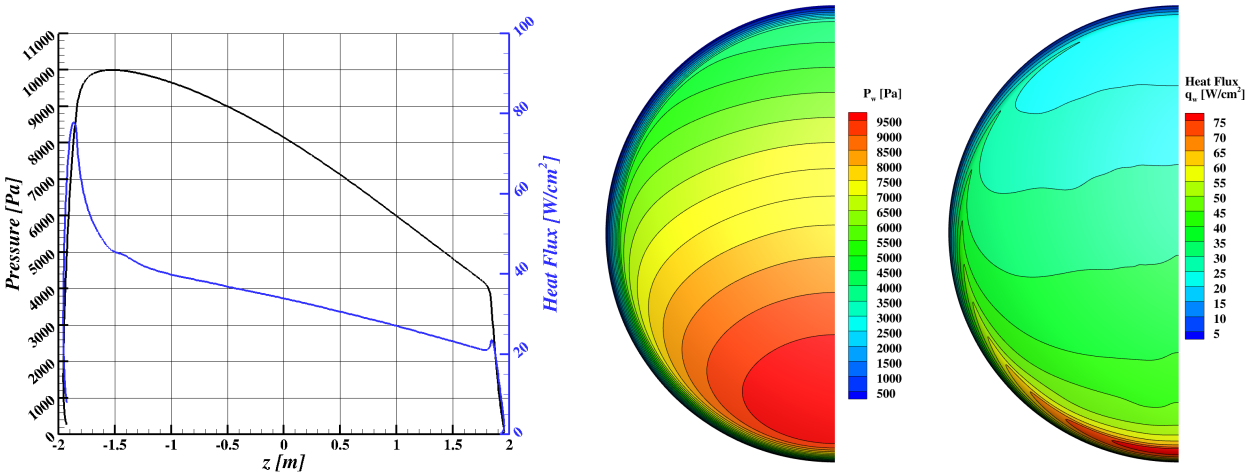

(a) Pitch plane pressure and heat flux (b) Pressure (c) Heat flux

Figure A70. Pressure and heat flux at velocity 6.0 km/s, altitude 60.0 km, and angle-of-attack 156.0 degrees.

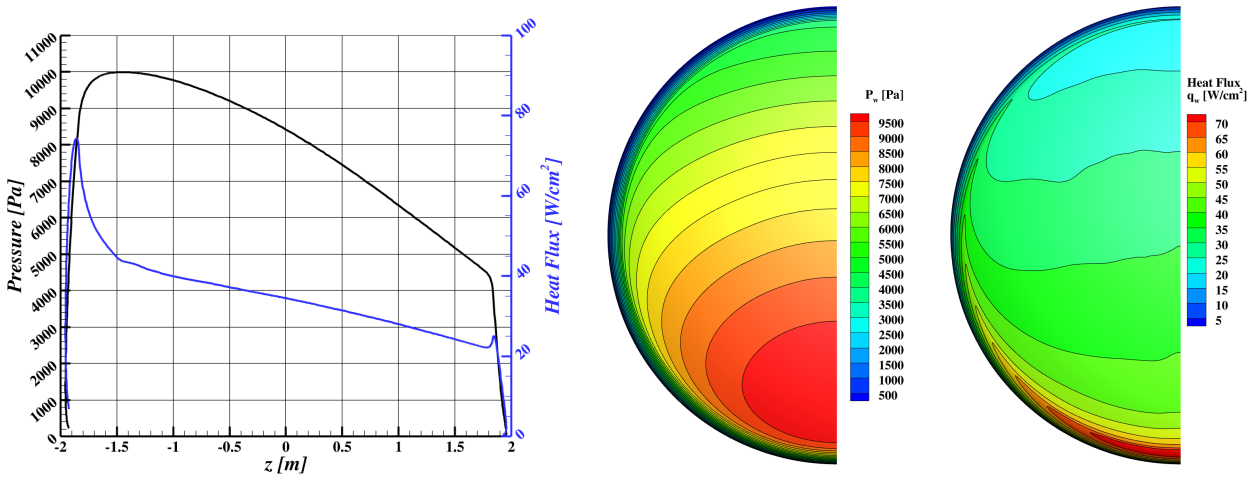

(a) Pitch plane pressure and heat flux (b) Pressure (c) Heat flux

Figure A71. Pressure and heat flux at velocity 6.0 km/s, altitude 60.0 km, and angle-of-attack 158.0 degrees.

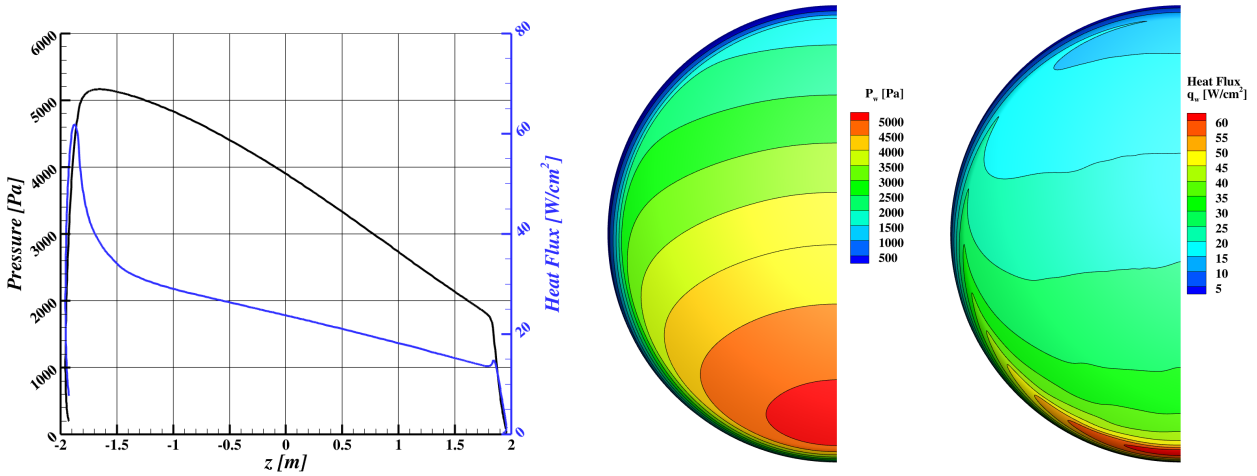

(a) Pitch plane pressure and heat flux (b) Pressure (c) Heat flux

Figure A72. Pressure and heat flux at velocity 6.0 km/s, altitude 65.0 km, and angle-of-attack 152.0 degrees.

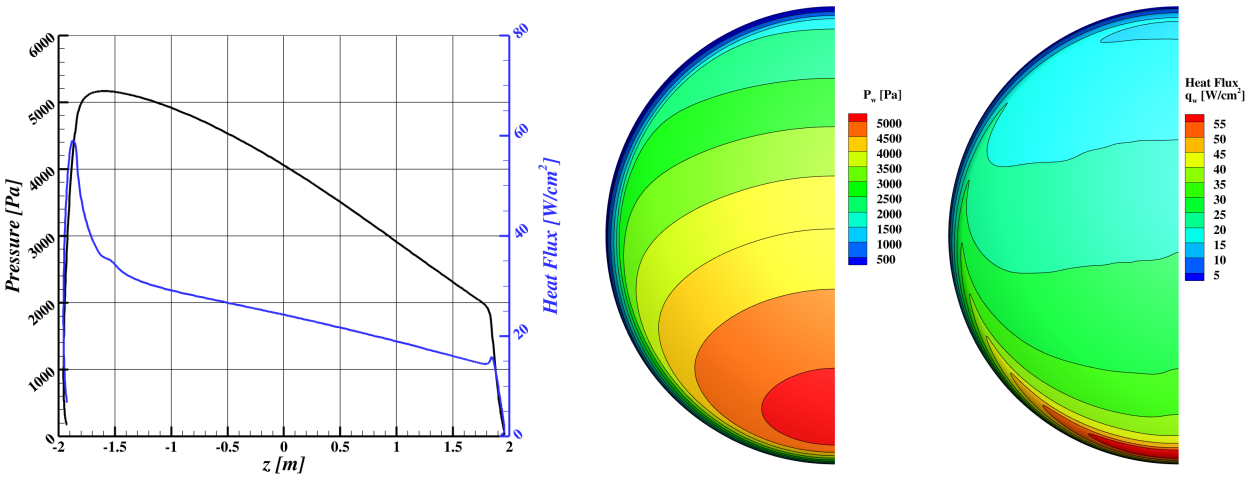

(a) Pitch plane pressure and heat flux (b) Pressure (c) Heat flux

Figure A73. Pressure and heat flux at velocity 6.0 km/s, altitude 65.0 km, and angle-of-attack 154.0 degrees.

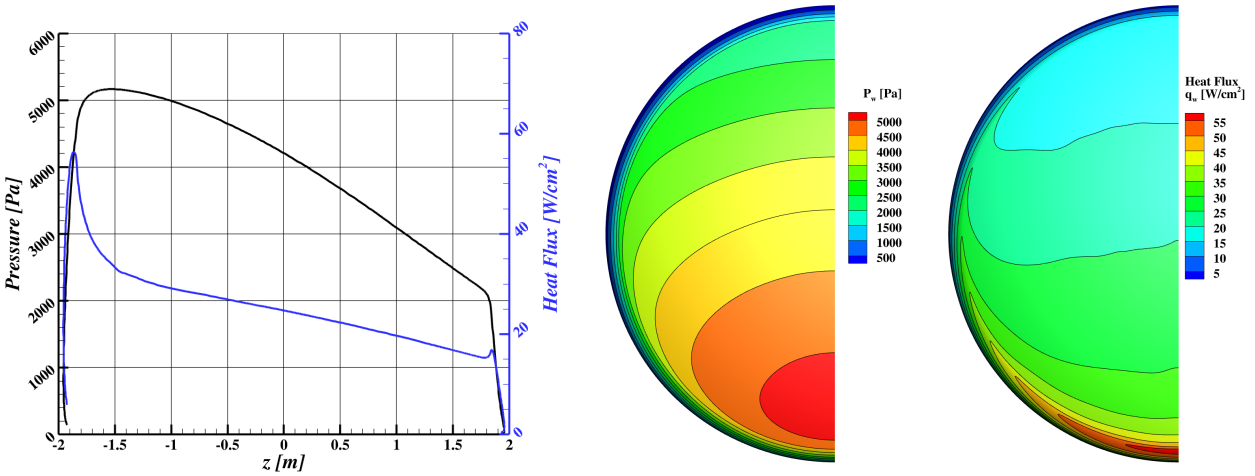

(a) Pitch plane pressure and heat flux (b) Pressure (c) Heat flux

Figure A74. Pressure and heat flux at velocity 6.0 km/s, altitude 65.0 km, and angle-of-attack 156.0 degrees.

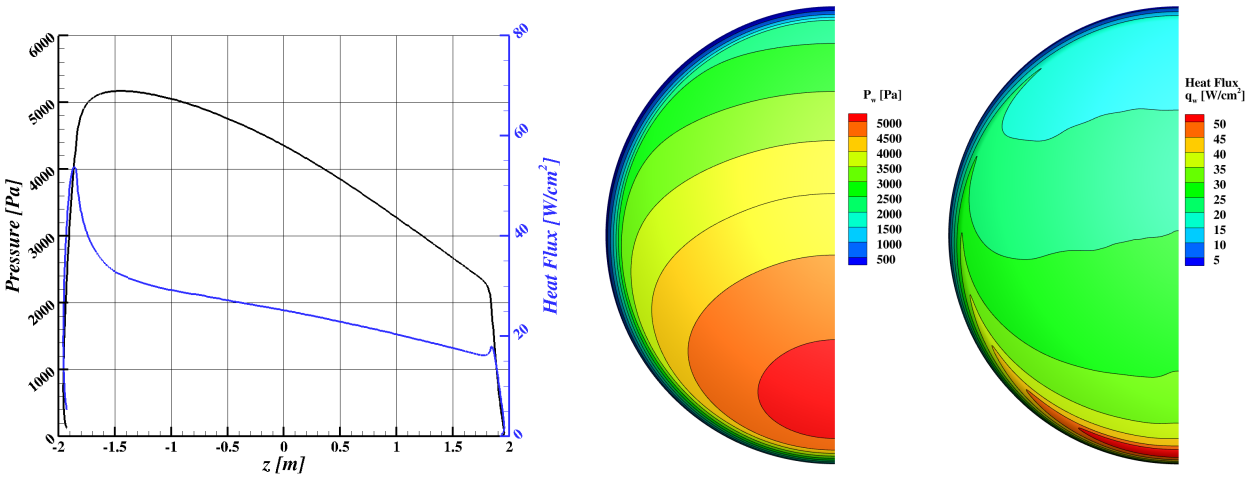

(a) Pitch plane pressure and heat flux (b) Pressure (c) Heat flux

Figure A75. Pressure and heat flux at velocity 6.0 km/s, altitude 65.0 km, and angle-of-attack 158.0 degrees.

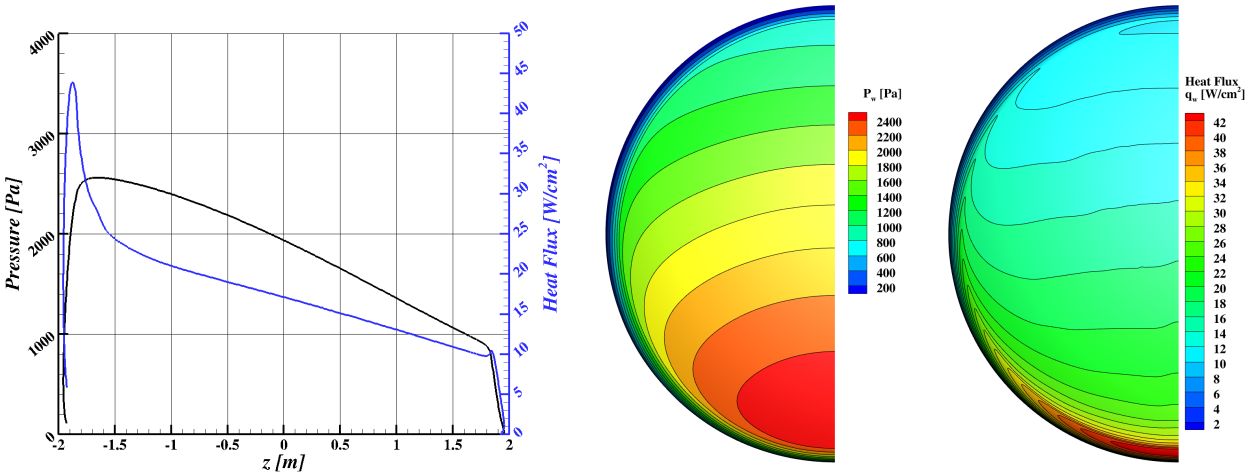

(a) Pitch plane pressure and heat flux (b) Pressure (c) Heat flux

Figure A76. Pressure and heat flux at velocity 6.0 km/s, altitude 70.0 km, and angle-of-attack 152.0 degrees.

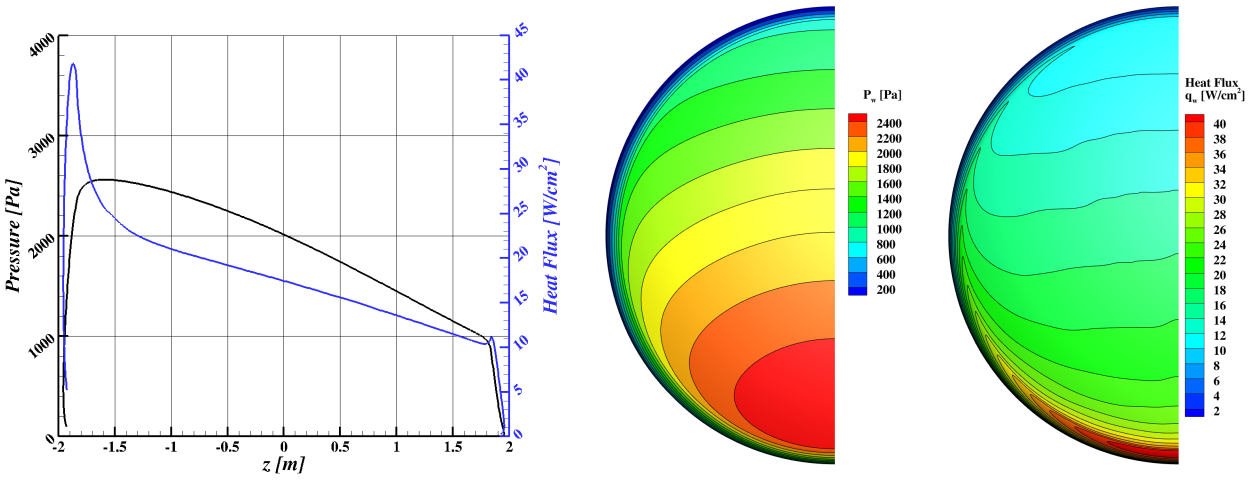

(a) Pitch plane pressure and heat flux (b) Pressure (c) Heat flux

Figure A77. Pressure and heat flux at velocity 6.0 km/s, altitude 70.0 km, and angle-of-attack 154.0 degrees.

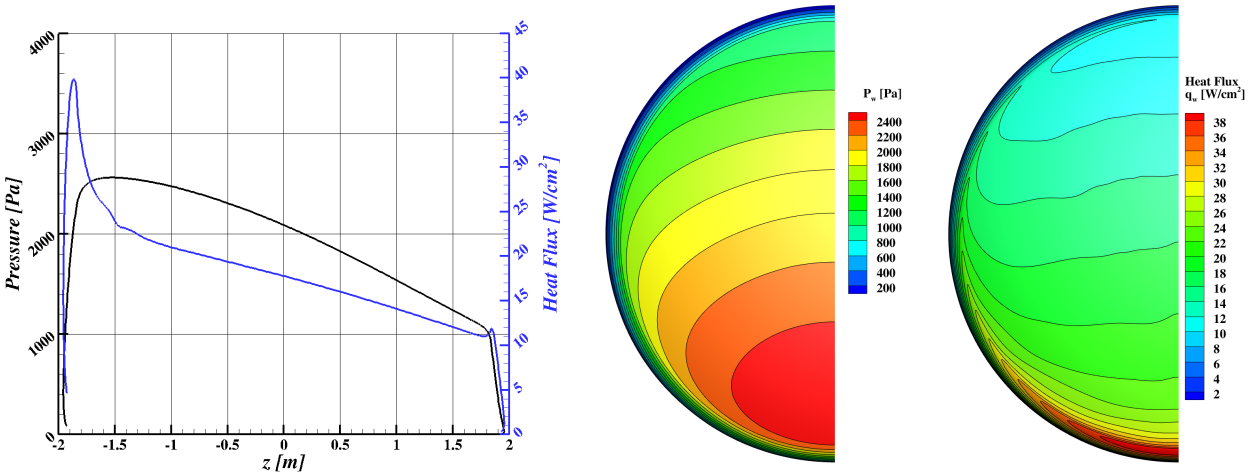

(a) Pitch plane pressure and heat flux (b) Pressure (c) Heat flux

Figure A78. Pressure and heat flux at velocity 6.0 km/s, altitude 70.0 km, and angle-of-attack 156.0 degrees.

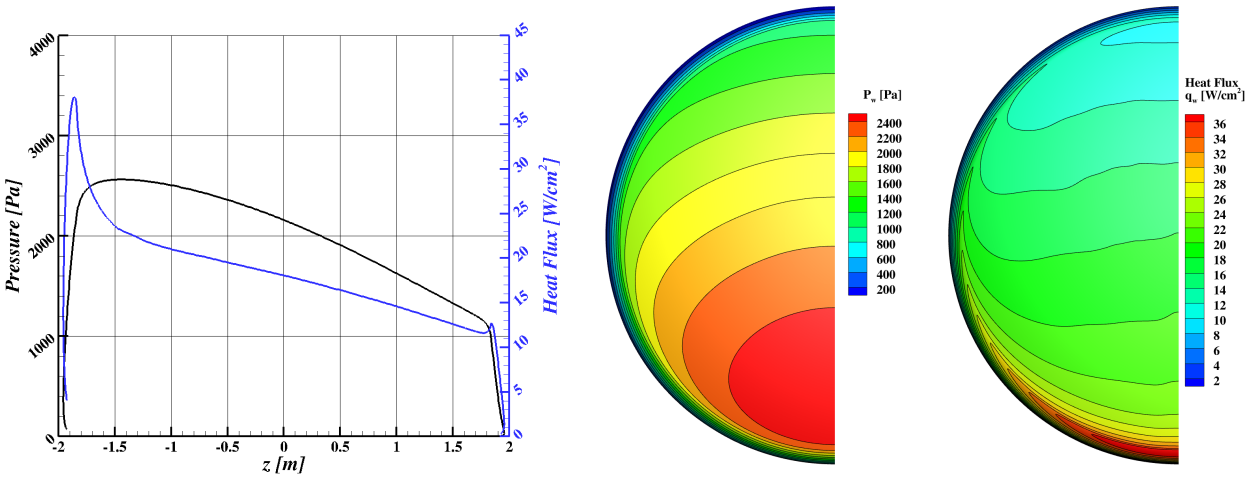

(a) Pitch plane pressure and heat flux (b) Pressure (c) Heat flux

Figure A79. Pressure and heat flux at velocity 6.0 km/s, altitude 70.0 km, and angle-of-attack 158.0 degrees.

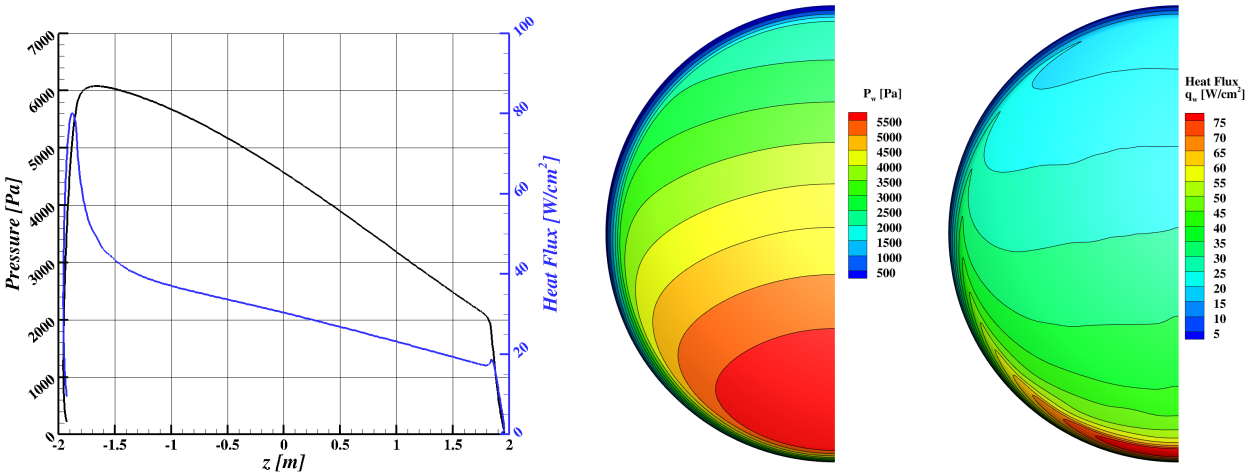

(a) Pitch plane pressure and heat flux (b) Pressure (c) Heat flux

Figure A80. Pressure and heat flux at velocity 6.5 km/s, altitude 65.0 km, and angle-of-attack 152.0 degrees.

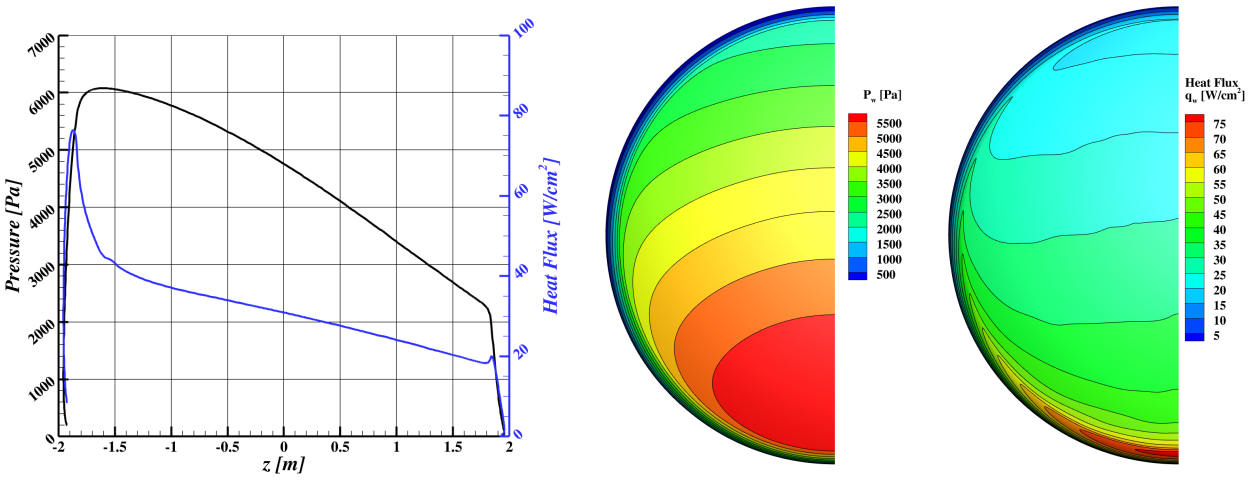

(a) Pitch plane pressure and heat flux (b) Pressure (c) Heat flux

Figure A81. Pressure and heat flux at velocity 6.5 km/s, altitude 65.0 km, and angle-of-attack 154.0 degrees.

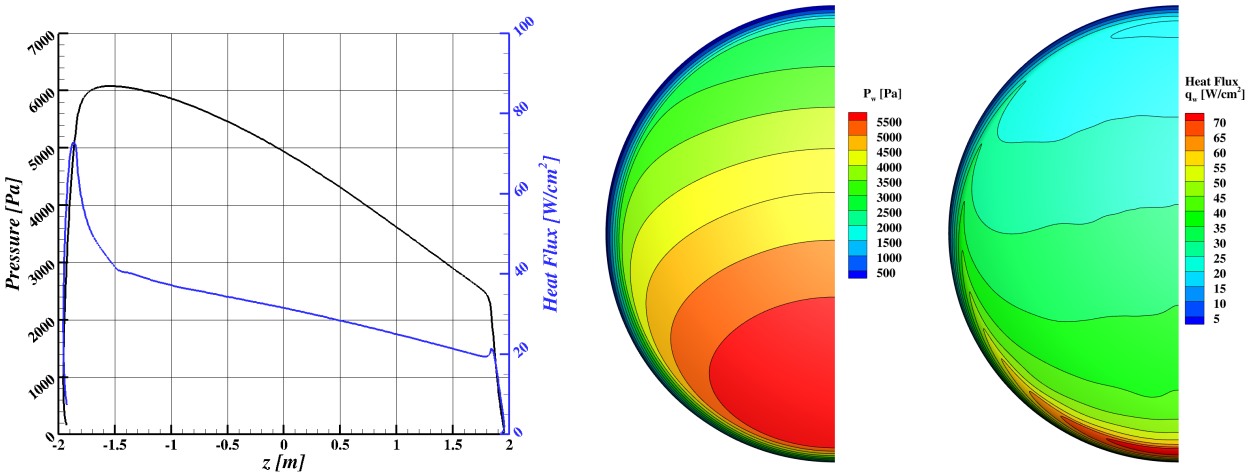

(a) Pitch plane pressure and heat flux (b) Pressure (c) Heat flux

Figure A82. Pressure and heat flux at velocity 6.5 km/s, altitude 65.0 km, and angle-of-attack 156.0 degrees.

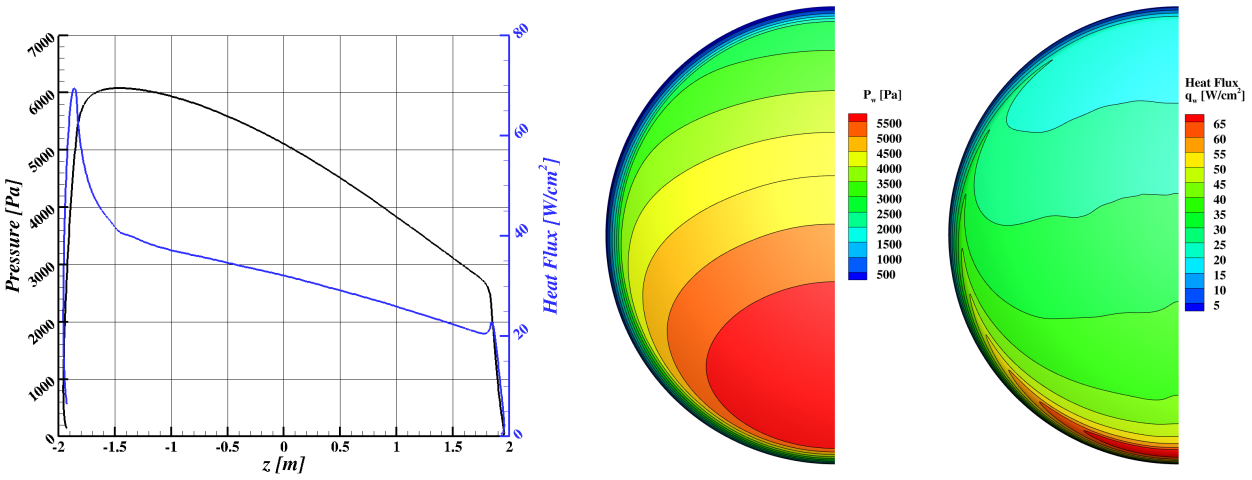

(a) Pitch plane pressure and heat flux (b) Pressure (c) Heat flux

Figure A83. Pressure and heat flux at velocity 6.5 km/s, altitude 65.0 km, and angle-of-attack 158.0 degrees.

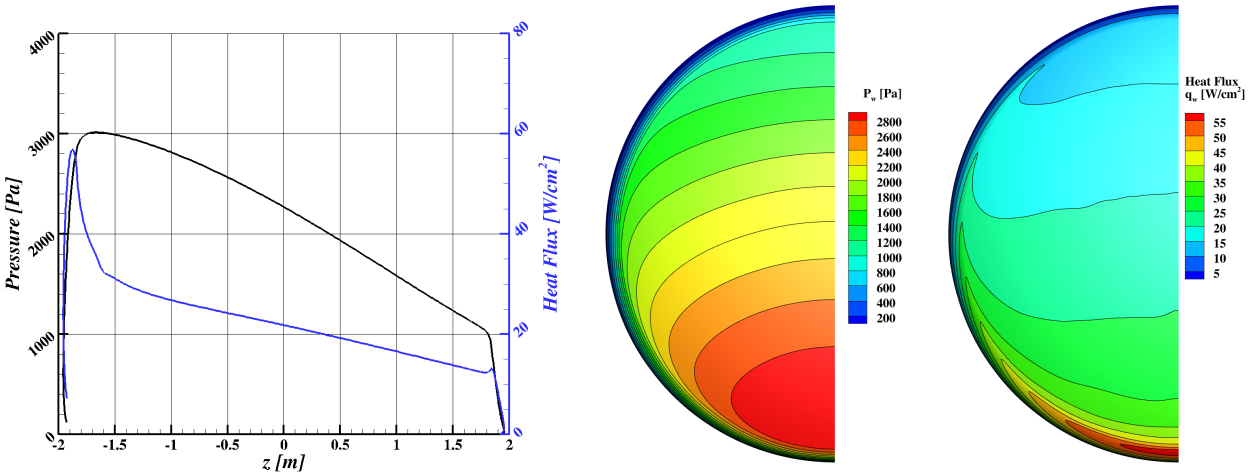

(a) Pitch plane pressure and heat flux (b) Pressure (c) Heat flux

Figure A84. Pressure and heat flux at velocity 6.5 km/s, altitude 70.0 km, and angle-of-attack 152.0 degrees.

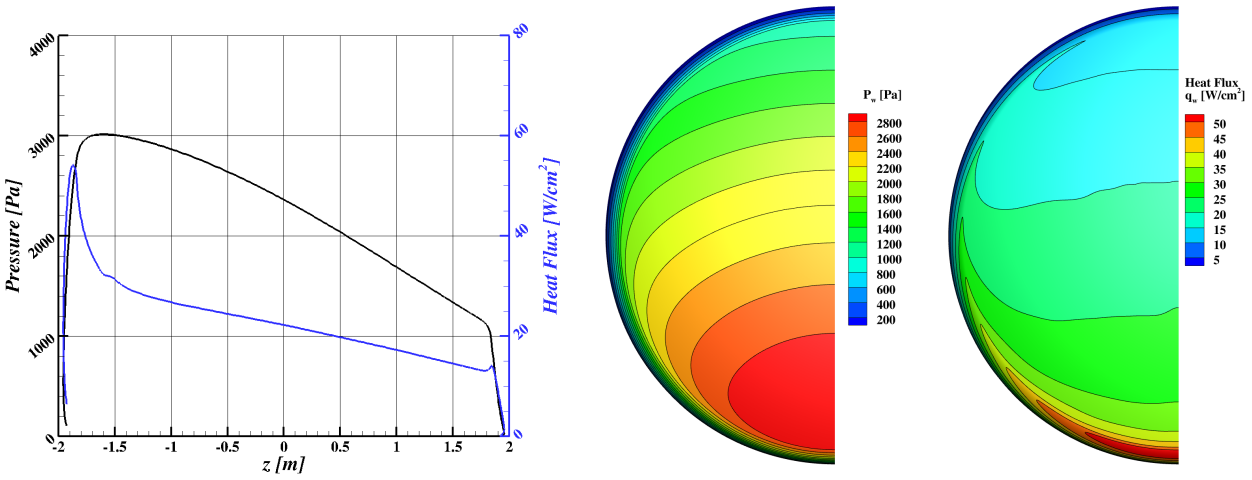

(a) Pitch plane pressure and heat flux (b) Pressure (c) Heat flux

Figure A85. Pressure and heat flux at velocity 6.5 km/s, altitude 70.0 km, and angle-of-attack 154.0 degrees.

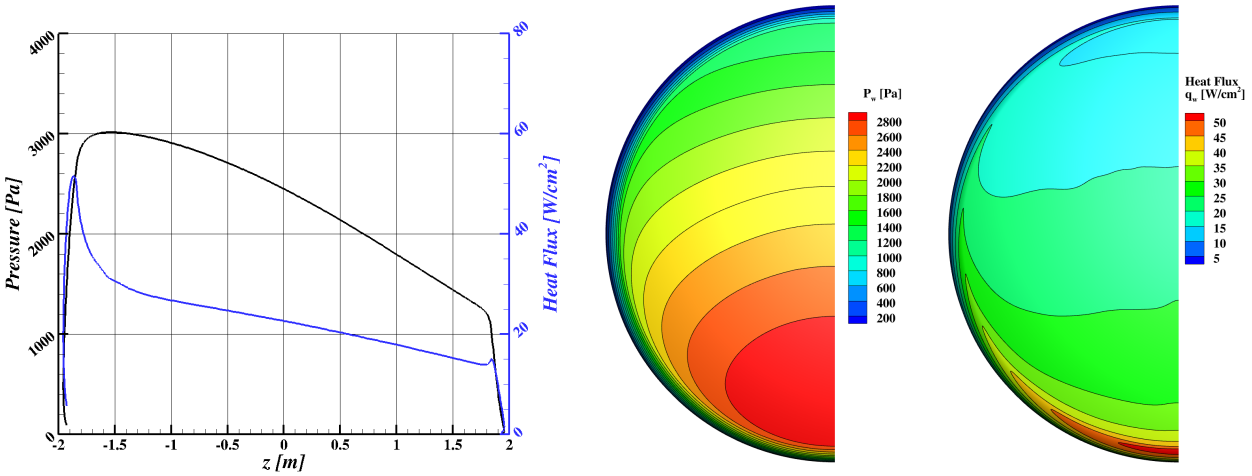

(a) Pitch plane pressure and heat flux (b) Pressure (c) Heat flux

Figure A86. Pressure and heat flux at velocity 6.5 km/s, altitude 70.0 km, and angle-of-attack 156.0 degrees.

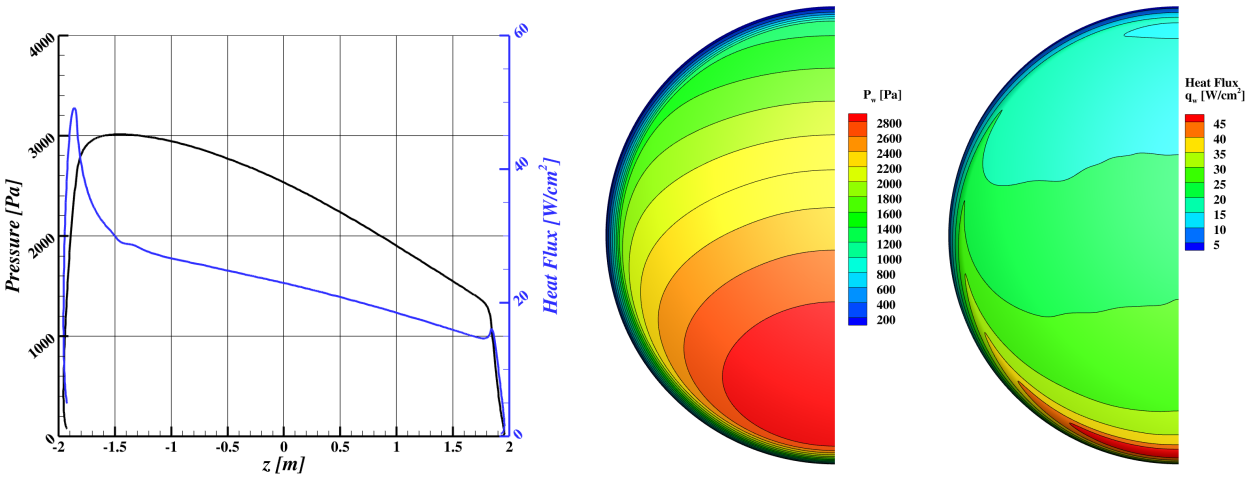

(a) Pitch plane pressure and heat flux (b) Pressure (c) Heat flux

Figure A87. Pressure and heat flux at velocity 6.5 km/s, altitude 70.0 km, and angle-of-attack 158.0 degrees.

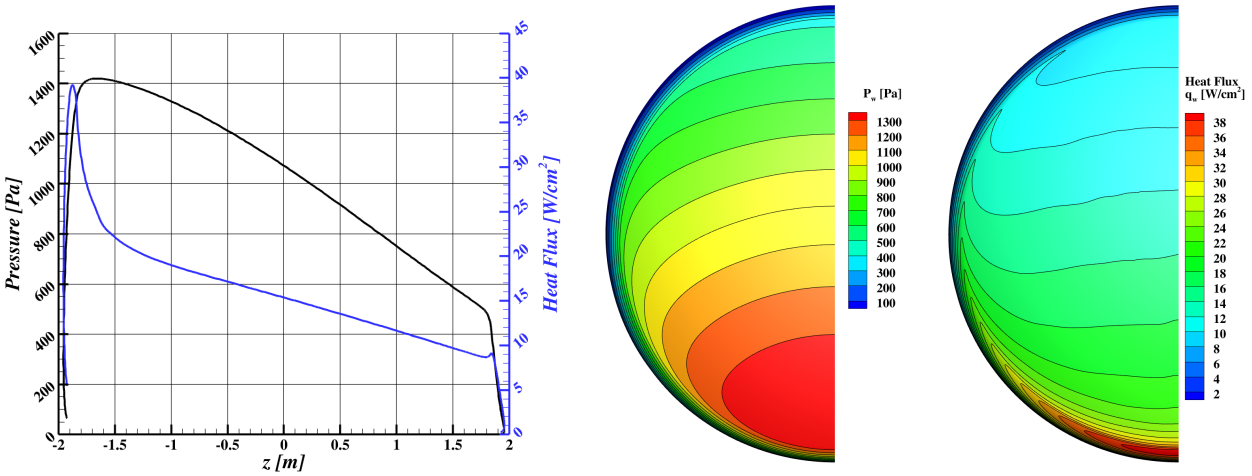

(a) Pitch plane pressure and heat flux (b) Pressure (c) Heat flux

Figure A88. Pressure and heat flux at velocity 6.5 km/s, altitude 75.0 km, and angle-of-attack 152.0 degrees.

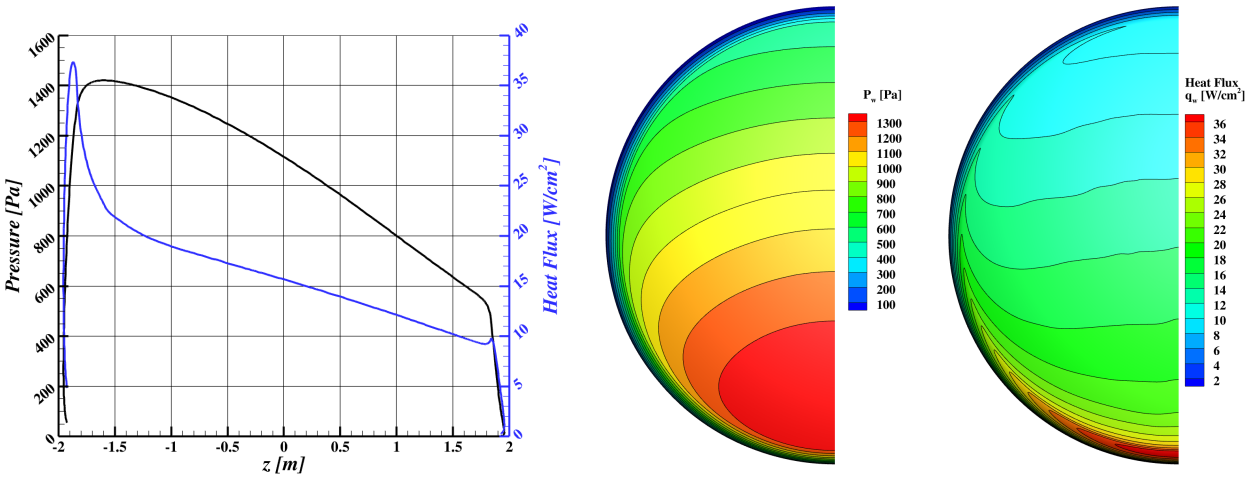

(a) Pitch plane pressure and heat flux (b) Pressure (c) Heat flux

Figure A89. Pressure and heat flux at velocity 6.5 km/s, altitude 75.0 km, and angle-of-attack 154.0 degrees.

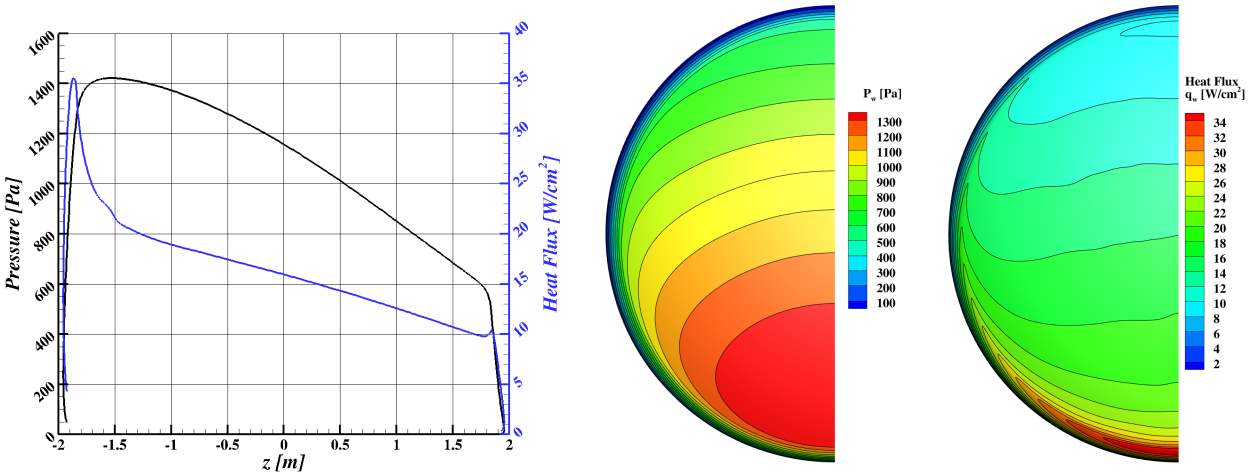

(a) Pitch plane pressure and heat flux (b) Pressure (c) Heat flux

Figure A90. Pressure and heat flux at velocity 6.5 km/s, altitude 75.0 km, and angle-of-attack 156.0 degrees.

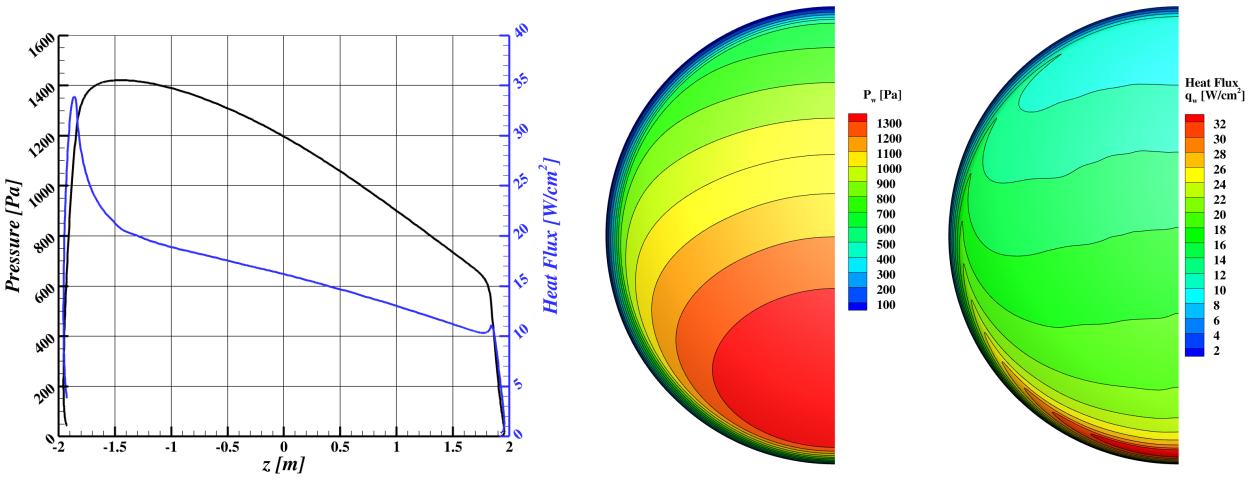

(a) Pitch plane pressure and heat flux (b) Pressure (c) Heat flux

Figure A91. Pressure and heat flux at velocity 6.5 km/s, altitude 75.0 km, and angle-of-attack 158.0 degrees.

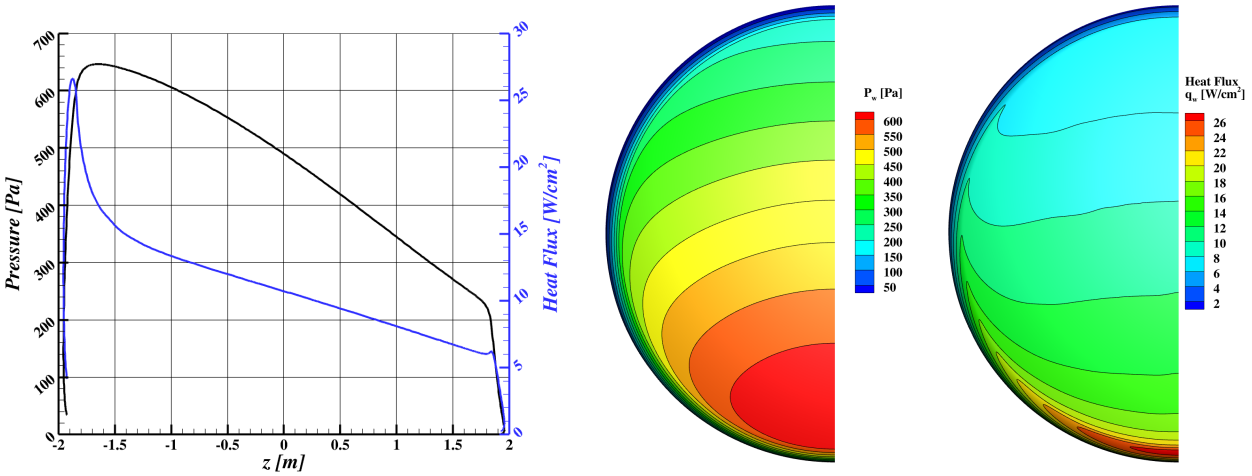

(a) Pitch plane pressure and heat flux (b) Pressure (c) Heat flux

Figure A92. Pressure and heat flux at velocity 6.5 km/s, altitude 80.0 km, and angle-of-attack 152.0 degrees.

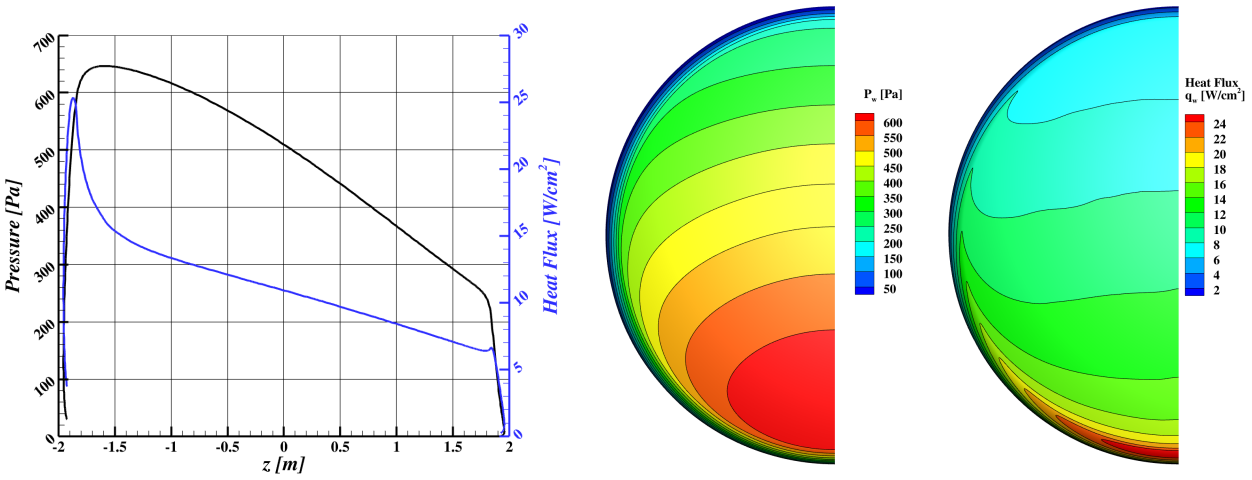

(a) Pitch plane pressure and heat flux (b) Pressure (c) Heat flux

Figure A93. Pressure and heat flux at velocity 6.5 km/s, altitude 80.0 km, and angle-of-attack 154.0 degrees.

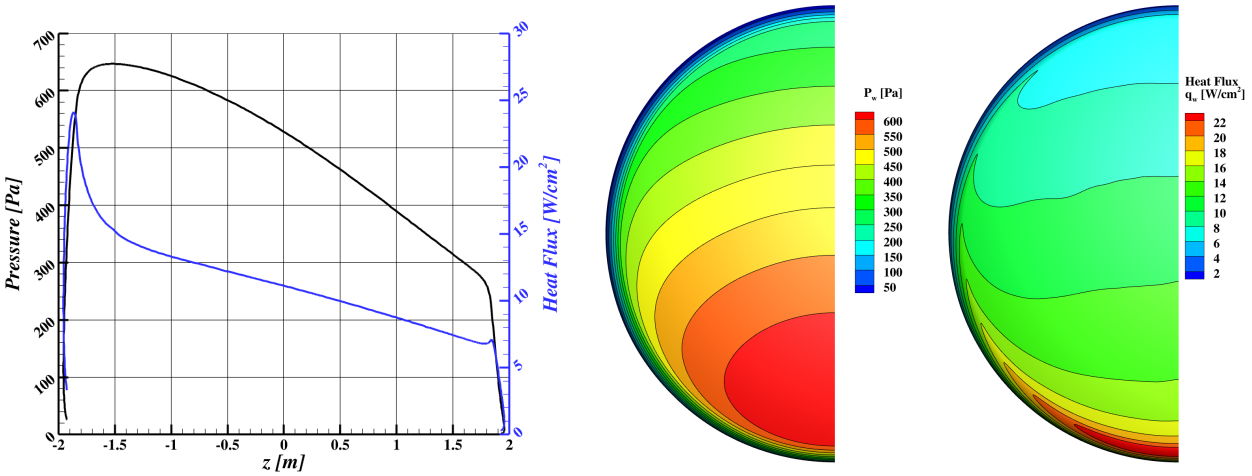

(a) Pitch plane pressure and heat flux (b) Pressure (c) Heat flux

Figure A94. Pressure and heat flux at velocity 6.5 km/s, altitude 80.0 km, and angle-of-attack 156.0 degrees.

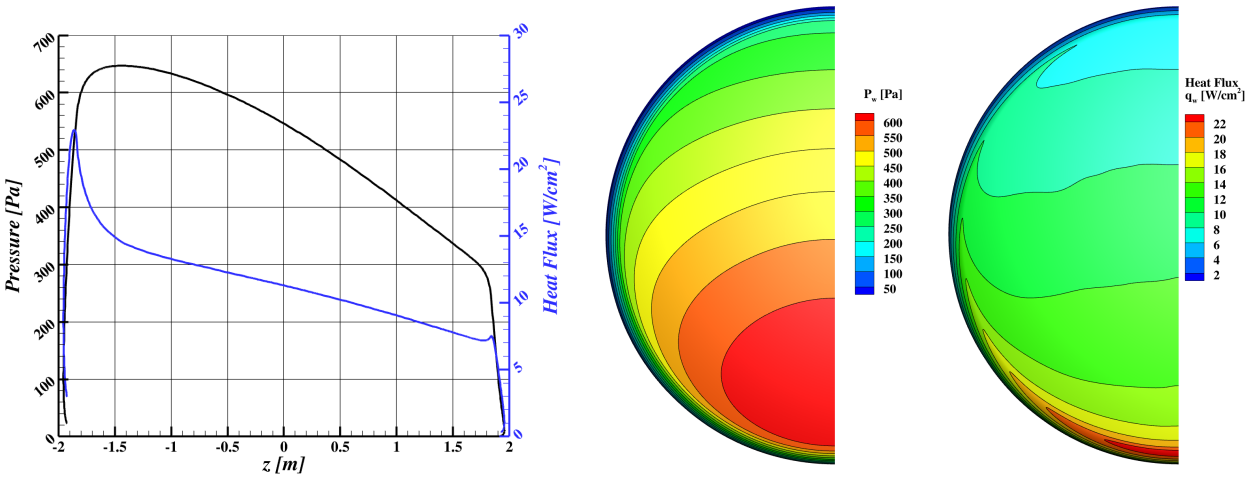

(a) Pitch plane pressure and heat flux (b) Pressure (c) Heat flux

Figure A95. Pressure and heat flux at velocity 6.5 km/s, altitude 80.0 km, and angle-of-attack 158.0 degrees.

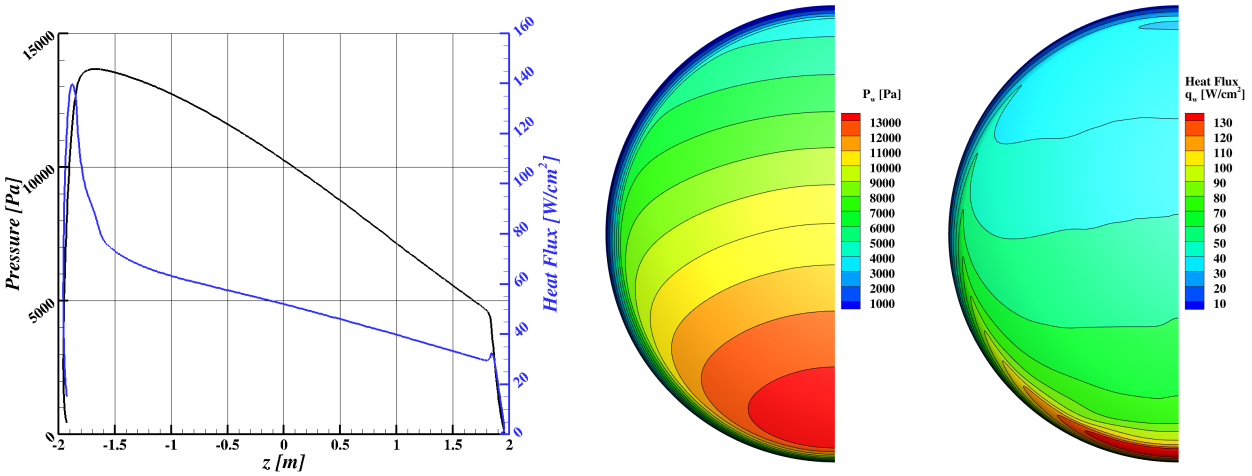

(a) Pitch plane pressure and heat flux (b) Pressure (c) Heat flux

Figure A96. Pressure and heat flux at velocity 7.0 km/s, altitude 60.0 km, and angle-of-attack 152.0 degrees.

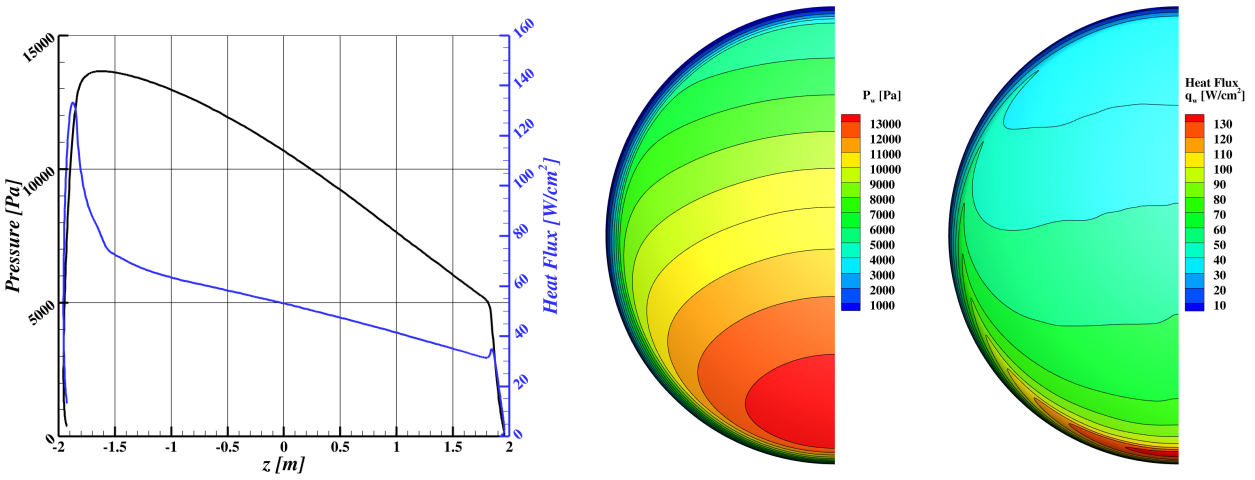

(a) Pitch plane pressure and heat flux (b) Pressure (c) Heat flux

Figure A97. Pressure and heat flux at velocity 7.0 km/s, altitude 60.0 km, and angle-of-attack 154.0 degrees.

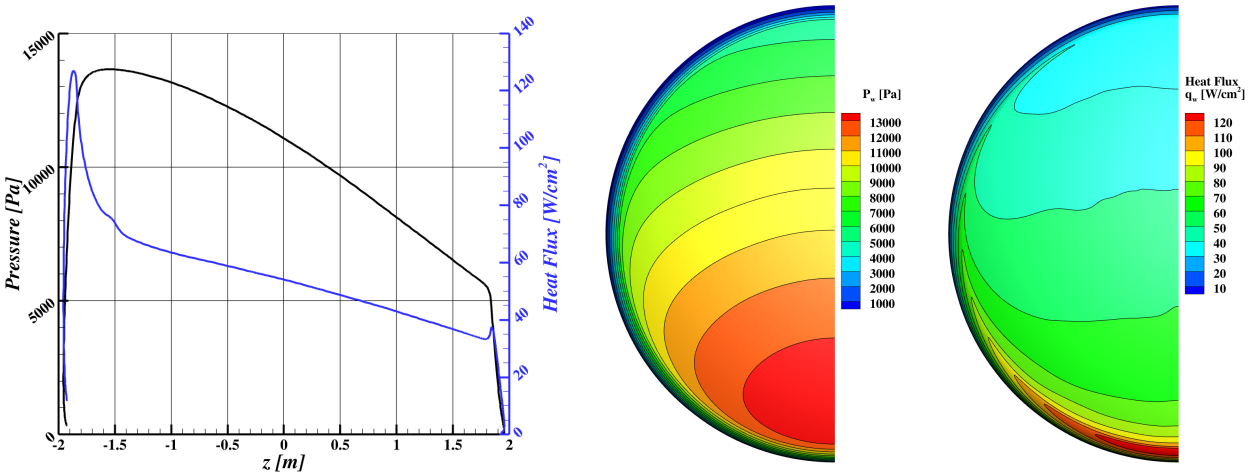

(a) Pitch plane pressure and heat flux (b) Pressure (c) Heat flux

Figure A98. Pressure and heat flux at velocity 7.0 km/s, altitude 60.0 km, and angle-of-attack 156.0 degrees.

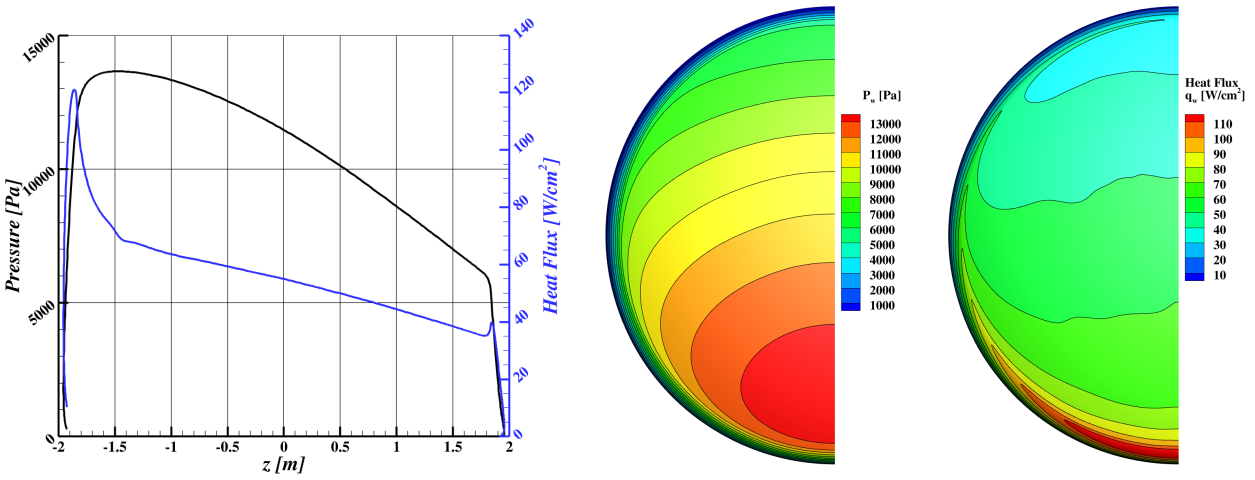

(a) Pitch plane pressure and heat flux (b) Pressure (c) Heat flux

Figure A99. Pressure and heat flux at velocity 7.0 km/s, altitude 60.0 km, and angle-of-attack 158.0 degrees.

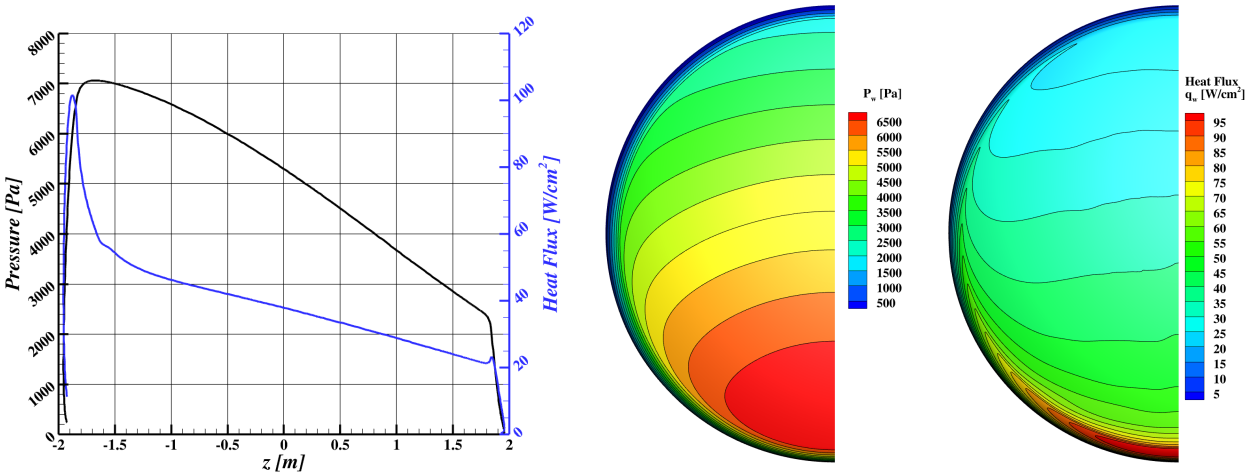

(a) Pitch plane pressure and heat flux (b) Pressure (c) Heat flux

Figure A100. Pressure and heat flux at velocity 7.0 km/s, altitude 65.0 km, and angle-of-attack 152.0 degrees.

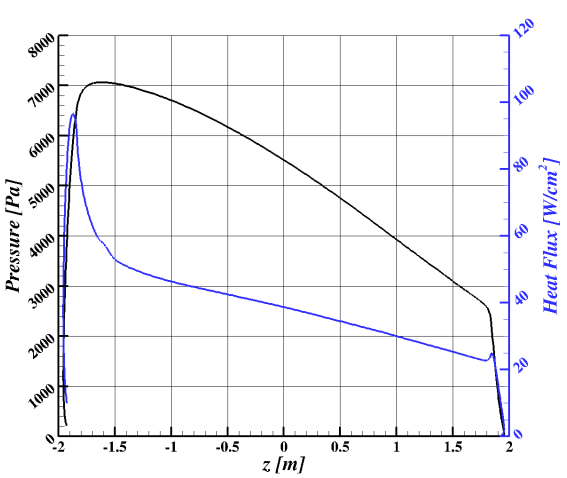

(a) Pitch plane pressure and heat flux

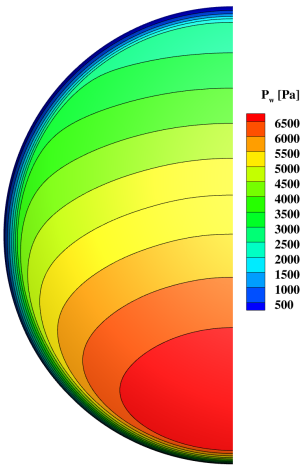

(b) Pressure

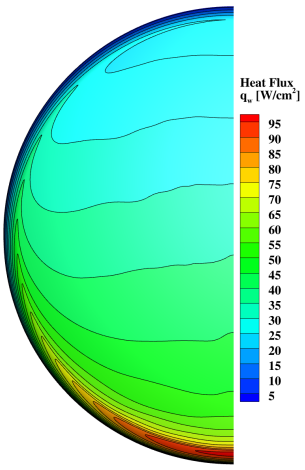

(c) Heat flux

Figure A101. Pressure and heat flux at velocity 7.0 km/s, altitude 65.0 km, and angle-of-attack 154.0 degrees.

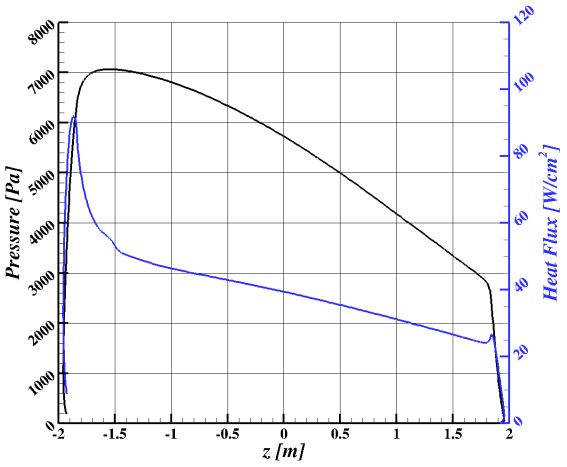

(a) Pitch plane pressure and heat flux

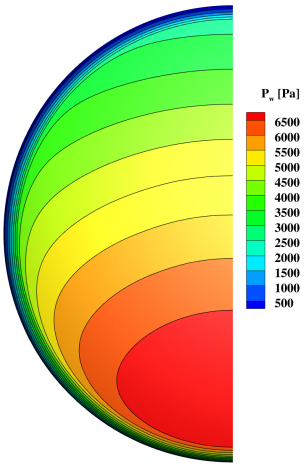

(b) Pressure

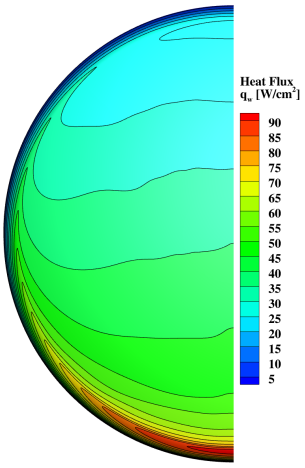

(c) Heat flux

Figure A102. Pressure and heat flux at velocity 7.0 km/s, altitude 65.0 km, and angle-of-attack 156.0 degrees.

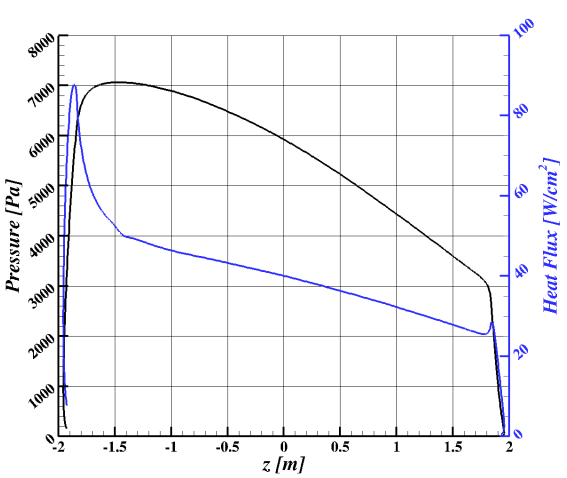

(a) Pitch plane pressure and heat flux

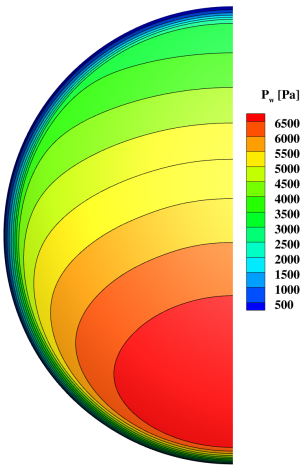

(b) Pressure

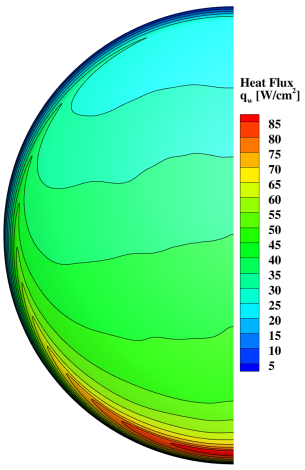

(c) Heat flux

Figure A103. Pressure and heat flux at velocity 7.0 km/s, altitude 65.0 km, and angle-of-attack 158.0 degrees.

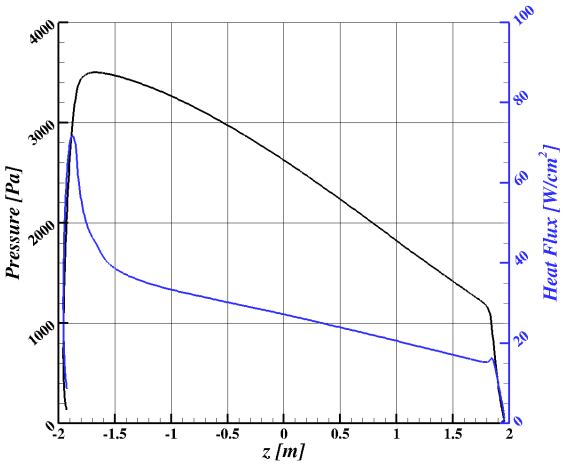

(a) Pitch plane pressure and heat flux

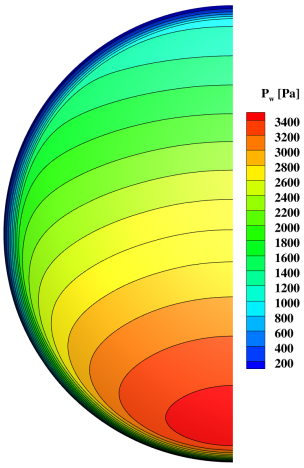

(b) Pressure

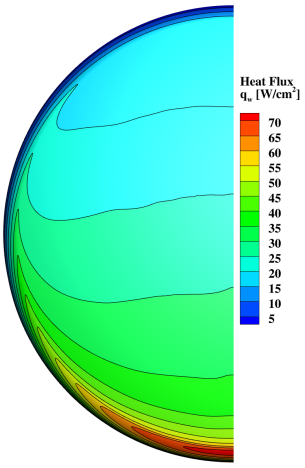

(c) Heat flux

Figure A104. Pressure and heat flux at velocity 7.0 km/s, altitude 70.0 km, and angle-of-attack 152.0 degrees.

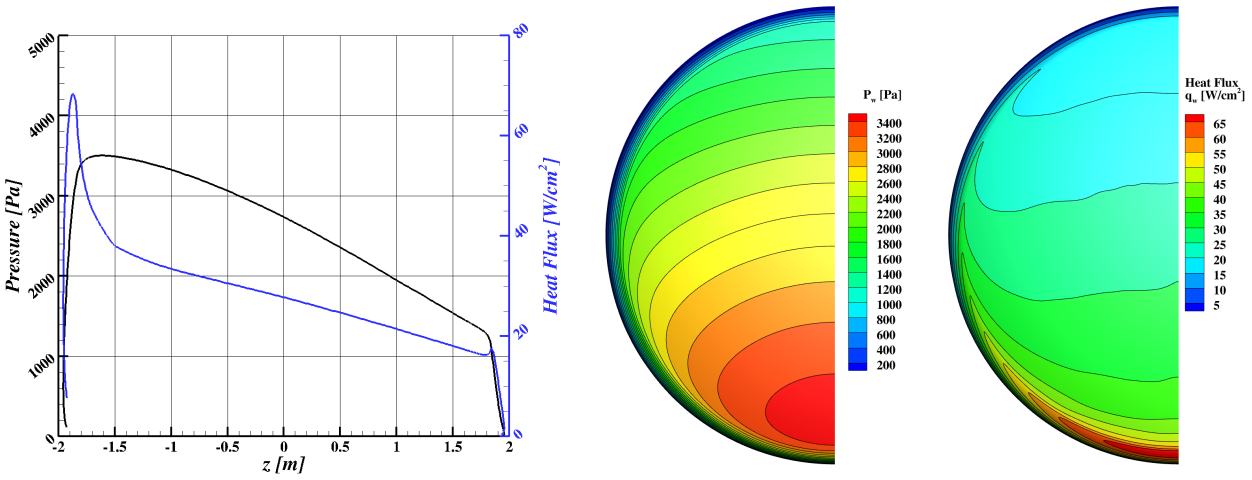

(a) Pitch plane pressure and heat flux (b) Pressure (c) Heat flux

Figure A105. Pressure and heat flux at velocity 7.0 km/s, altitude 70.0 km, and angle-of-attack 154.0 degrees.

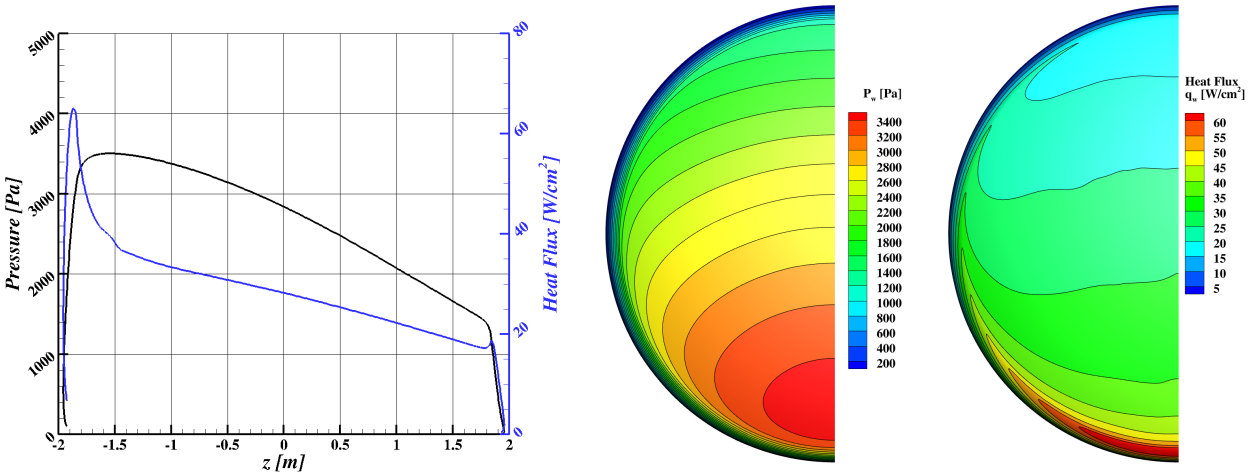

(a) Pitch plane pressure and heat flux (b) Pressure (c) Heat flux

Figure A106. Pressure and heat flux at velocity 7.0 km/s, altitude 70.0 km, and angle-of-attack 156.0 degrees.

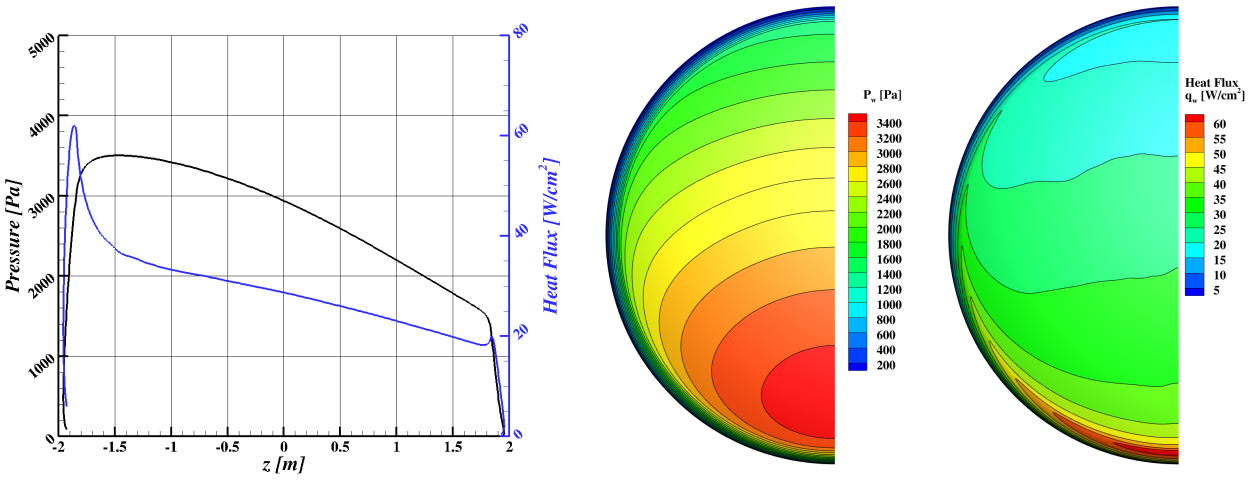

(a) Pitch plane pressure and heat flux (b) Pressure (c) Heat flux

Figure A107. Pressure and heat flux at velocity 7.0 km/s, altitude 70.0 km, and angle-of-attack 158.0 degrees.

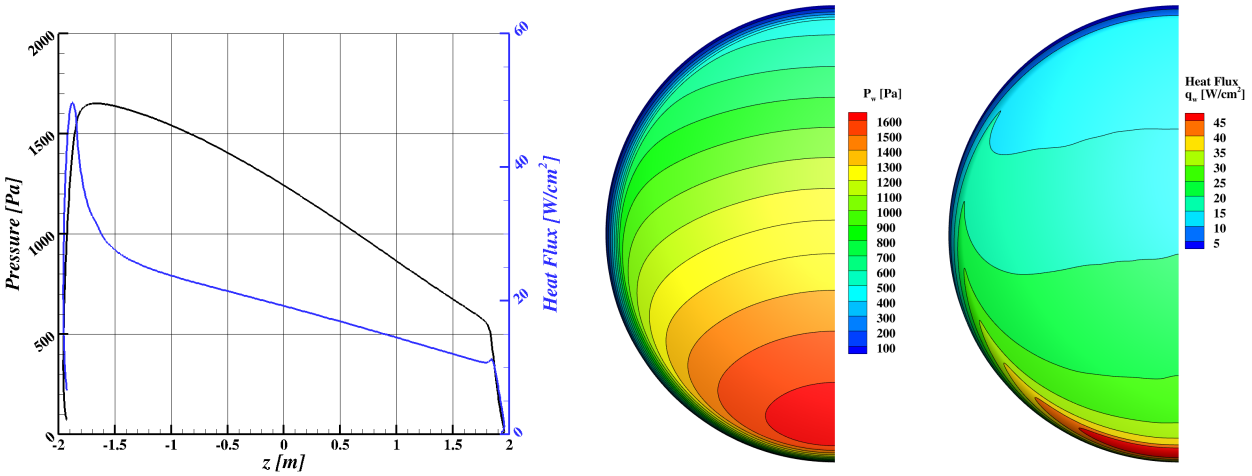

(a) Pitch plane pressure and heat flux (b) Pressure (c) Heat flux

Figure A108. Pressure and heat flux at velocity 7.0 km/s, altitude 75.0 km, and angle-of-attack 152.0 degrees.

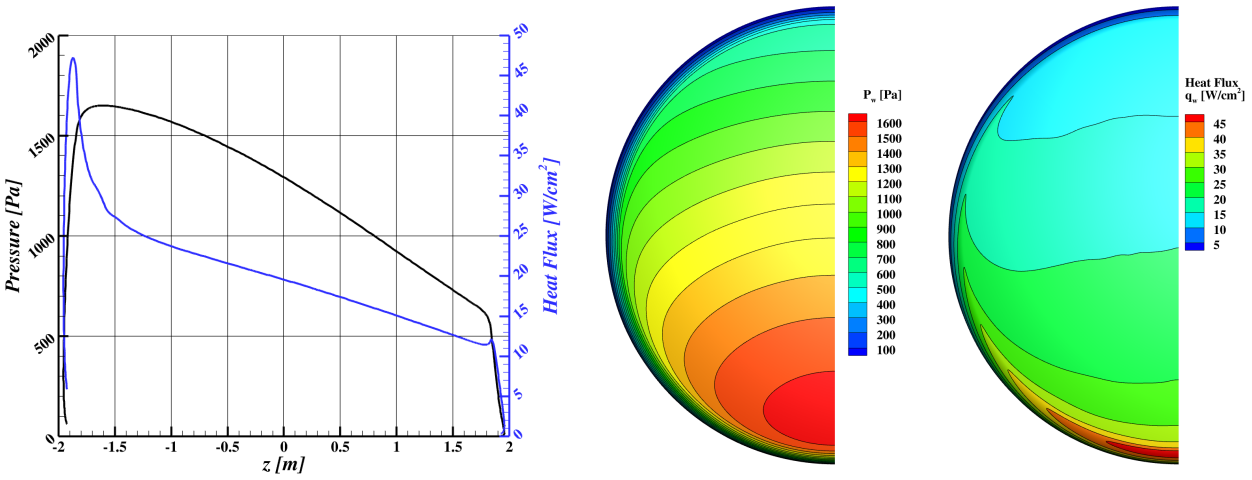

(a) Pitch plane pressure and heat flux (b) Pressure (c) Heat flux

Figure A109. Pressure and heat flux at velocity 7.0 km/s, altitude 75.0 km, and angle-of-attack 154.0 degrees.

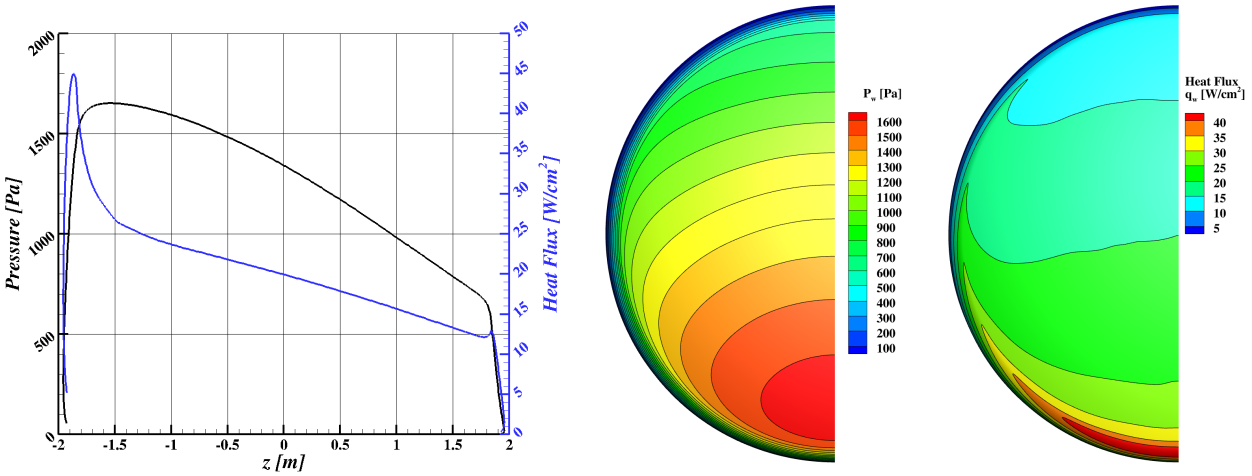

(a) Pitch plane pressure and heat flux (b) Pressure (c) Heat flux

Figure A110. Pressure and heat flux at velocity 7.0 km/s, altitude 75.0 km, and angle-of-attack 156.0 degrees.

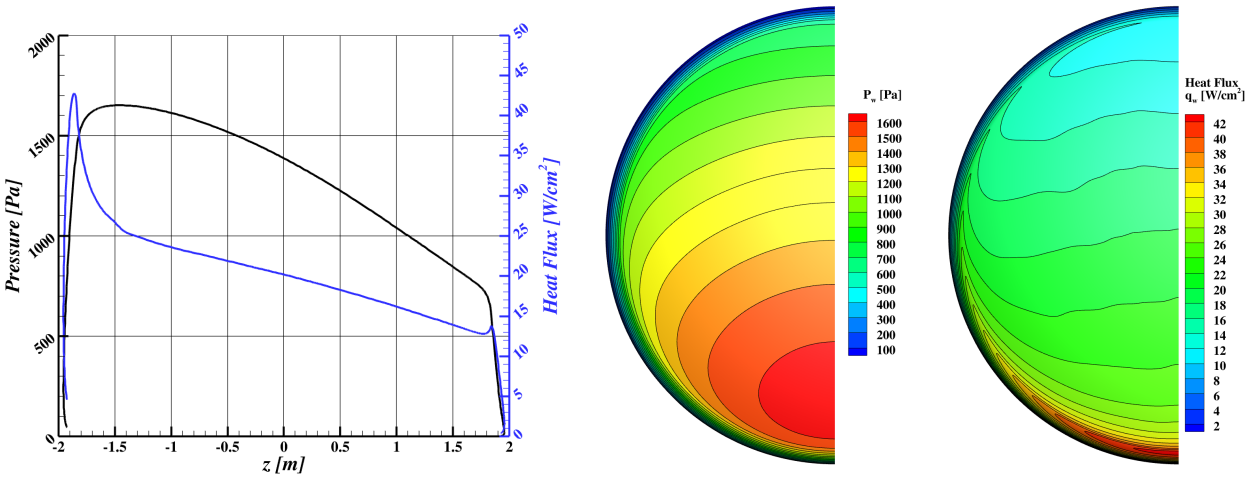

(a) Pitch plane pressure and heat flux (b) Pressure (c) Heat flux

Figure A111. Pressure and heat flux at velocity 7.0 km/s, altitude 75.0 km, and angle-of-attack 158.0 degrees.

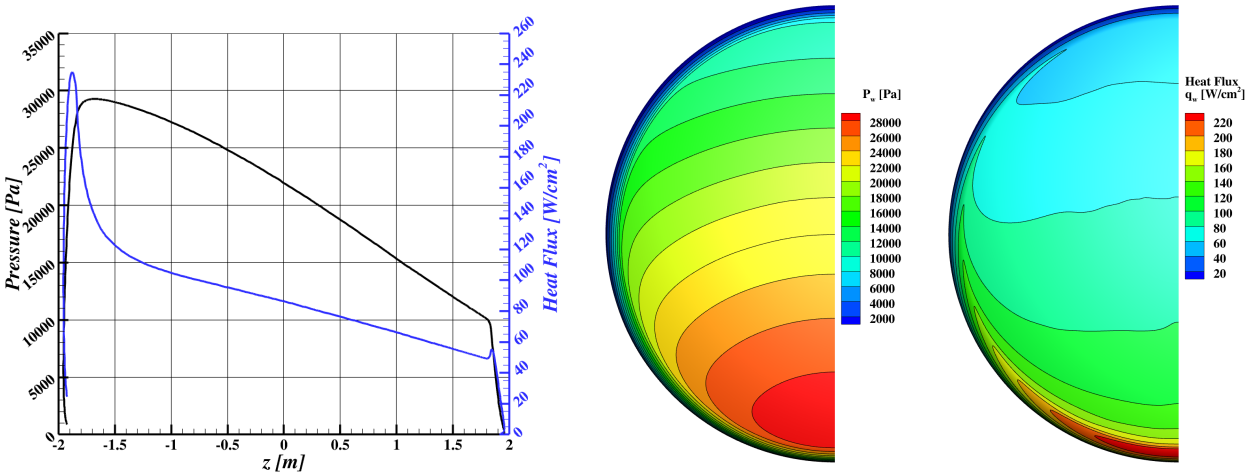

(a) Pitch plane pressure and heat flux (b) Pressure (c) Heat flux

Figure A112. Pressure and heat flux at velocity 7.5 km/s, altitude 55.0 km, and angle-of-attack 152.0 degrees.

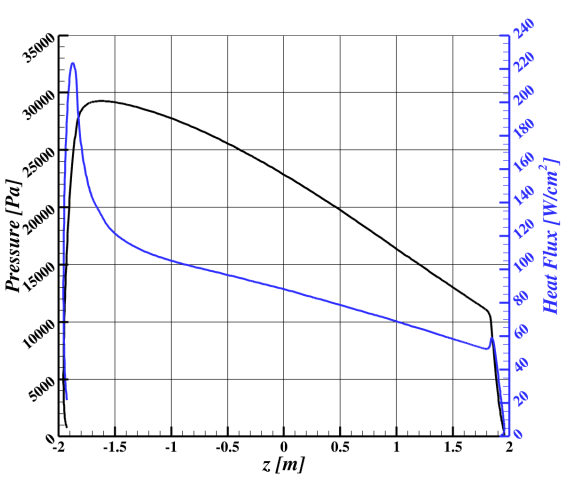

(a) Pitch plane pressure and heat flux

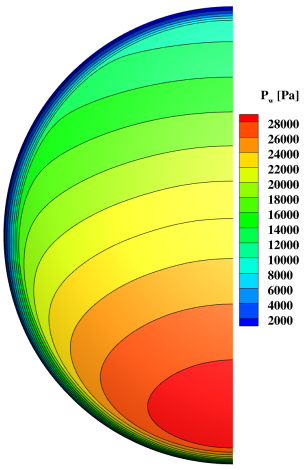

(b) Pressure

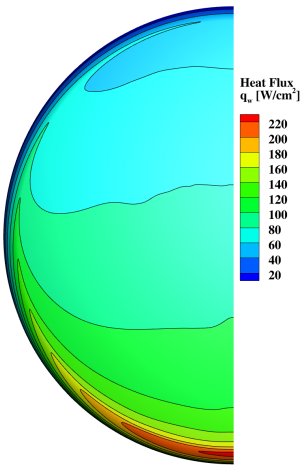

(c) Heat flux

Figure A113. Pressure and heat flux at velocity 7.5 km/s, altitude 55.0 km, and angle-of-attack 154.0 degrees.

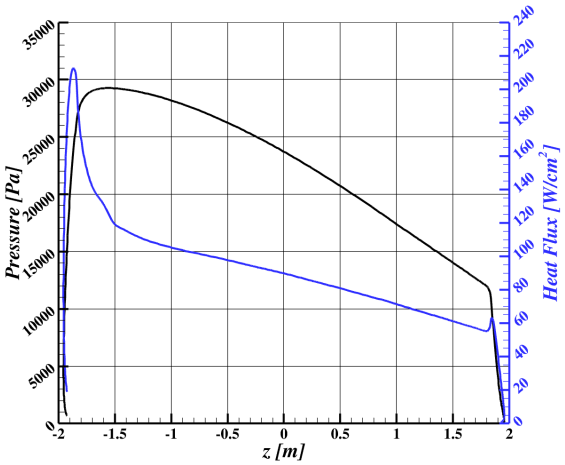

(a) Pitch plane pressure and heat flux

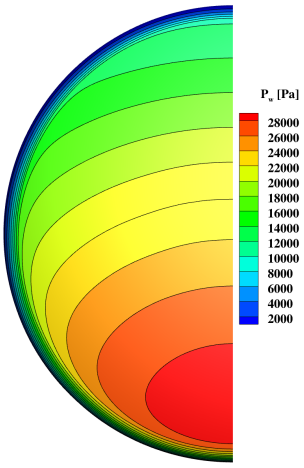

(b) Pressure

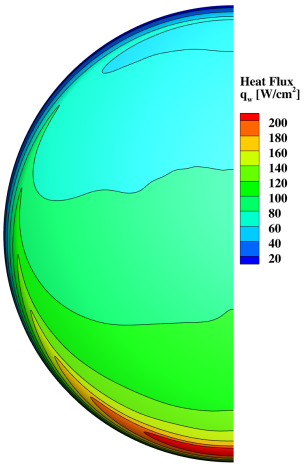

(c) Heat flux

Figure A114. Pressure and heat flux at velocity 7.5 km/s, altitude 55.0 km, and angle-of-attack 156.0 degrees.

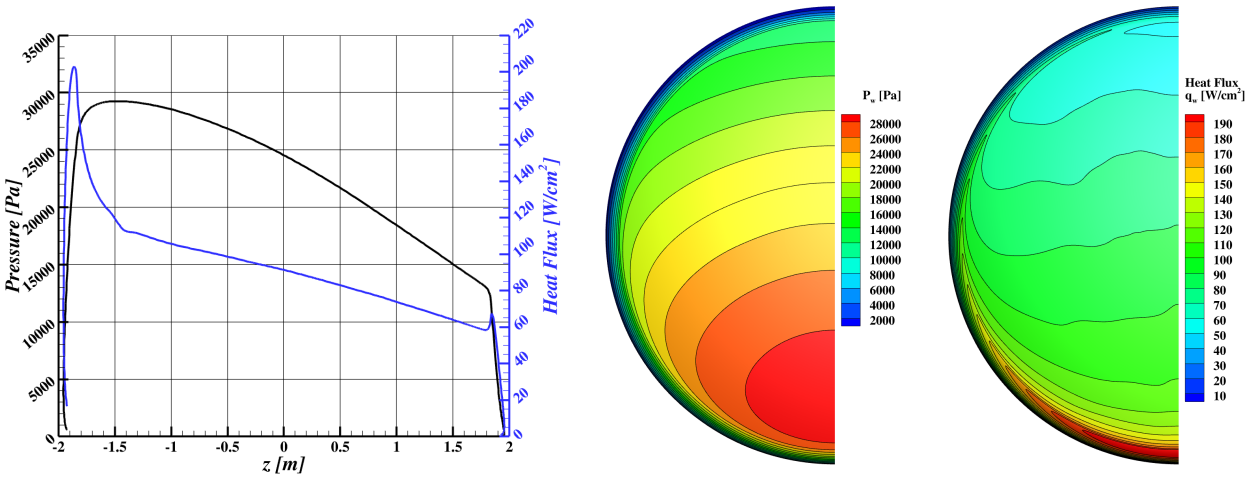

(a) Pitch plane pressure and heat flux (b) Pressure (c) Heat flux

Figure A115. Pressure and heat flux at velocity 7.5 km/s, altitude 55.0 km, and angle-of-attack 158.0 degrees.

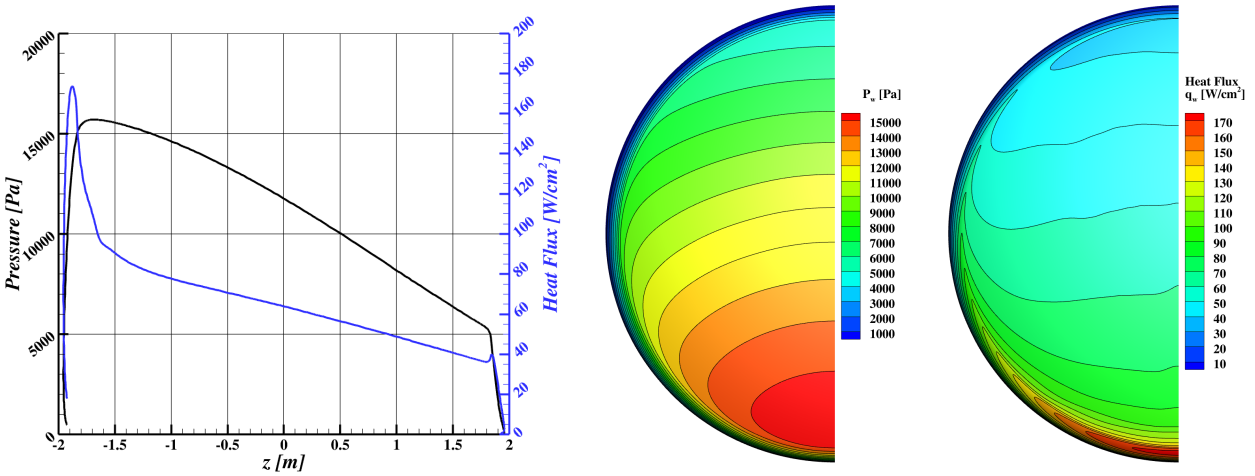

(a) Pitch plane pressure and heat flux (b) Pressure (c) Heat flux

Figure A116. Pressure and heat flux at velocity 7.5 km/s, altitude 60.0 km, and angle-of-attack 152.0 degrees.

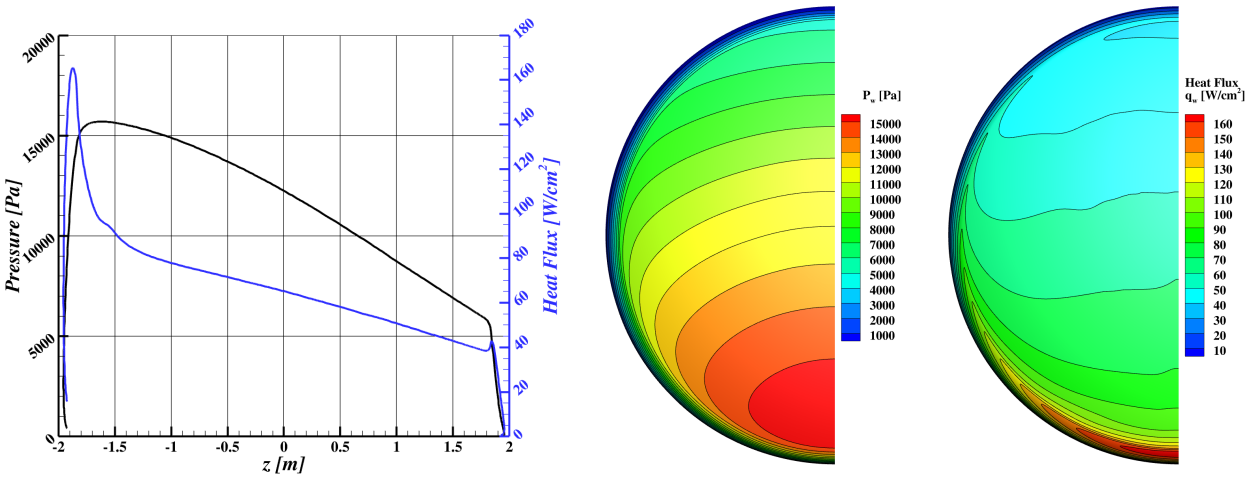

(a) Pitch plane pressure and heat flux (b) Pressure (c) Heat flux

Figure A117. Pressure and heat flux at velocity 7.5 km/s, altitude 60.0 km, and angle-of-attack 154.0 degrees.

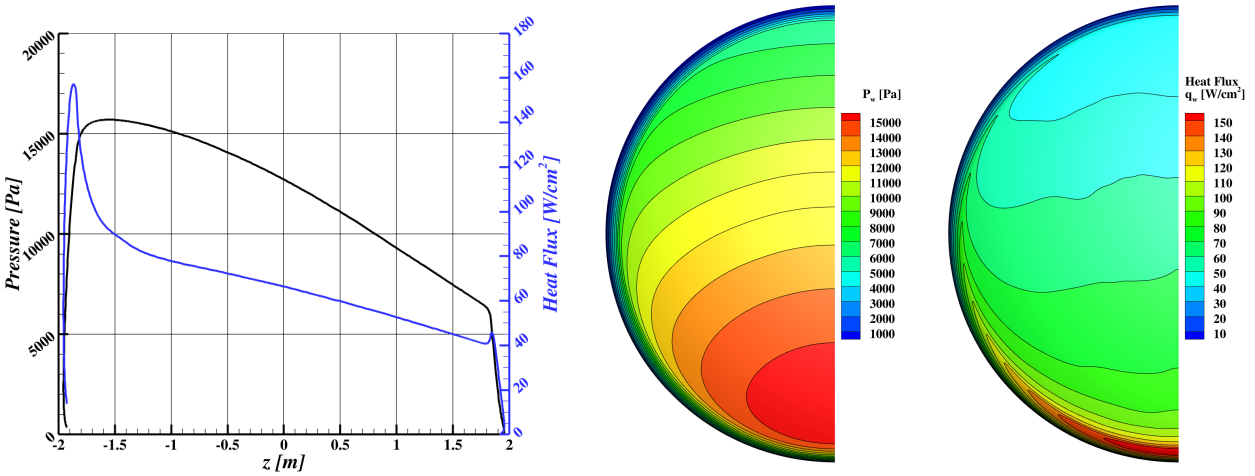

(a) Pitch plane pressure and heat flux (b) Pressure (c) Heat flux

Figure A118. Pressure and heat flux at velocity 7.5 km/s, altitude 60.0 km, and angle-of-attack 156.0 degrees.

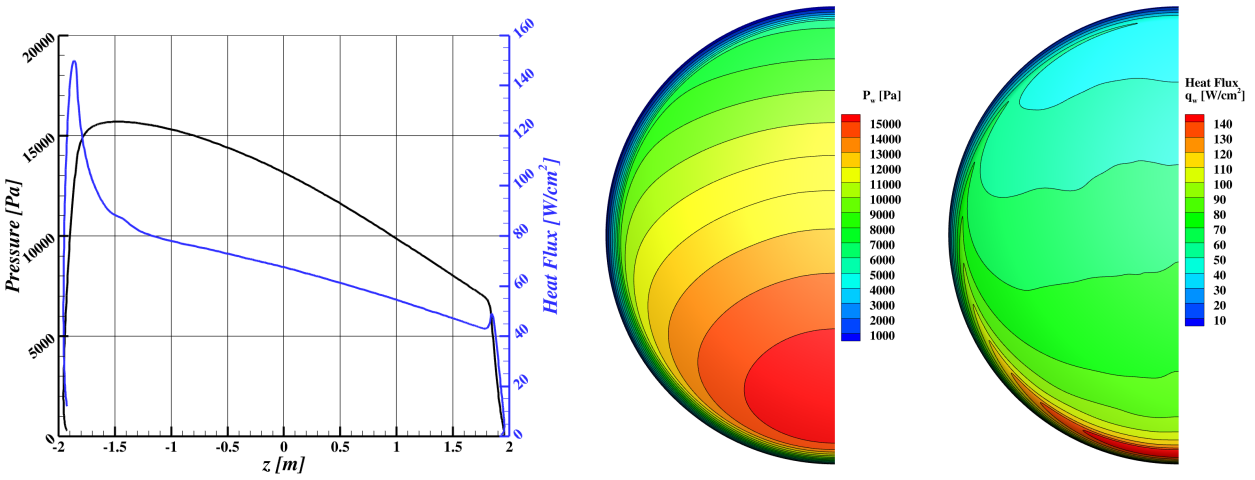

(a) Pitch plane pressure and heat flux (b) Pressure (c) Heat flux

Figure A119. Pressure and heat flux at velocity 7.5 km/s, altitude 60.0 km, and angle-of-attack 158.0 degrees.

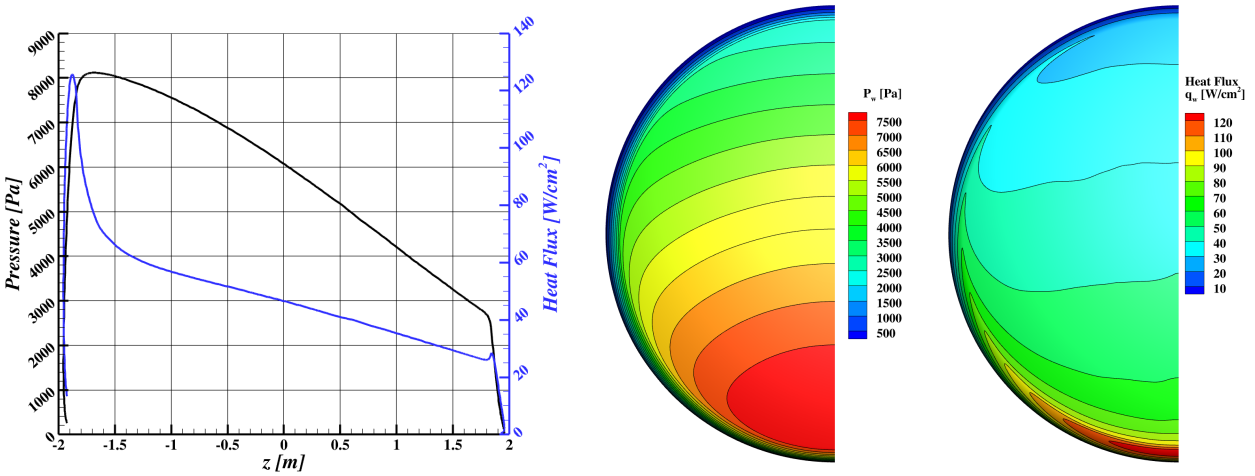

(a) Pitch plane pressure and heat flux (b) Pressure (c) Heat flux

Figure A120. Pressure and heat flux at velocity 7.5 km/s, altitude 65.0 km, and angle-of-attack 152.0 degrees.

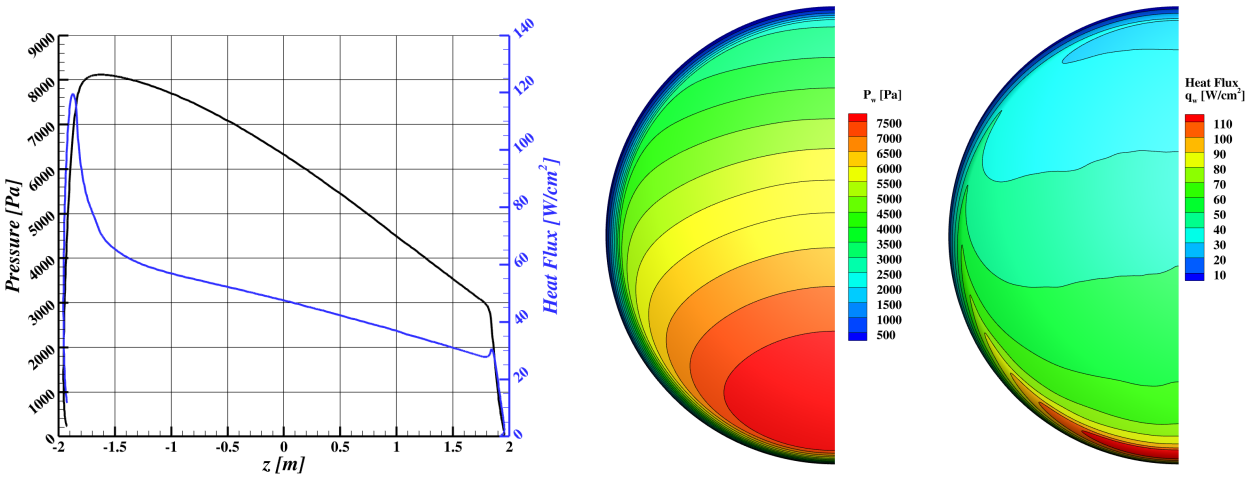

(a) Pitch plane pressure and heat flux (b) Pressure (c) Heat flux

Figure A121. Pressure and heat flux at velocity 7.5 km/s, altitude 65.0 km, and angle-of-attack 154.0 degrees.

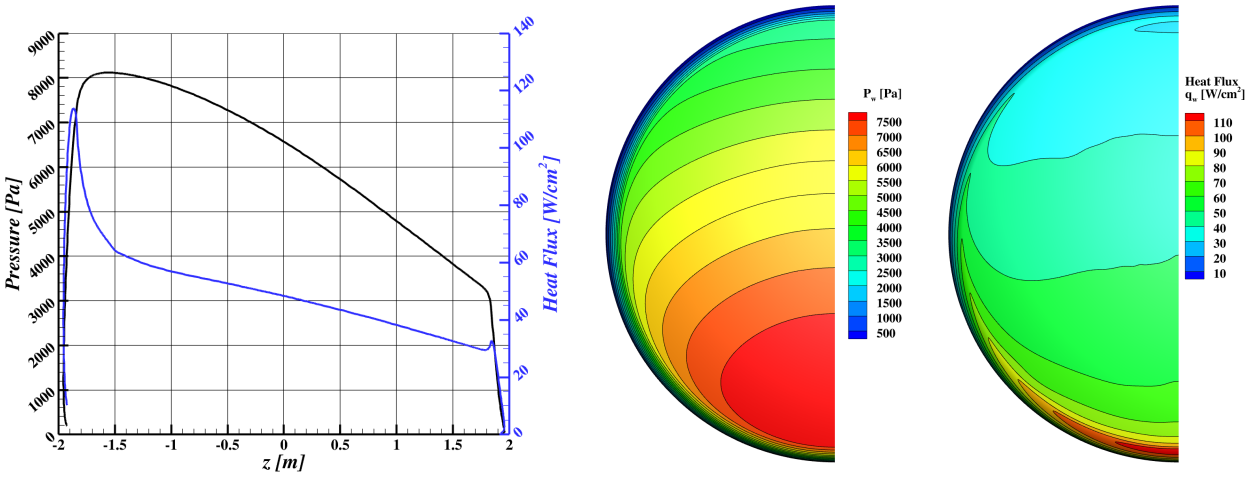

(a) Pitch plane pressure and heat flux (b) Pressure (c) Heat flux

Figure A122. Pressure and heat flux at velocity 7.5 km/s, altitude 65.0 km, and angle-of-attack 156.0 degrees.

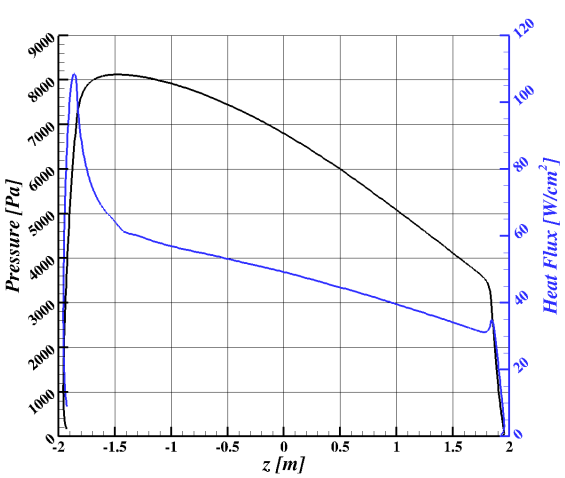

(a) Pitch plane pressure and heat flux

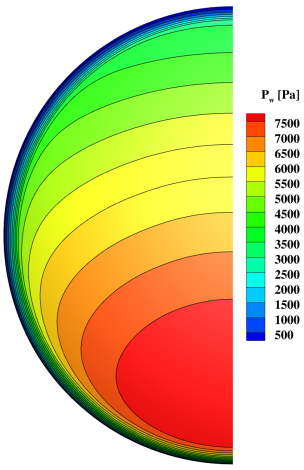

(b) Pressure

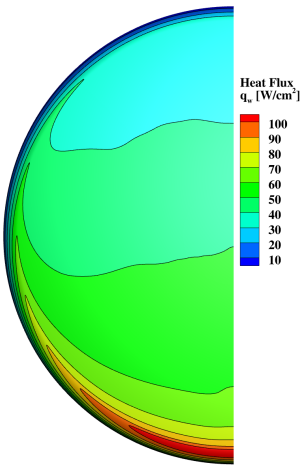

(c) Heat flux

Figure A123. Pressure and heat flux at velocity 7.5 km/s, altitude 65.0 km, and angle-of-attack 158.0 degrees.

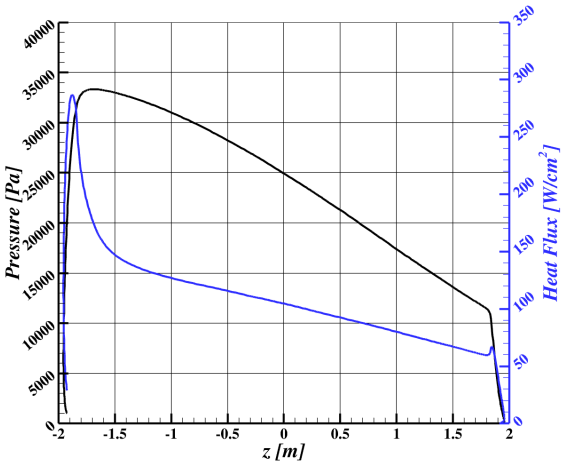

(a) Pitch plane pressure and heat flux

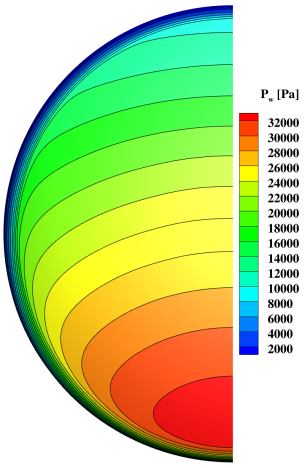

(b) Pressure

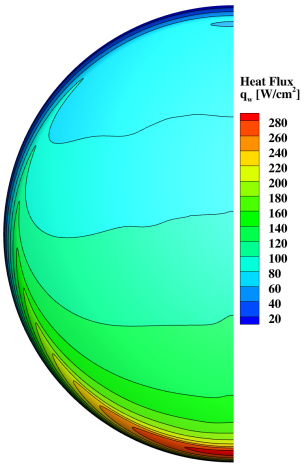

(c) Heat flux

Figure A124. Pressure and heat flux at velocity 8.0 km/s, altitude 55.0 km, and angle-of-attack 152.0 degrees.

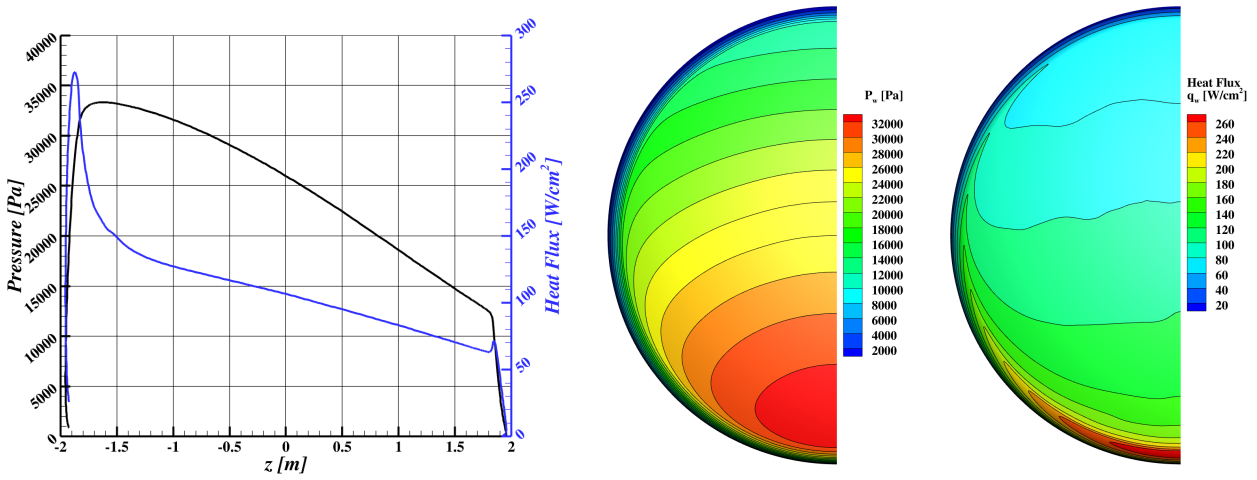

(a) Pitch plane pressure and heat flux (b) Pressure (c) Heat flux

Figure A125. Pressure and heat flux at velocity 8.0 km/s, altitude 55.0 km, and angle-of-attack 154.0 degrees.

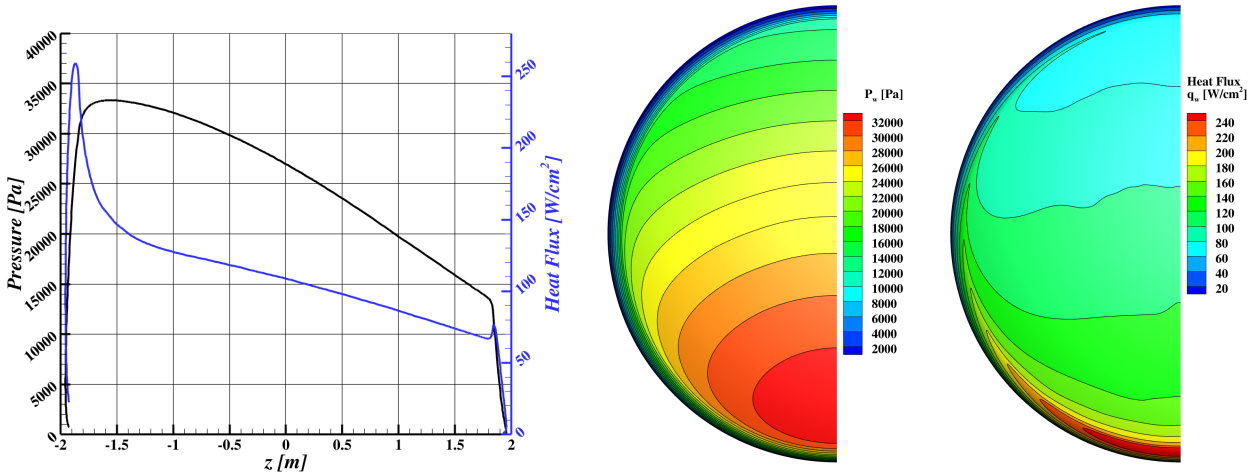

(a) Pitch plane pressure and heat flux (b) Pressure (c) Heat flux

Figure A126. Pressure and heat flux at velocity 8.0 km/s, altitude 55.0 km, and angle-of-attack 156.0 degrees.

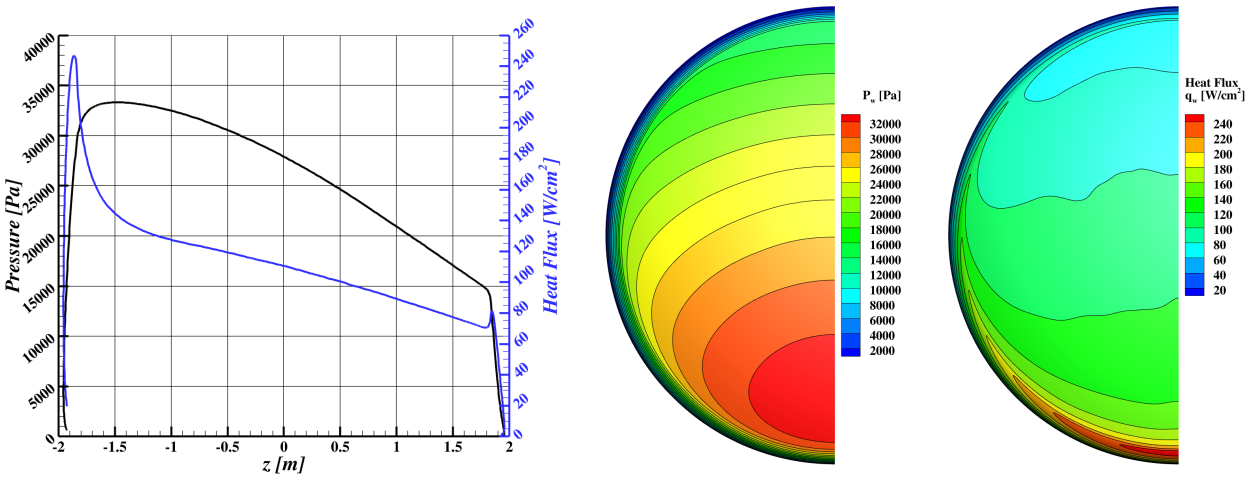

(a) Pitch plane pressure and heat flux (b) Pressure (c) Heat flux

Figure A127. Pressure and heat flux at velocity 8.0 km/s, altitude 55.0 km, and angle-of-attack 158.0 degrees.

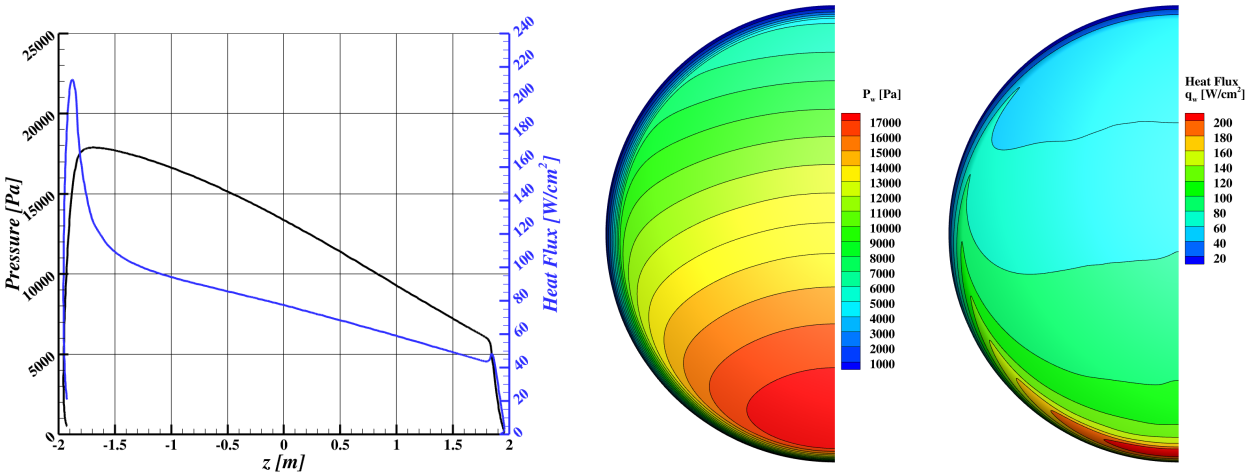

(a) Pitch plane pressure and heat flux (b) Pressure (c) Heat flux

Figure A128. Pressure and heat flux at velocity 8.0 km/s, altitude 60.0 km, and angle-of-attack 152.0 degrees.

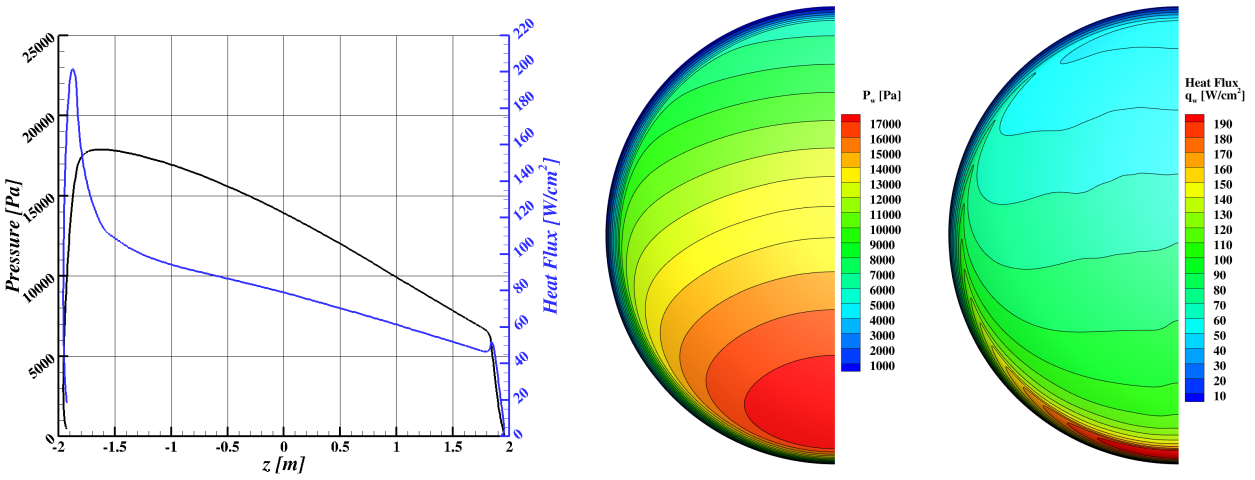

(a) Pitch plane pressure and heat flux (b) Pressure (c) Heat flux

Figure A129. Pressure and heat flux at velocity 8.0 km/s, altitude 60.0 km, and angle-of-attack 154.0 degrees.

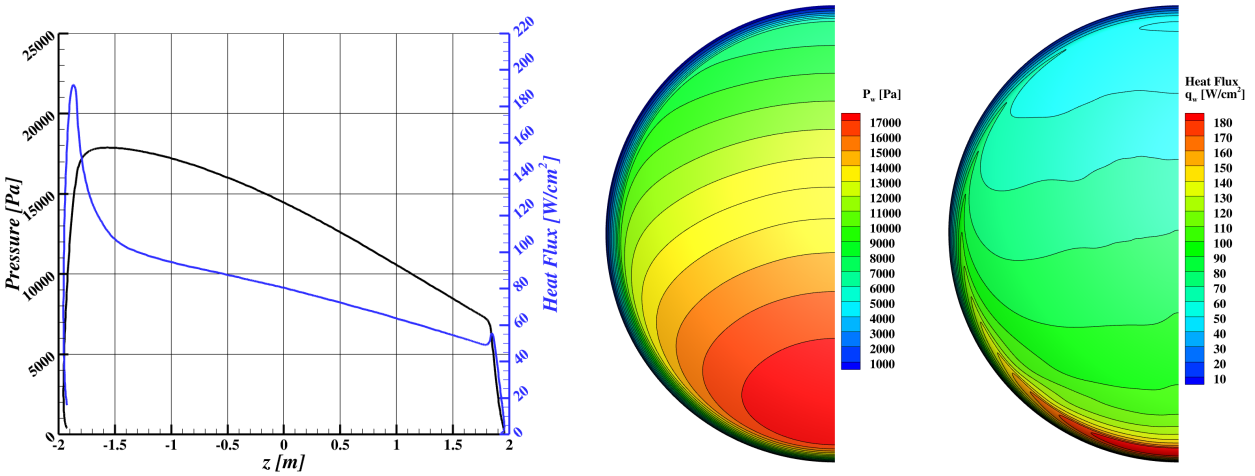

(a) Pitch plane pressure and heat flux (b) Pressure (c) Heat flux

Figure A130. Pressure and heat flux at velocity 8.0 km/s, altitude 60.0 km, and angle-of-attack 156.0 degrees.

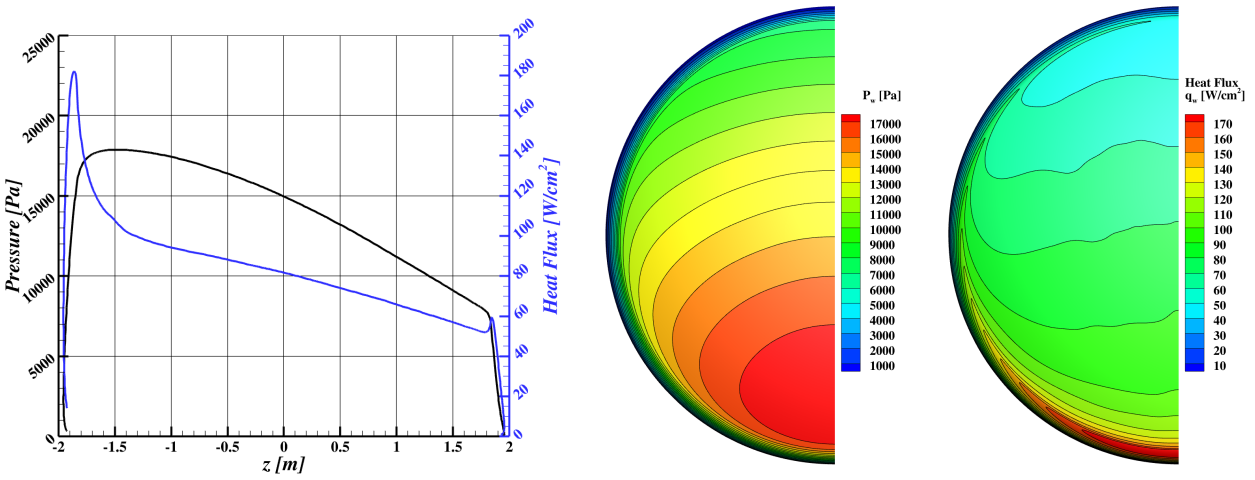

(a) Pitch plane pressure and heat flux (b) Pressure (c) Heat flux

Figure A131. Pressure and heat flux at velocity 8.0 km/s, altitude 60.0 km, and angle-of-attack 158.0 degrees.

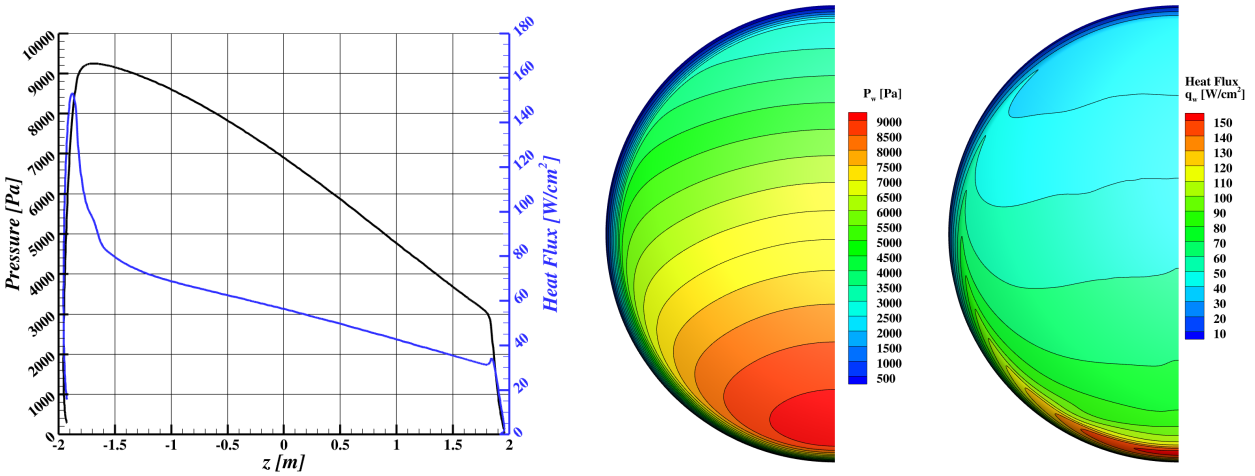

(a) Pitch plane pressure and heat flux (b) Pressure (c) Heat flux

Figure A132. Pressure and heat flux at velocity 8.0 km/s, altitude 65.0 km, and angle-of-attack 152.0 degrees.

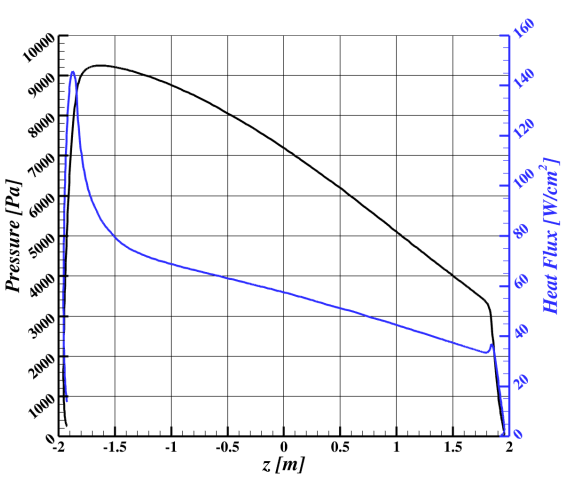

(a) Pitch plane pressure and heat flux

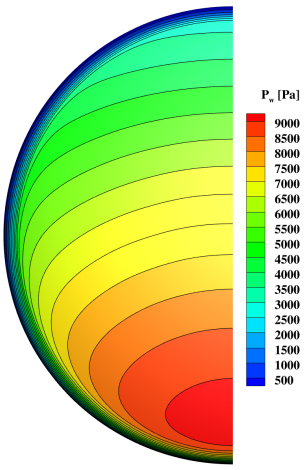

(b) Pressure

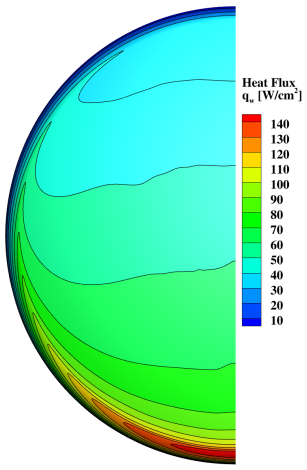

(c) Heat flux

Figure A133. Pressure and heat flux at velocity 8.0 km/s, altitude 65.0 km, and angle-of-attack 154.0 degrees.

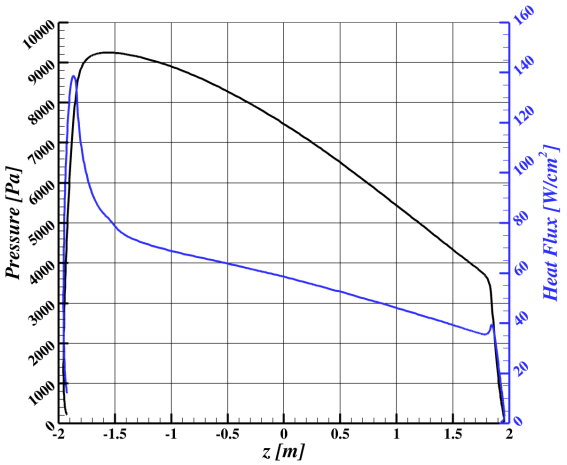

(a) Pitch plane pressure and heat flux

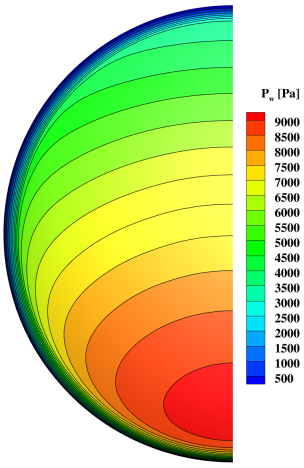

(b) Pressure

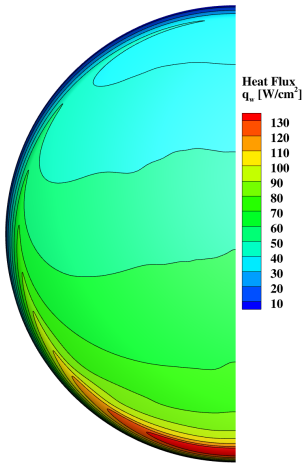

(c) Heat flux

Figure A134. Pressure and heat flux at velocity 8.0 km/s, altitude 65.0 km, and angle-of-attack 156.0 degrees.

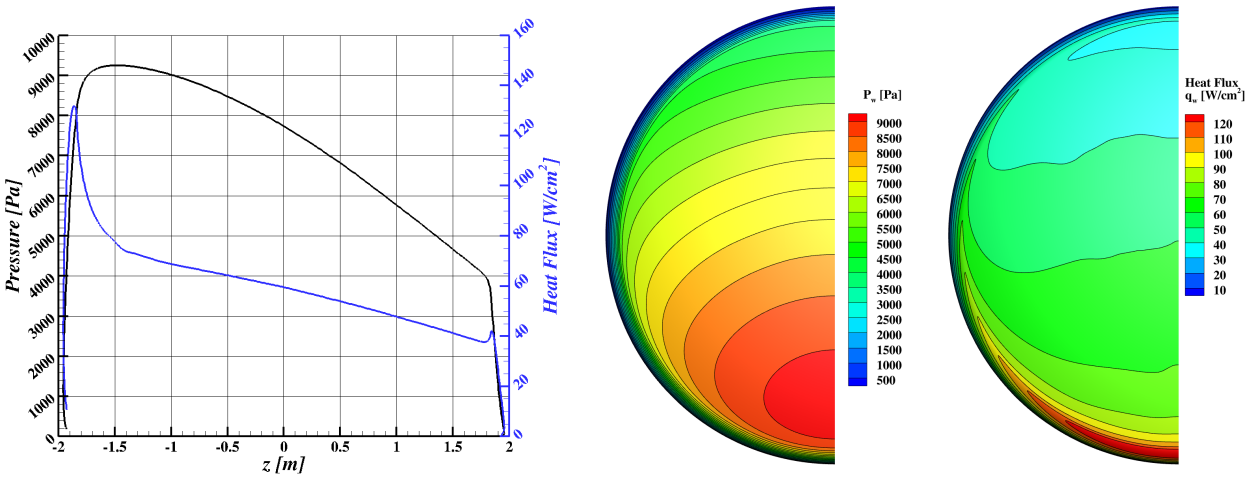

(a) Pitch plane pressure and heat flux (b) Pressure (c) Heat flux

Figure A135. Pressure and heat flux at velocity 8.0 km/s, altitude 65.0 km, and angle-of-attack 158.0 degrees.

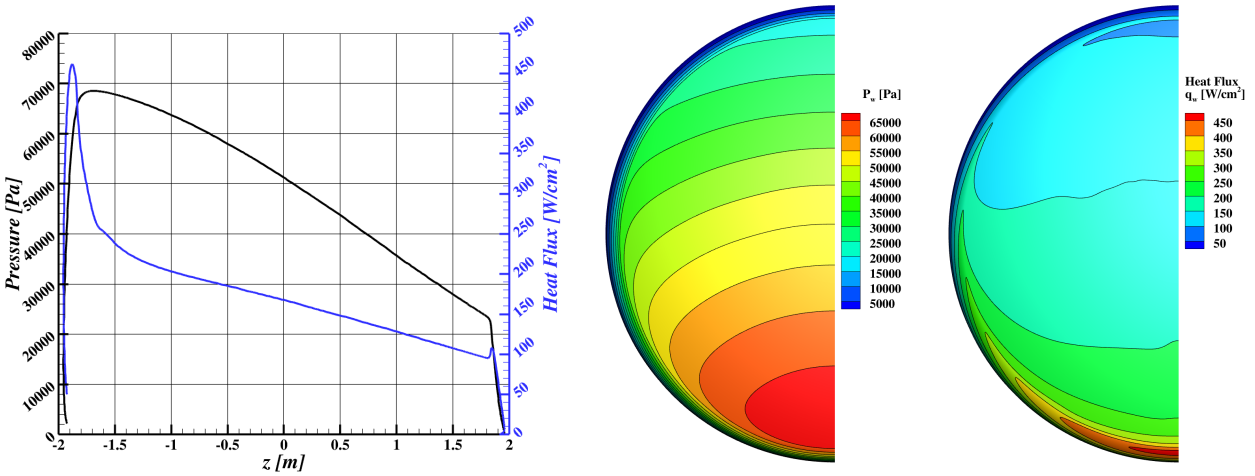

(a) Pitch plane pressure and heat flux (b) Pressure (c) Heat flux

Figure A136. Pressure and heat flux at velocity 8.5 km/s, altitude 50.0 km, and angle-of-attack 152.0 degrees.

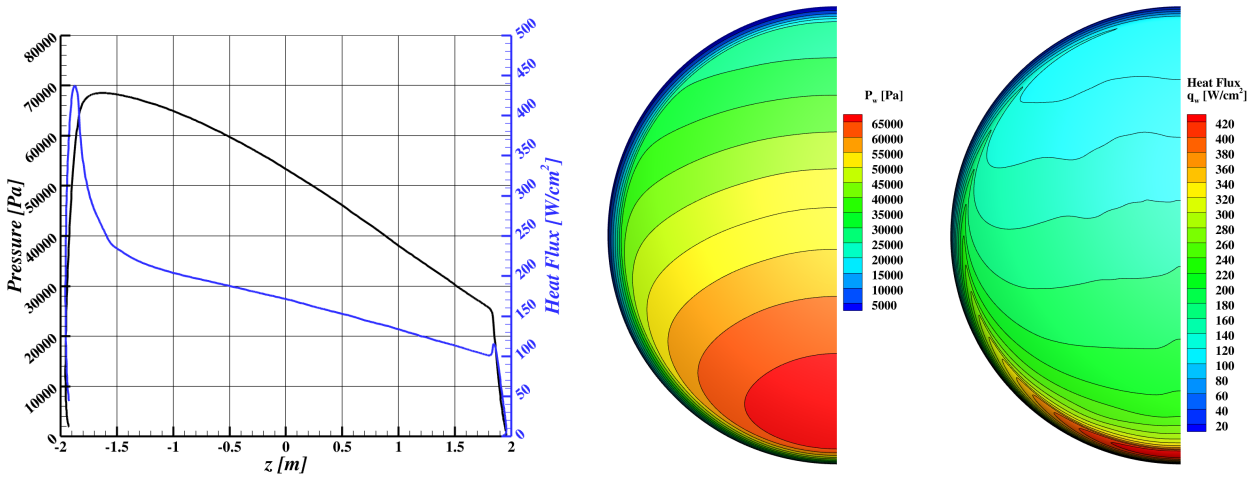

(a) Pitch plane pressure and heat flux (b) Pressure (c) Heat flux

Figure A137. Pressure and heat flux at velocity 8.5 km/s, altitude 50.0 km, and angle-of-attack 154.0 degrees.

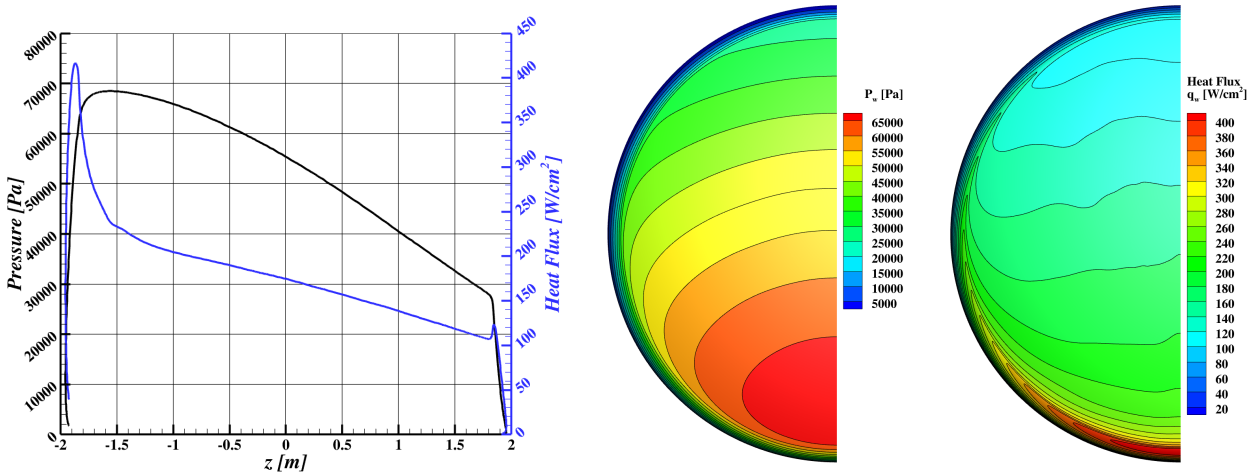

(a) Pitch plane pressure and heat flux (b) Pressure (c) Heat flux

Figure A138. Pressure and heat flux at velocity 8.5 km/s, altitude 50.0 km, and angle-of-attack 156.0 degrees.

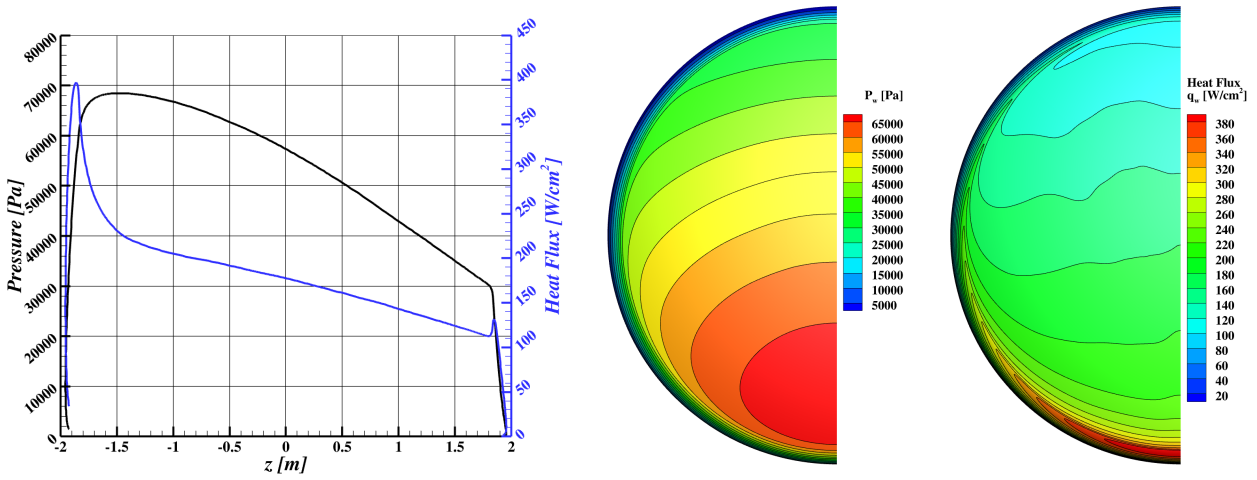

(a) Pitch plane pressure and heat flux (b) Pressure (c) Heat flux

Figure A139. Pressure and heat flux at velocity 8.5 km/s, altitude 50.0 km, and angle-of-attack 158.0 degrees.

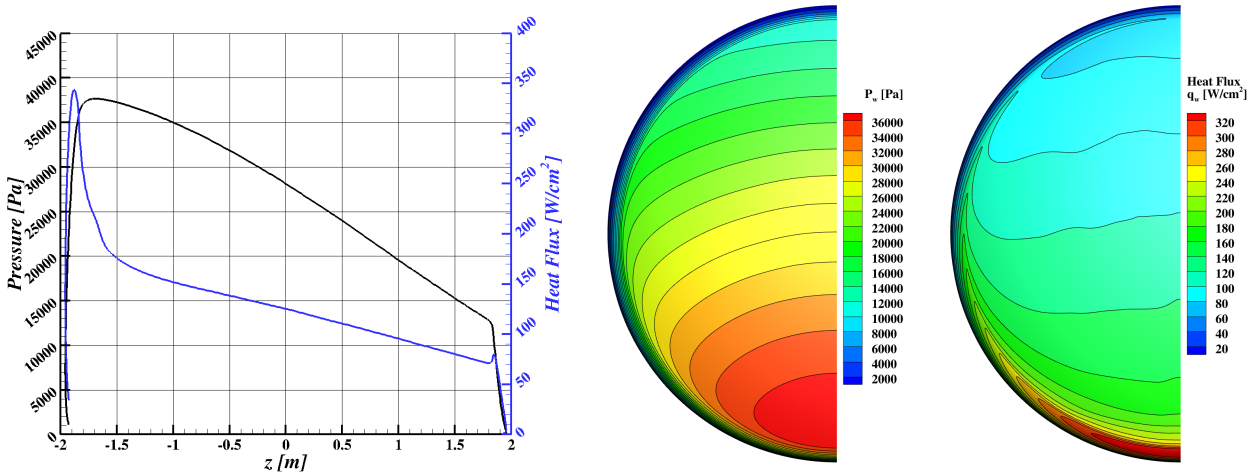

(a) Pitch plane pressure and heat flux (b) Pressure (c) Heat flux

Figure A140. Pressure and heat flux at velocity 8.5 km/s, altitude 55.0 km, and angle-of-attack 152.0 degrees.

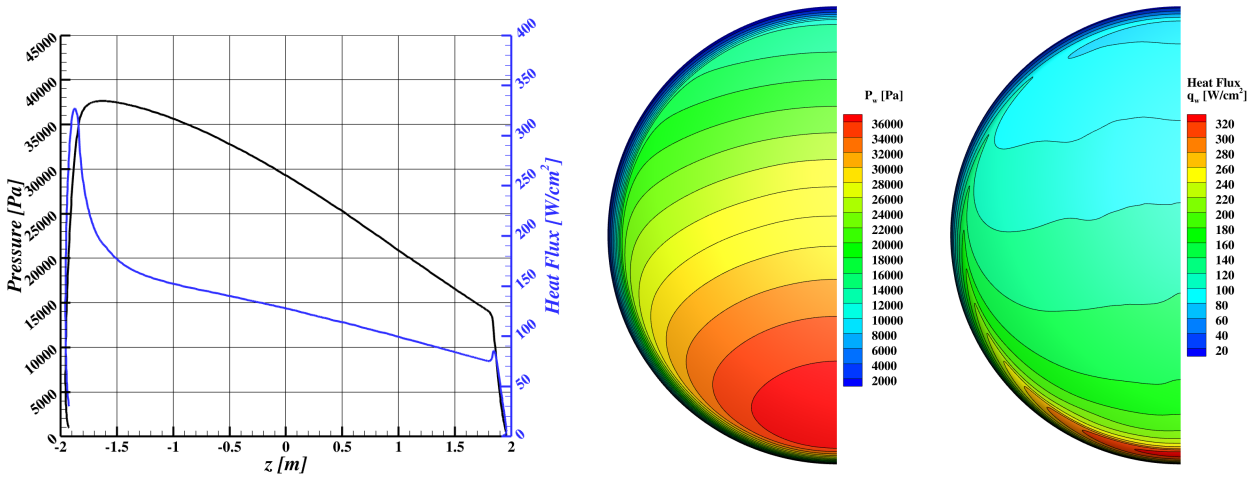

(a) Pitch plane pressure and heat flux (b) Pressure (c) Heat flux

Figure A141. Pressure and heat flux at velocity 8.5 km/s, altitude 55.0 km, and angle-of-attack 154.0 degrees.

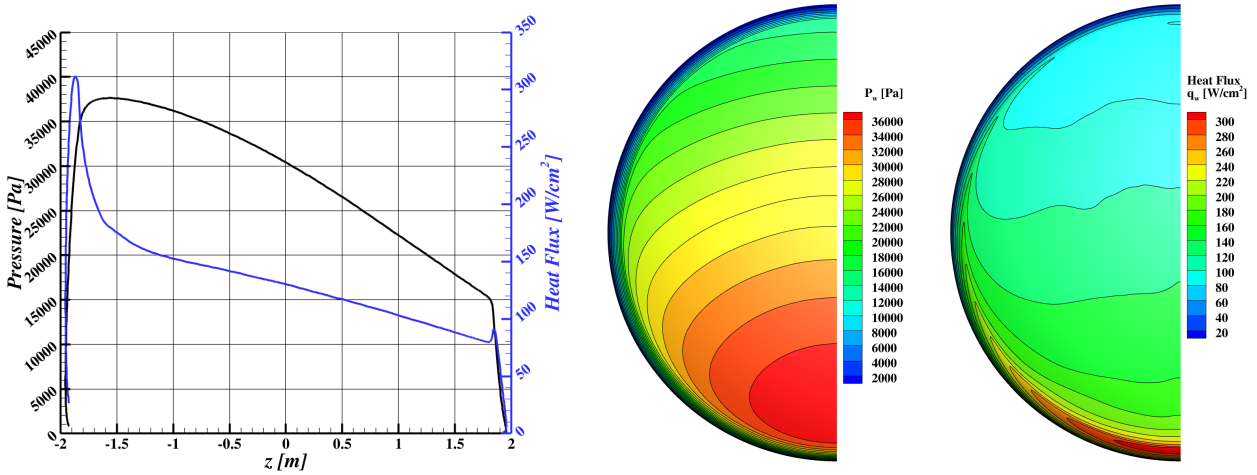

(a) Pitch plane pressure and heat flux (b) Pressure (c) Heat flux

Figure A142. Pressure and heat flux at velocity 8.5 km/s, altitude 55.0 km, and angle-of-attack 156.0 degrees.

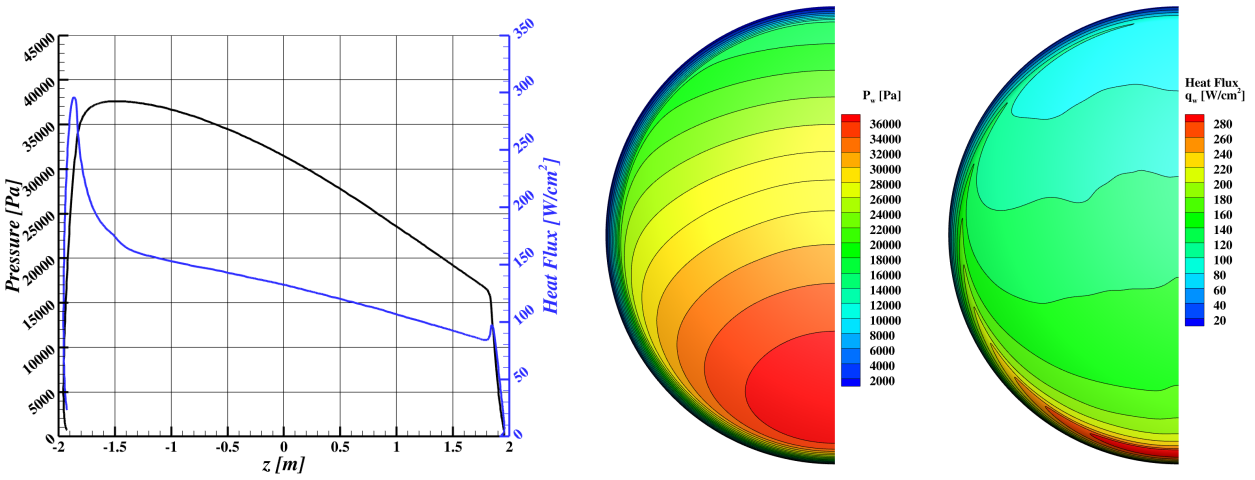

(a) Pitch plane pressure and heat flux (b) Pressure (c) Heat flux

Figure A143. Pressure and heat flux at velocity 8.5 km/s, altitude 55.0 km, and angle-of-attack 158.0 degrees.

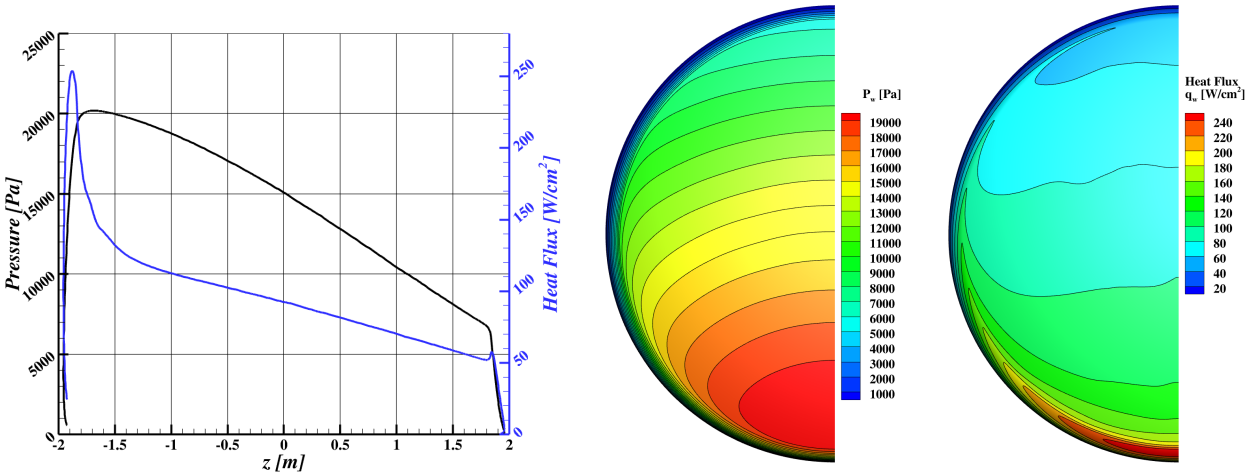

(a) Pitch plane pressure and heat flux (b) Pressure (c) Heat flux

Figure A144. Pressure and heat flux at velocity 8.5 km/s, altitude 60.0 km, and angle-of-attack 152.0 degrees.

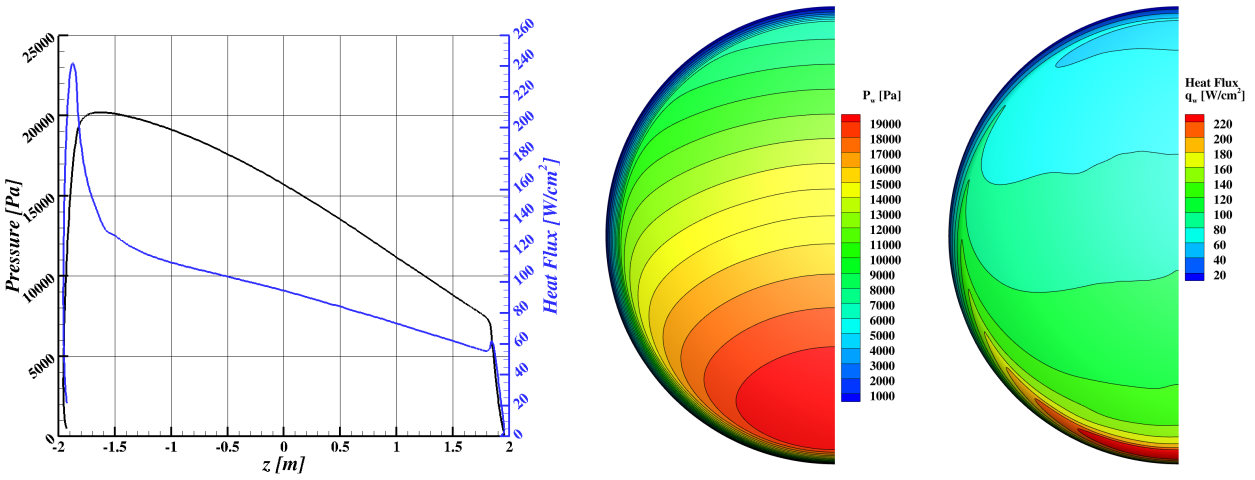

(a) Pitch plane pressure and heat flux (b) Pressure (c) Heat flux

Figure A145. Pressure and heat flux at velocity 8.5 km/s, altitude 60.0 km, and angle-of-attack 154.0 degrees.

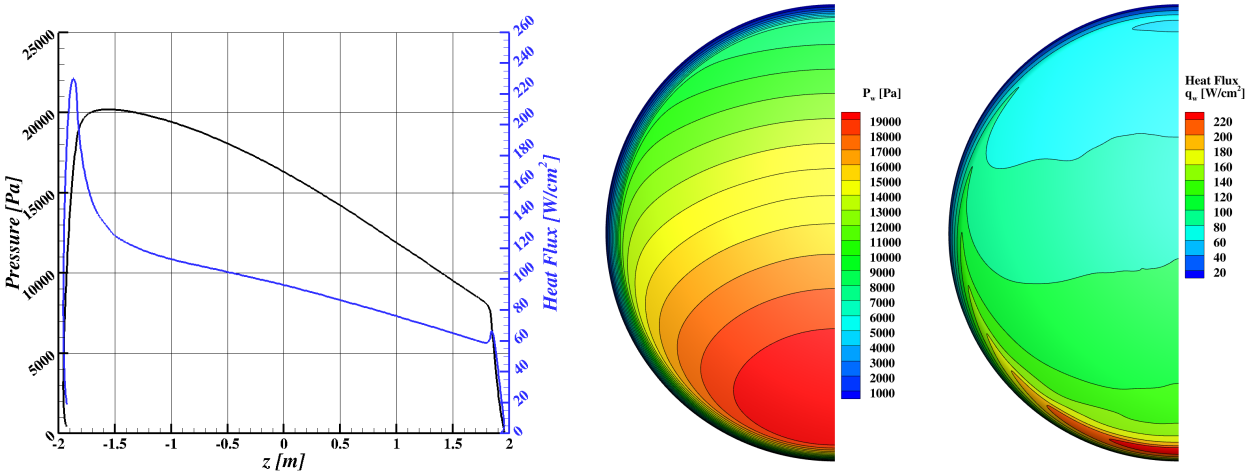

(a) Pitch plane pressure and heat flux (b) Pressure (c) Heat flux

Figure A146. Pressure and heat flux at velocity 8.5 km/s, altitude 60.0 km, and angle-of-attack 156.0 degrees.

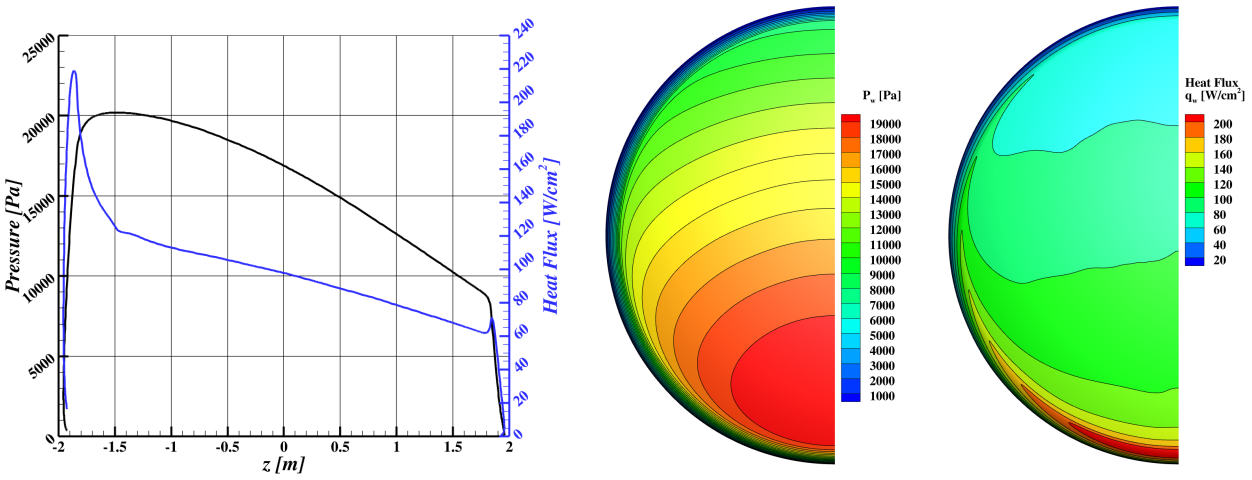

(a) Pitch plane pressure and heat flux (b) Pressure (c) Heat flux

Figure A147. Pressure and heat flux at velocity 8.5 km/s, altitude 60.0 km, and angle-of-attack 158.0 degrees.

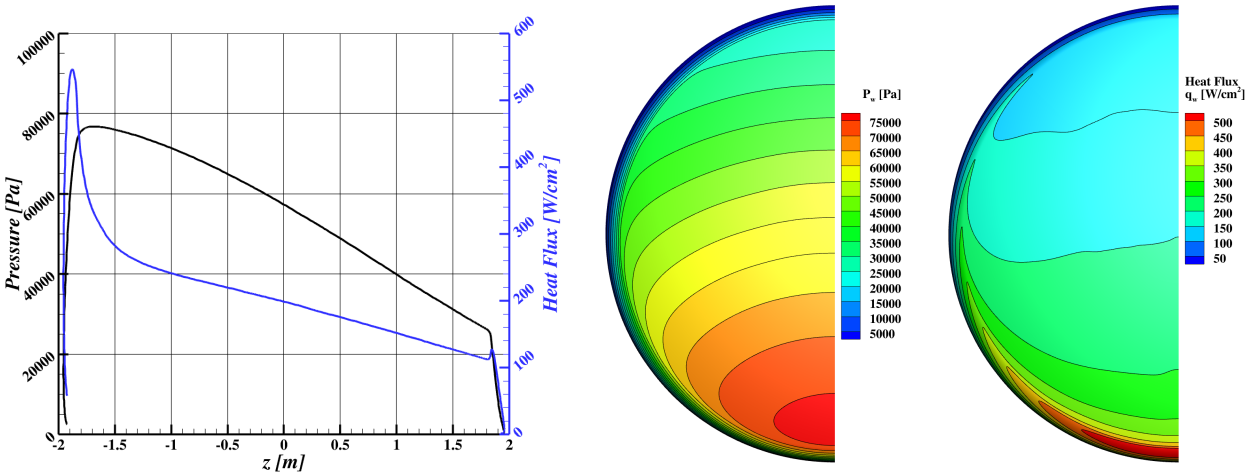

(a) Pitch plane pressure and heat flux (b) Pressure (c) Heat flux

Figure A148. Pressure and heat flux at velocity 9.0 km/s, altitude 50.0 km, and angle-of-attack 152.0 degrees.

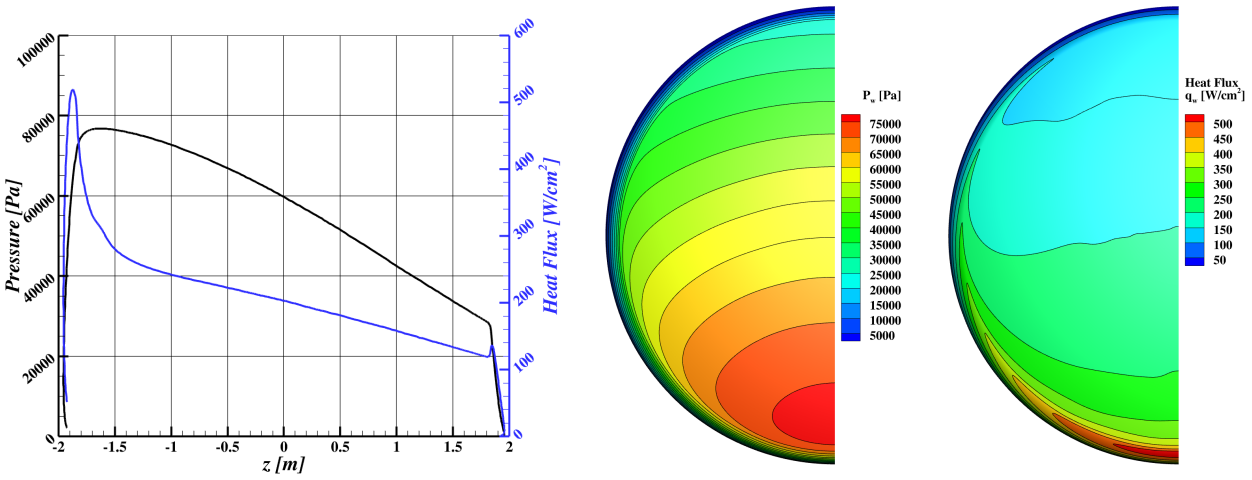

(a) Pitch plane pressure and heat flux (b) Pressure (c) Heat flux

Figure A149. Pressure and heat flux at velocity 9.0 km/s, altitude 50.0 km, and angle-of-attack 154.0 degrees.

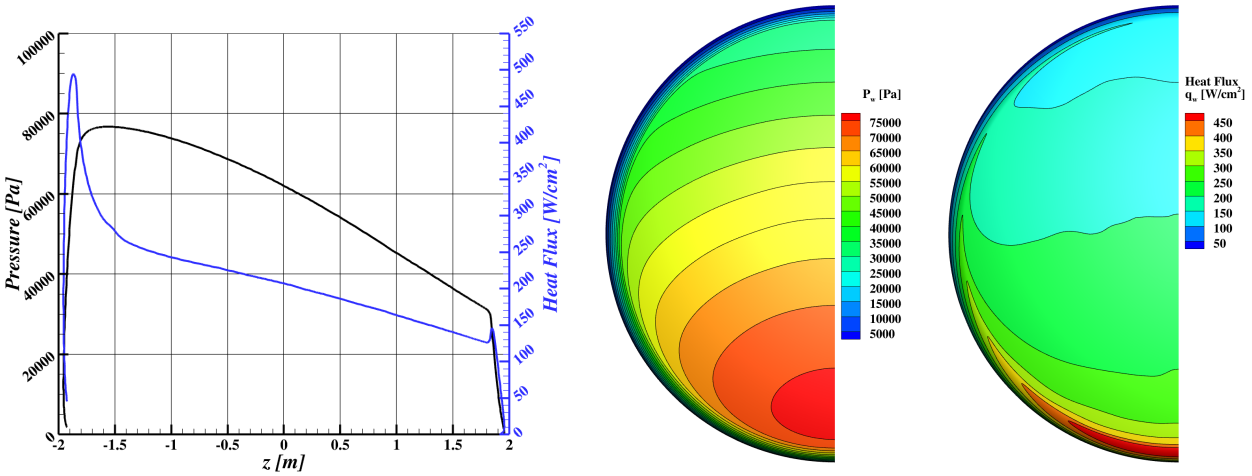

(a) Pitch plane pressure and heat flux (b) Pressure (c) Heat flux

Figure A150. Pressure and heat flux at velocity 9.0 km/s, altitude 50.0 km, and angle-of-attack 156.0 degrees.

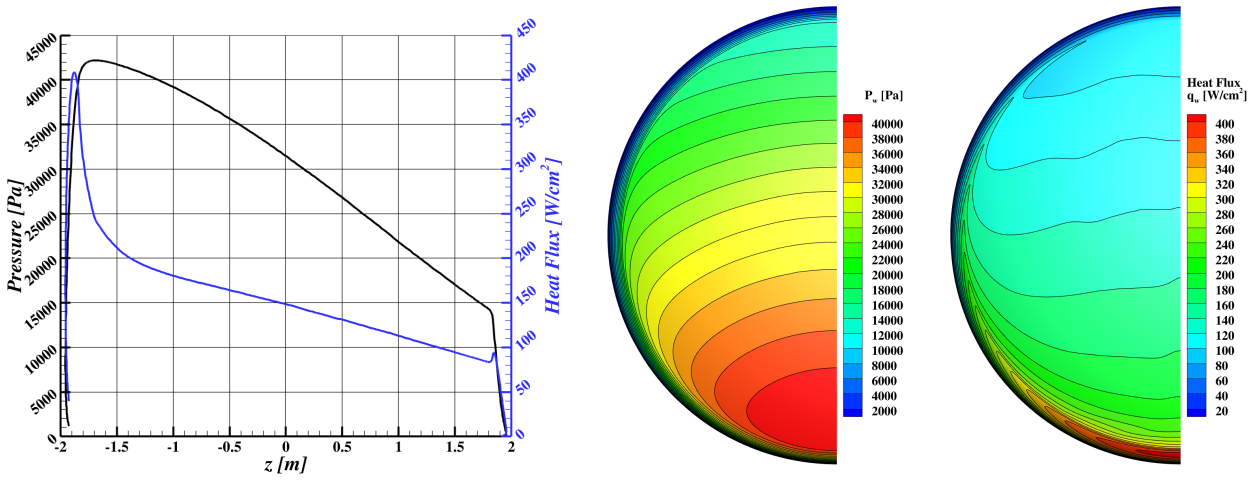

(a) Pitch plane pressure and heat flux (b) Pressure (c) Heat flux

Figure A151. Pressure and heat flux at velocity 9.0 km/s, altitude 55.0 km, and angle-of-attack 152.0 degrees.

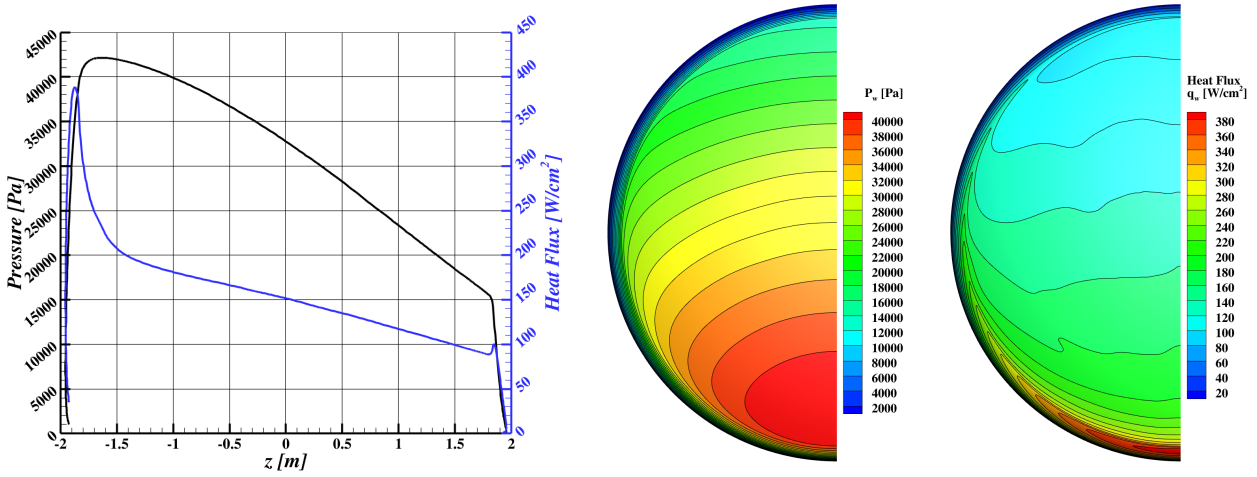

(a) Pitch plane pressure and heat flux (b) Pressure (c) Heat flux

Figure A152. Pressure and heat flux at velocity 9.0 km/s, altitude 55.0 km, and angle-of-attack 154.0 degrees.

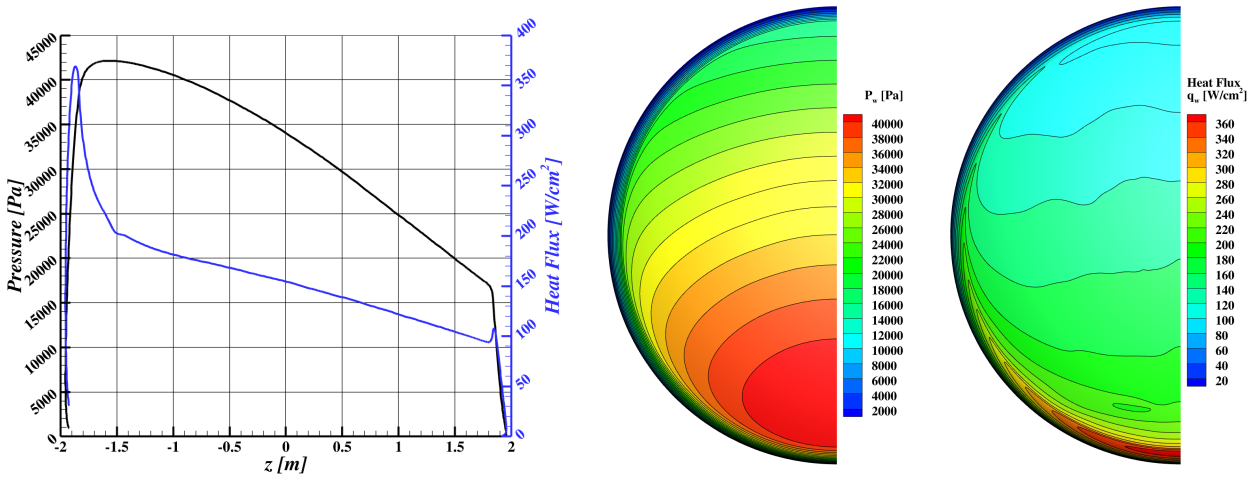

(a) Pitch plane pressure and heat flux (b) Pressure (c) Heat flux

Figure A153. Pressure and heat flux at velocity 9.0 km/s, altitude 55.0 km, and angle-of-attack 156.0 degrees.

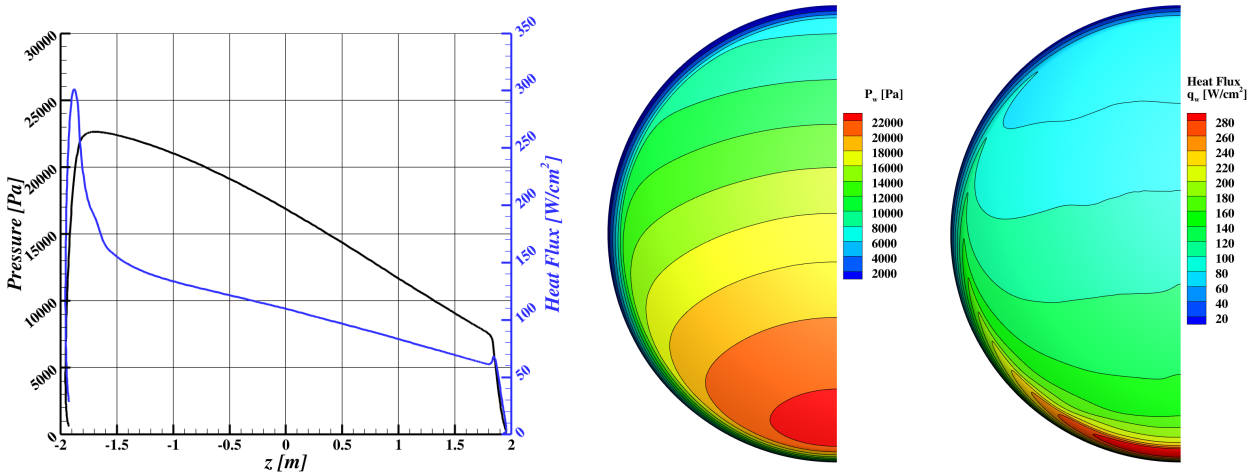

(a) Pitch plane pressure and heat flux (b) Pressure (c) Heat flux

Figure A154. Pressure and heat flux at velocity 9.0 km/s, altitude 60.0 km, and angle-of-attack 152.0 degrees.

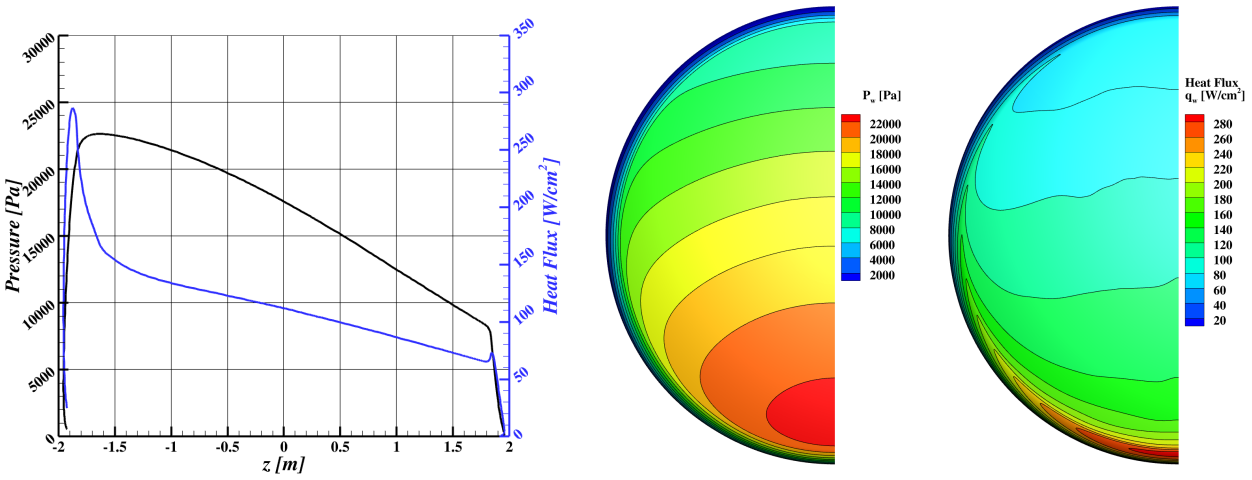

(a) Pitch plane pressure and heat flux (b) Pressure (c) Heat flux

Figure A155. Pressure and heat flux at velocity 9.0 km/s, altitude 60.0 km, and angle-of-attack 154.0 degrees.

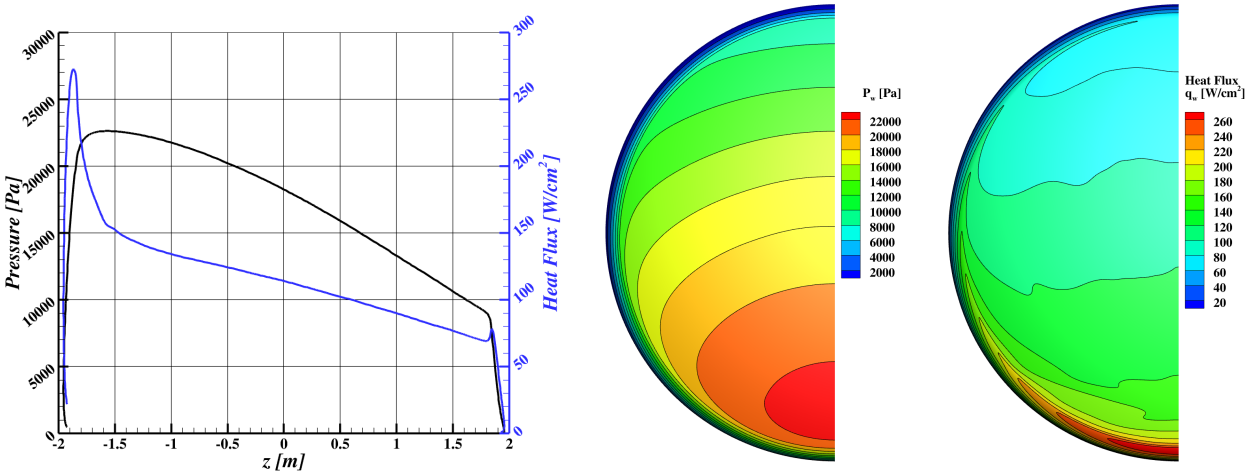

(a) Pitch plane pressure and heat flux (b) Pressure (c) Heat flux

Figure A156. Pressure and heat flux at velocity 9.0 km/s, altitude 60.0 km, and angle-of-attack 156.0 degrees.

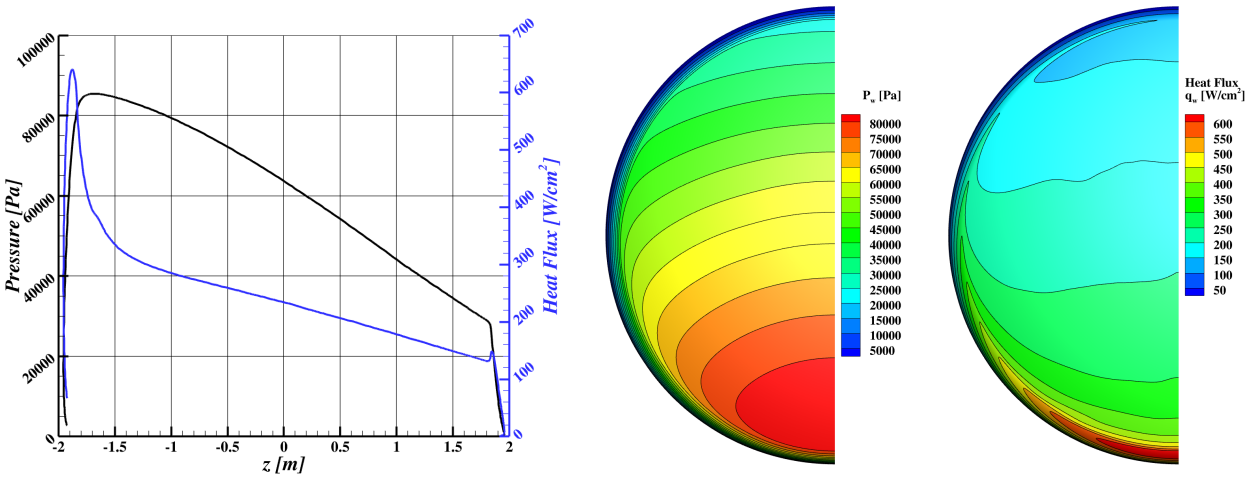

(a) Pitch plane pressure and heat flux (b) Pressure (c) Heat flux

Figure A157. Pressure and heat flux at velocity 9.5 km/s, altitude 50.0 km, and angle-of-attack 152.0 degrees.

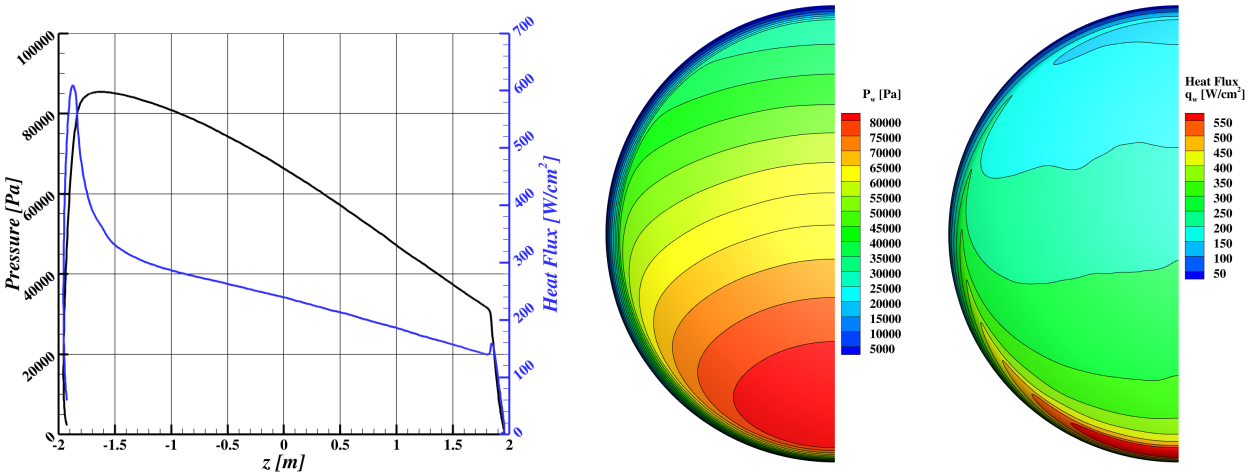

(a) Pitch plane pressure and heat flux (b) Pressure (c) Heat flux

Figure A158. Pressure and heat flux at velocity 9.5 km/s, altitude 50.0 km, and angle-of-attack 154.0 degrees.

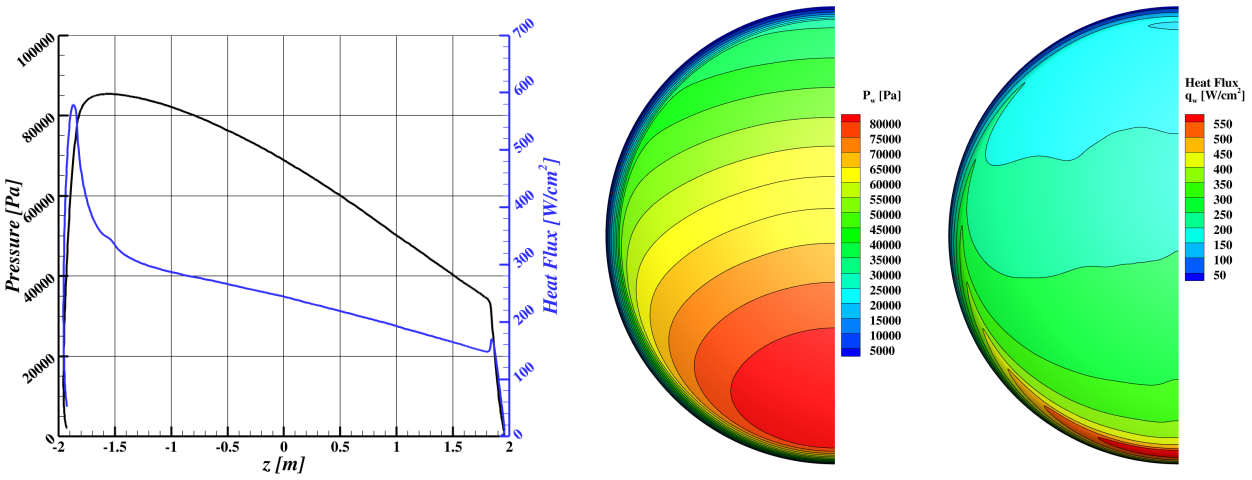

(a) Pitch plane pressure and heat flux (b) Pressure (c) Heat flux

Figure A159. Pressure and heat flux at velocity 9.5 km/s, altitude 50.0 km, and angle-of-attack 156.0 degrees.

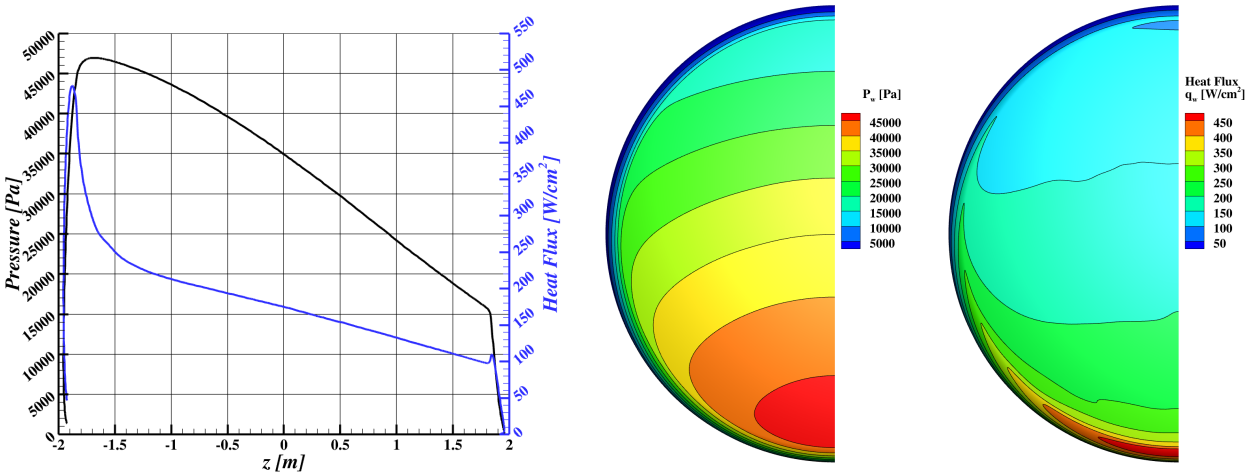

(a) Pitch plane pressure and heat flux (b) Pressure (c) Heat flux

Figure A160. Pressure and heat flux at velocity 9.5 km/s, altitude 55.0 km, and angle-of-attack 152.0 degrees.

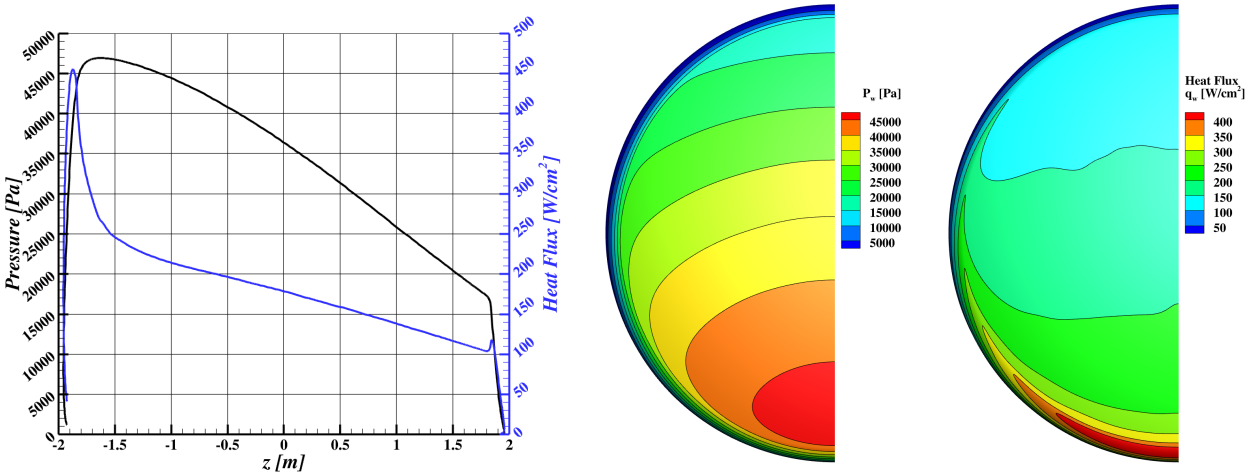

(a) Pitch plane pressure and heat flux (b) Pressure (c) Heat flux

Figure A161. Pressure and heat flux at velocity 9.5 km/s, altitude 55.0 km, and angle-of-attack 154.0 degrees.

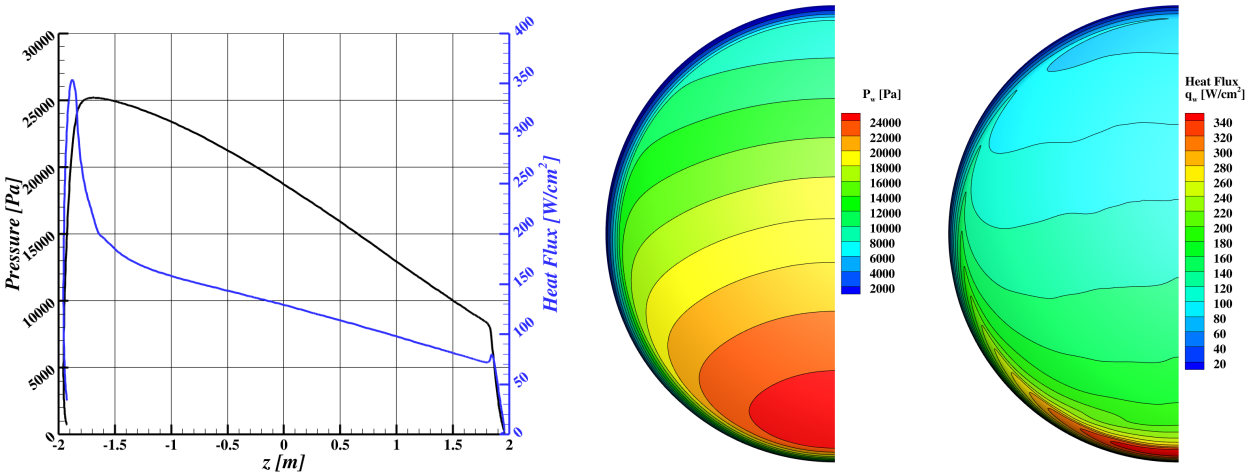

(a) Pitch plane pressure and heat flux (b) Pressure (c) Heat flux

Figure A162. Pressure and heat flux at velocity 9.5 km/s, altitude 60.0 km, and angle-of-attack 152.0 degrees.

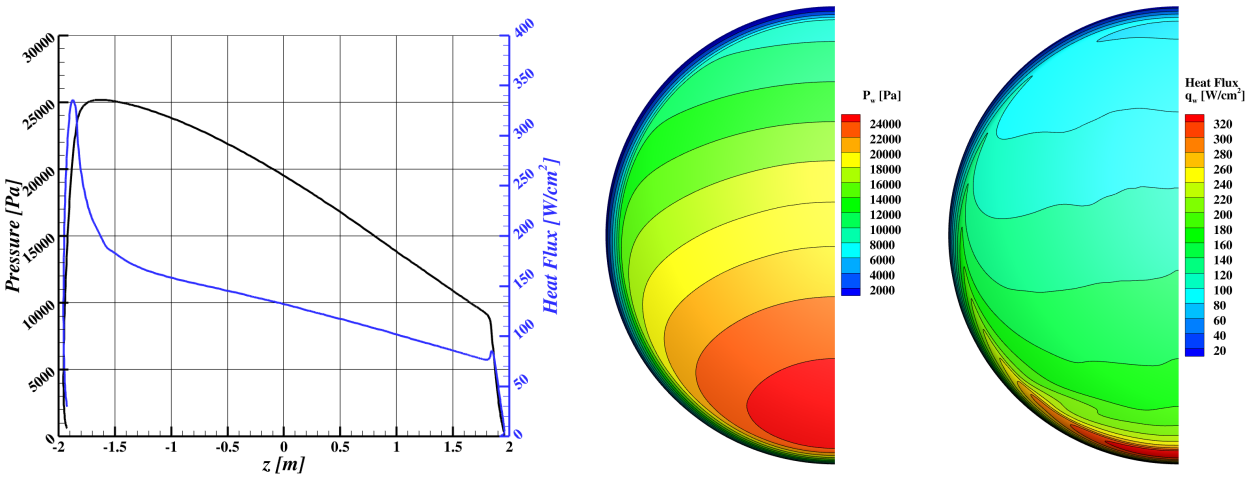

(a) Pitch plane pressure and heat flux (b) Pressure (c) Heat flux

Figure A163. Pressure and heat flux at velocity 9.5 km/s, altitude 60.0 km, and angle-of-attack 154.0 degrees.

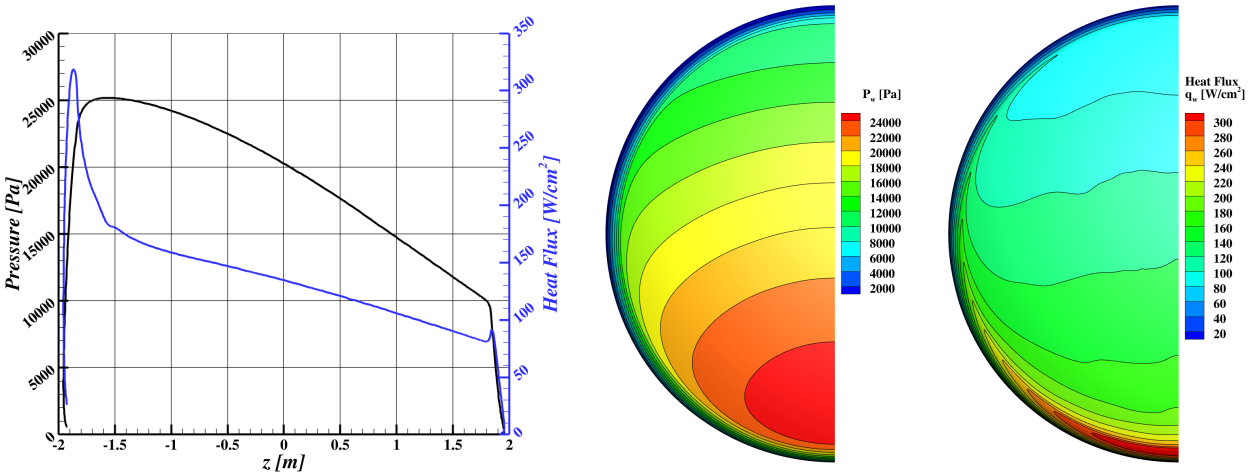

(a) Pitch plane pressure and heat flux (b) Pressure (c) Heat flux

Figure A164. Pressure and heat flux at velocity 9.5 km/s, altitude 60.0 km, and angle-of-attack 156.0 degrees.

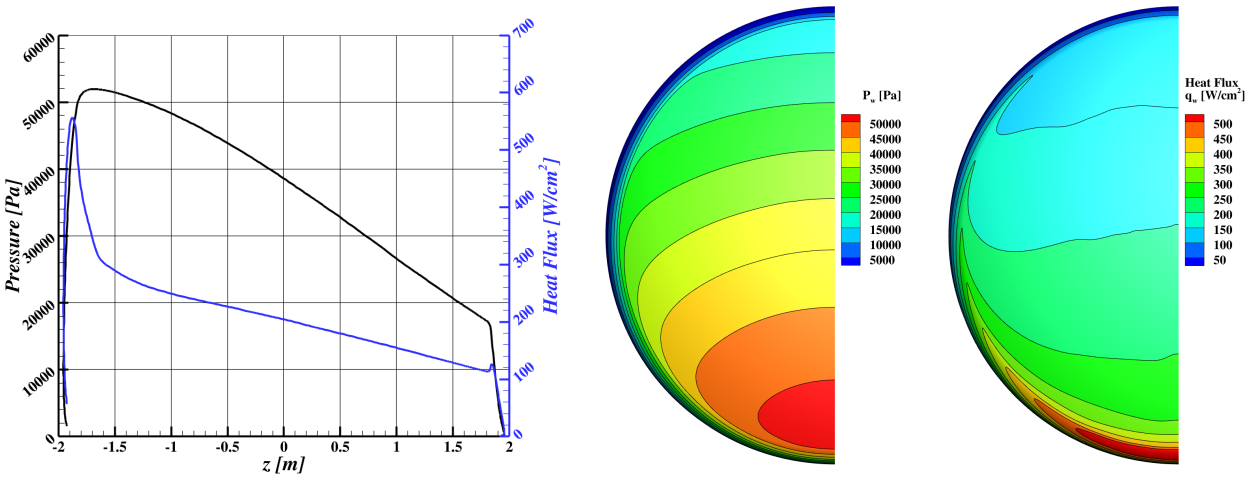

(a) Pitch plane pressure and heat flux (b) Pressure (c) Heat flux

Figure A165. Pressure and heat flux at velocity 10.0 km/s, altitude 55.0 km, and angle-of-attack 152.0 degrees.

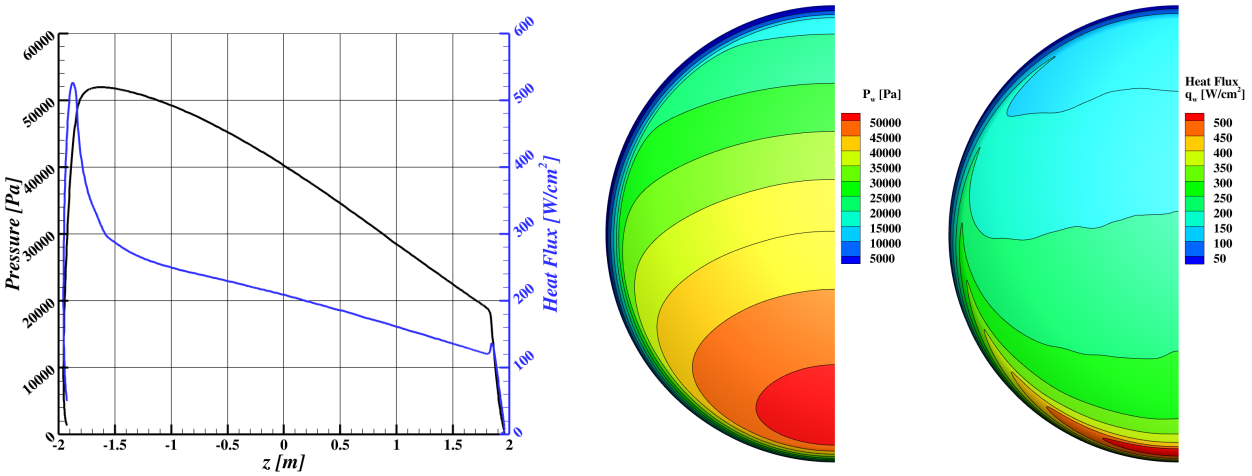

(a) Pitch plane pressure and heat flux (b) Pressure (c) Heat flux

Figure A166. Pressure and heat flux at velocity 10.0 km/s, altitude 55.0 km, and angle-of-attack 154.0 degrees.

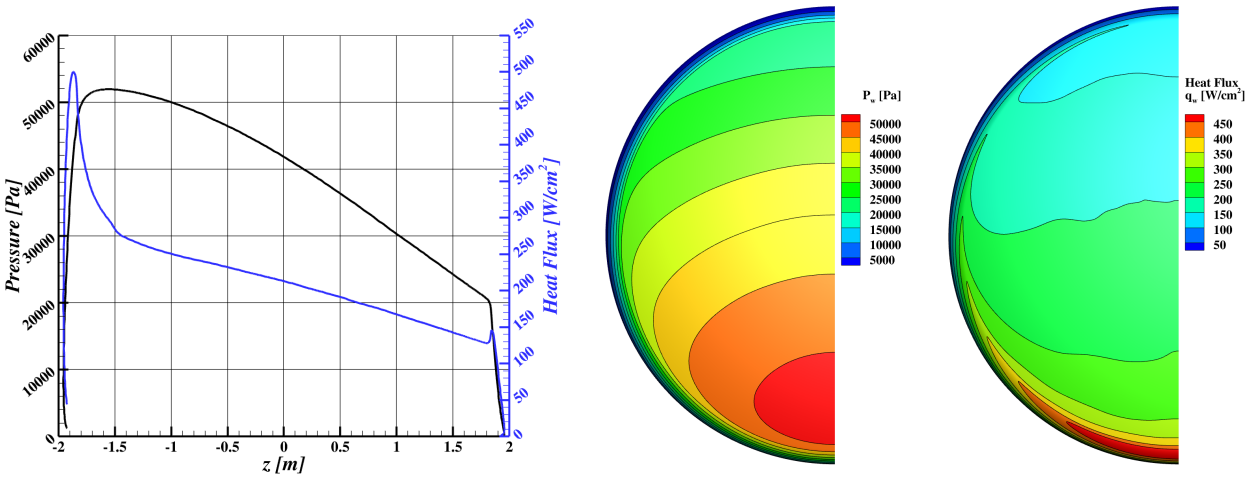

(a) Pitch plane pressure and heat flux (b) Pressure (c) Heat flux

Figure A167. Pressure and heat flux at velocity 10.0 km/s, altitude 55.0 km, and angle-of-attack 156.0 degrees.

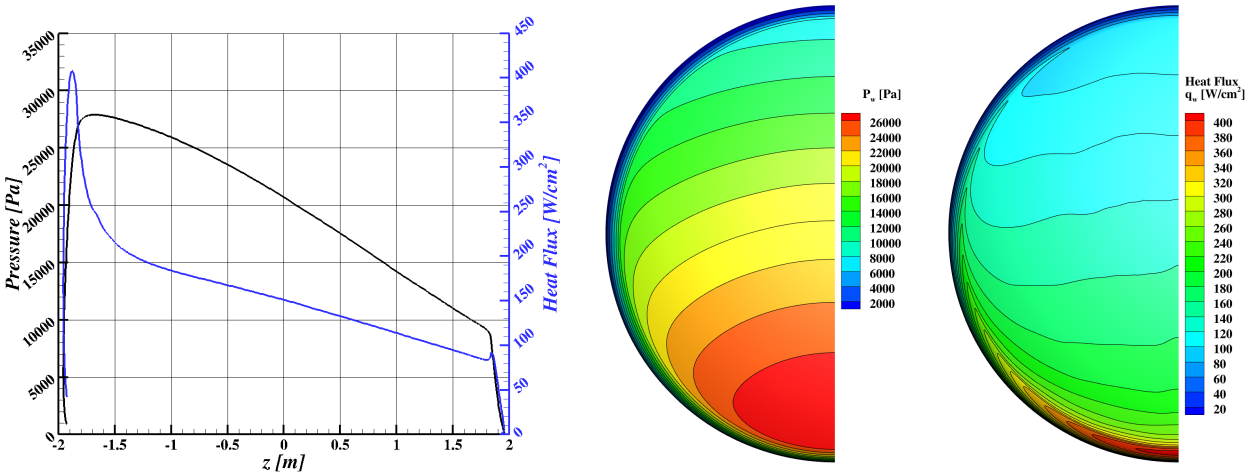

(a) Pitch plane pressure and heat flux (b) Pressure (c) Heat flux

Figure A168. Pressure and heat flux at velocity 10.0 km/s, altitude 60.0 km, and angle-of-attack 152.0 degrees.

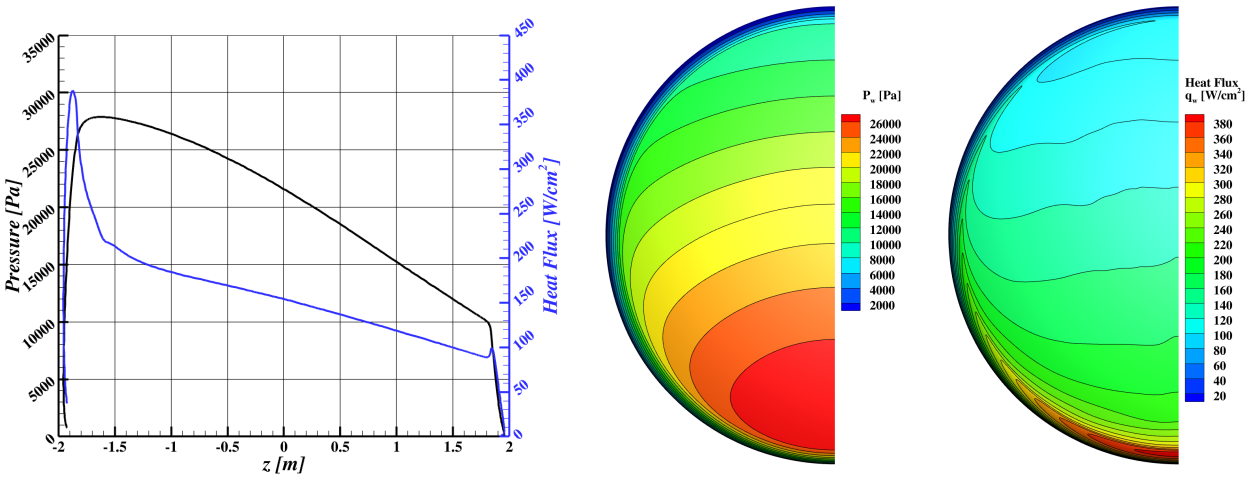

(a) Pitch plane pressure and heat flux (b) Pressure (c) Heat flux

Figure A169. Pressure and heat flux at velocity 10.0 km/s, altitude 60.0 km, and angle-of-attack 154.0 degrees.

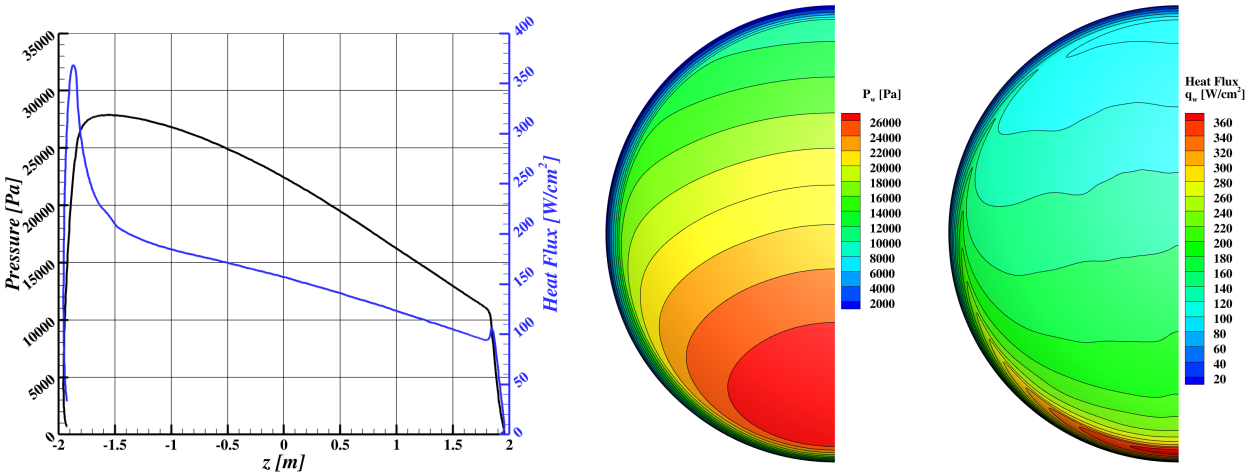

(a) Pitch plane pressure and heat flux (b) Pressure (c) Heat flux

Figure A170. Pressure and heat flux at velocity 10.0 km/s, altitude 60.0 km, and angle-of-attack 156.0 degrees.

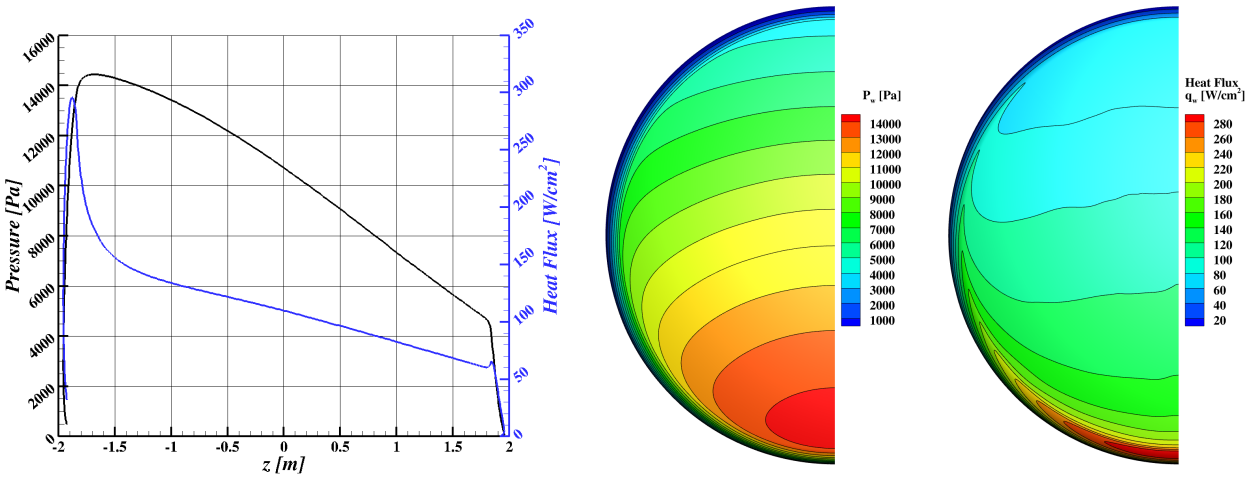

(a) Pitch plane pressure and heat flux (b) Pressure (c) Heat flux

Figure A171. Pressure and heat flux at velocity 10.0 km/s, altitude 65.0 km, and angle-of-attack 152.0 degrees.

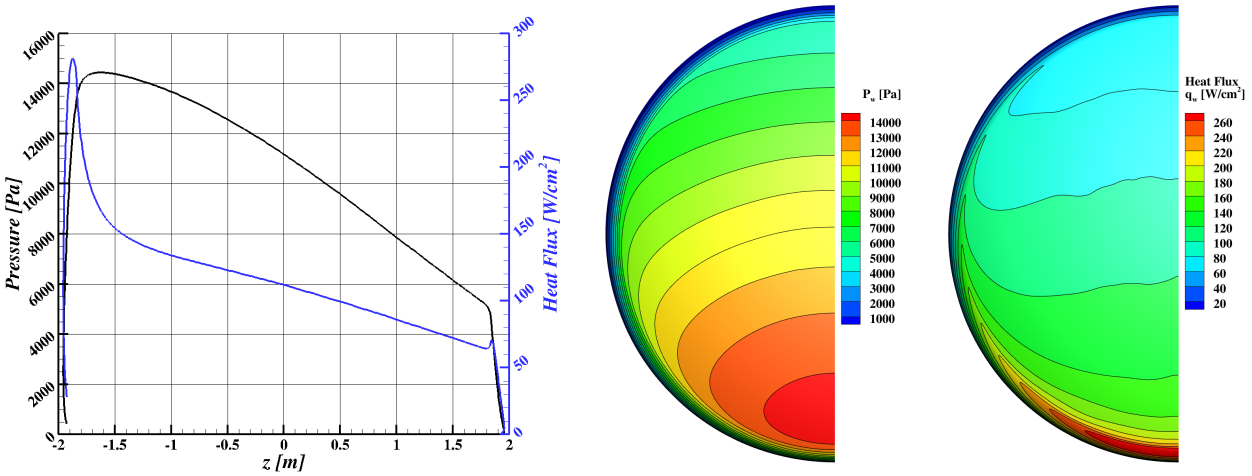

(a) Pitch plane pressure and heat flux (b) Pressure (c) Heat flux

Figure A172. Pressure and heat flux at velocity 10.0 km/s, altitude 65.0 km, and angle-of-attack 154.0 degrees.

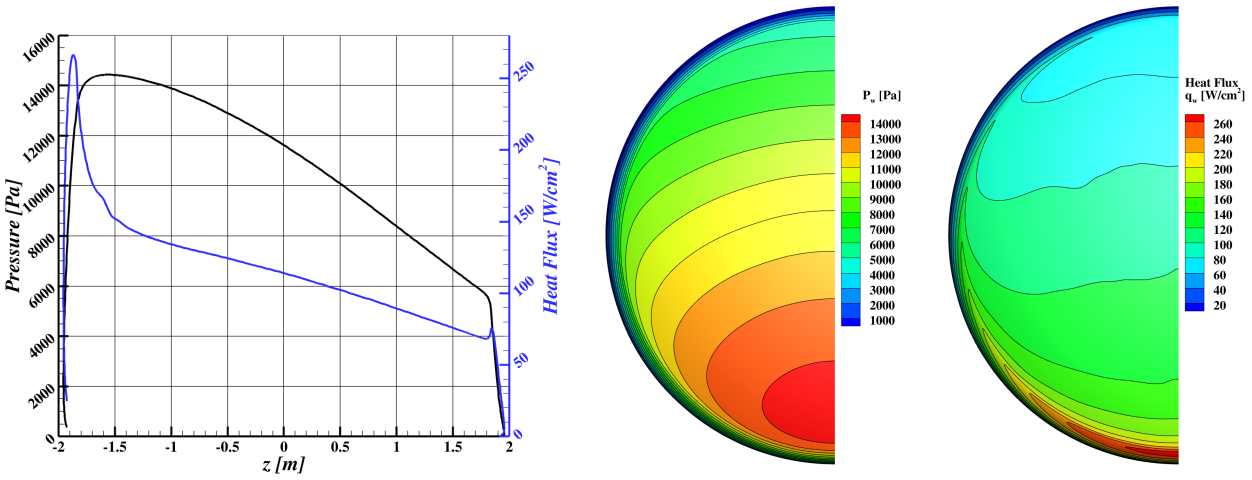

(a) Pitch plane pressure and heat flux (b) Pressure (c) Heat flux

Figure A173. Pressure and heat flux at velocity 10.0 km/s, altitude 65.0 km, and angle-of-attack 156.0 degrees.

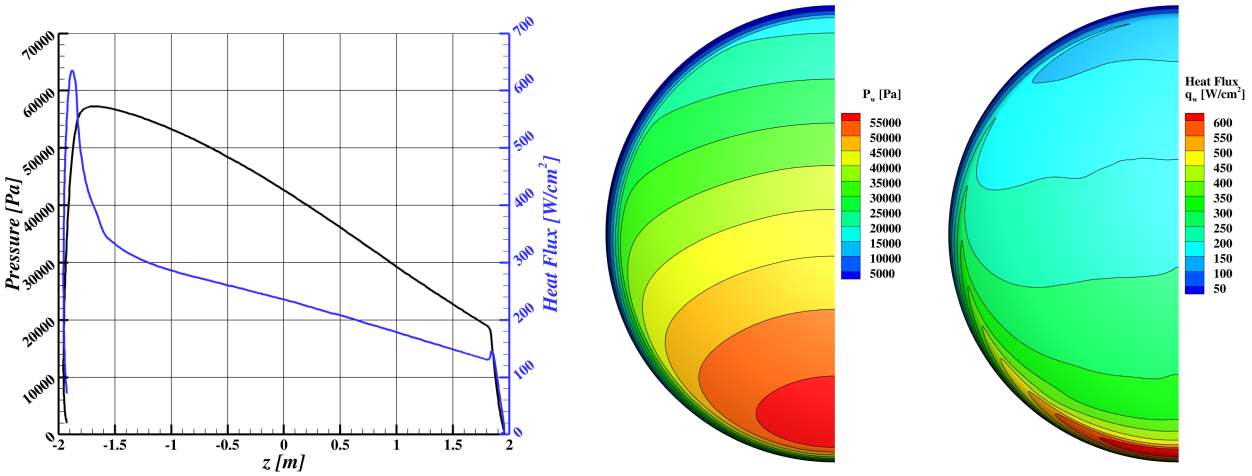

(a) Pitch plane pressure and heat flux (b) Pressure (c) Heat flux

Figure A174. Pressure and heat flux at velocity 10.5 km/s, altitude 55.0 km, and angle-of-attack 152.0 degrees.

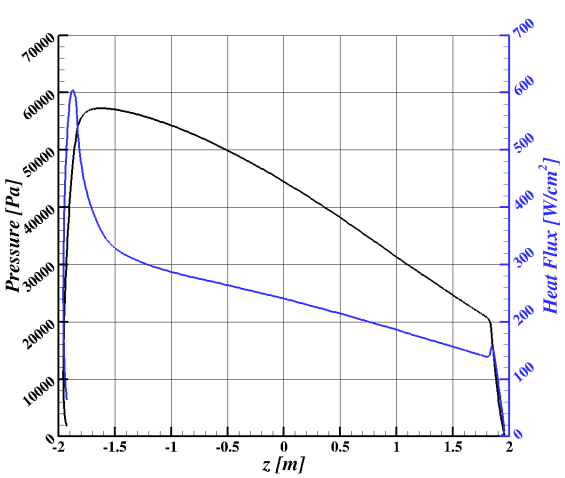

(a) Pitch plane pressure and heat flux

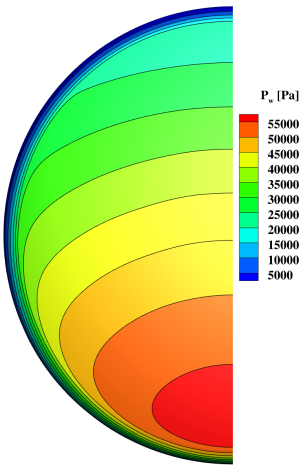

(b) Pressure

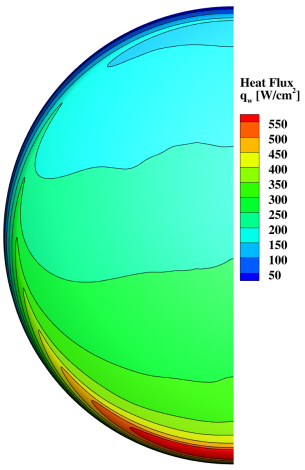

(c) Heat flux

Figure A175. Pressure and heat flux at velocity 10.5 km/s, altitude 55.0 km, and angle-of-attack 154.0 degrees.

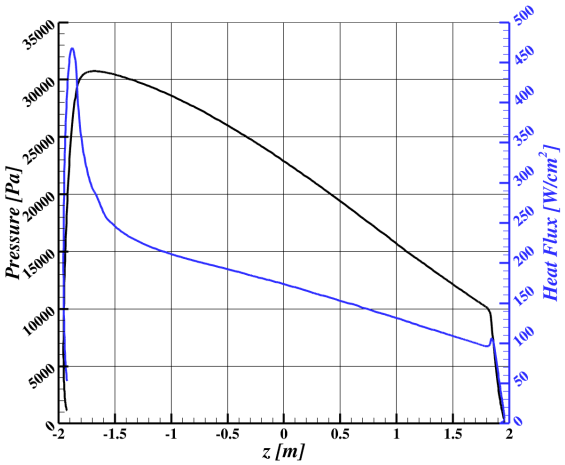

(a) Pitch plane pressure and heat flux

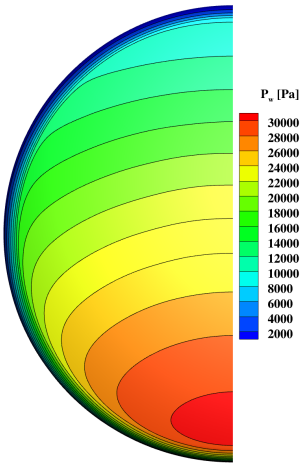

(b) Pressure

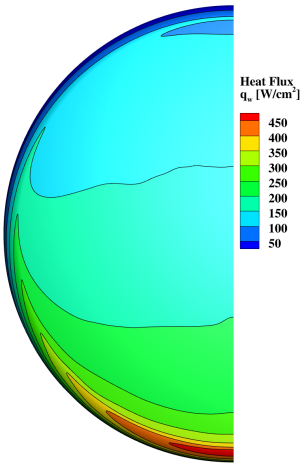

(c) Heat flux

Figure A176. Pressure and heat flux at velocity 10.5 km/s, altitude 60.0 km, and angle-of-attack 152.0 degrees.

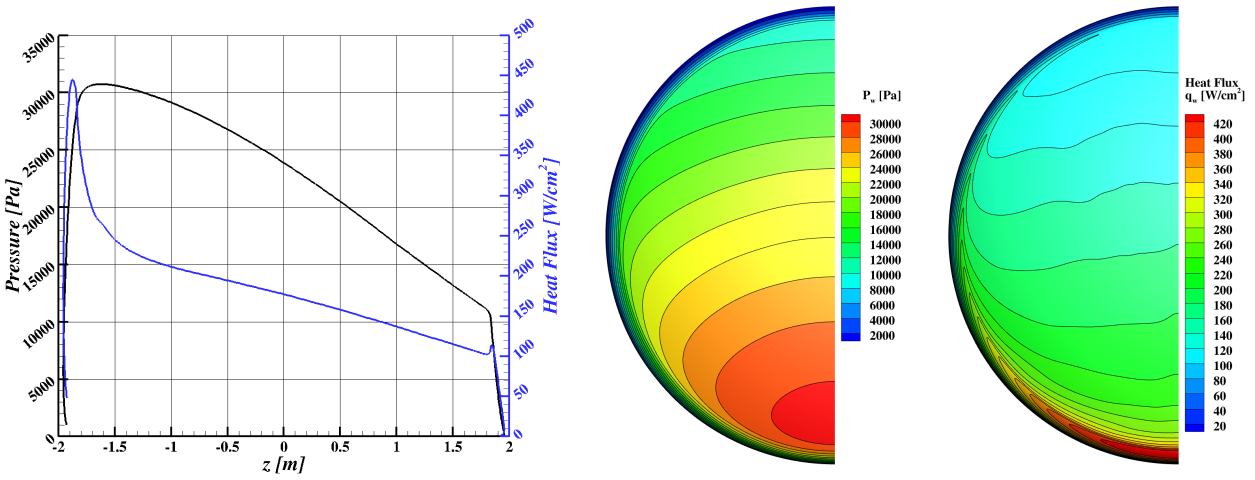

(a) Pitch plane pressure and heat flux (b) Pressure (c) Heat flux

Figure A177. Pressure and heat flux at velocity 10.5 km/s, altitude 60.0 km, and angle-of-attack 154.0 degrees.

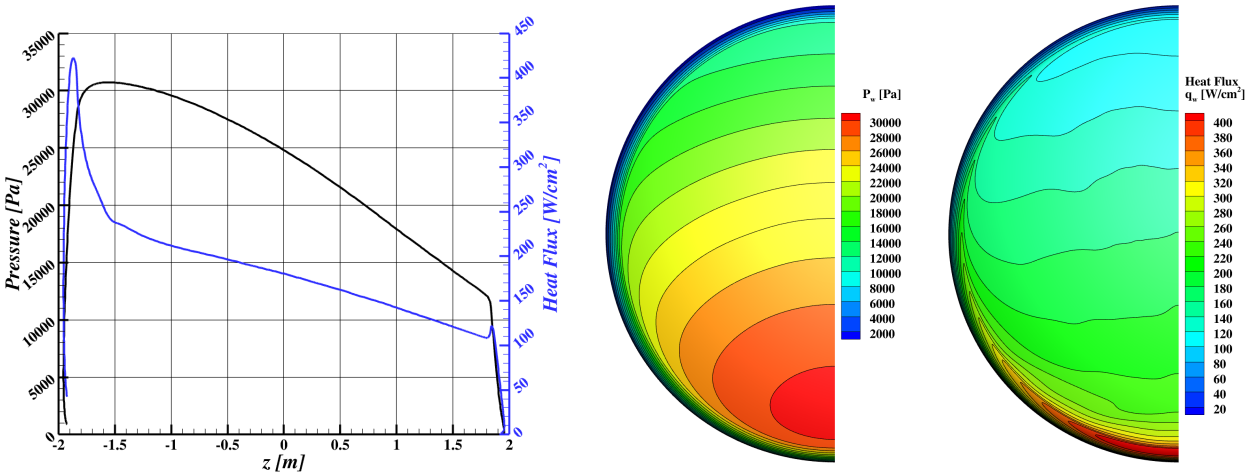

(a) Pitch plane pressure and heat flux (b) Pressure (c) Heat flux

Figure A178. Pressure and heat flux at velocity 10.5 km/s, altitude 60.0 km, and angle-of-attack 156.0 degrees.

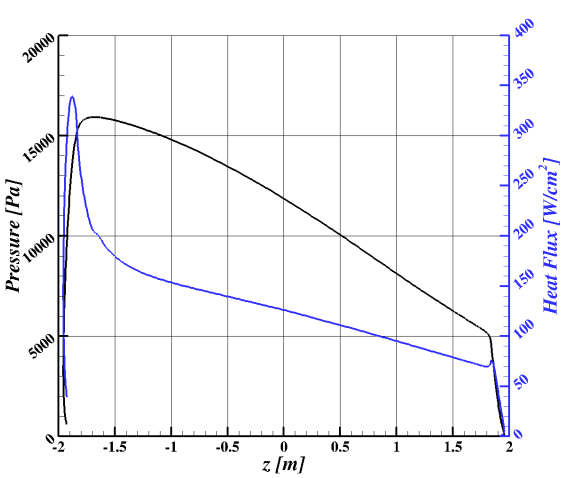

(a) Pitch plane pressure and heat flux

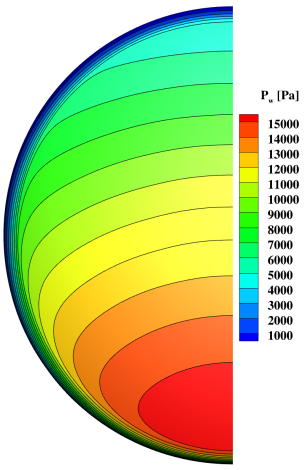

(b) Pressure

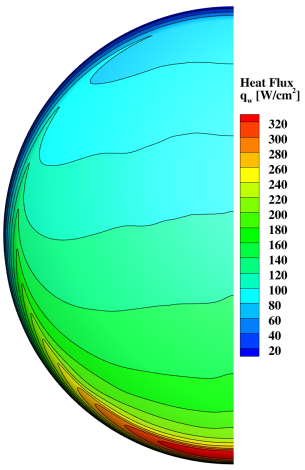

(c) Heat flux

Figure A179. Pressure and heat flux at velocity 10.5 km/s, altitude 65.0 km, and angle-of-attack 152.0 degrees.

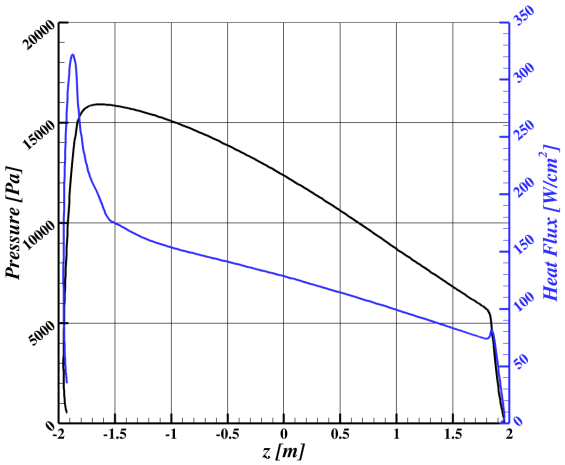

(a) Pitch plane pressure and heat flux

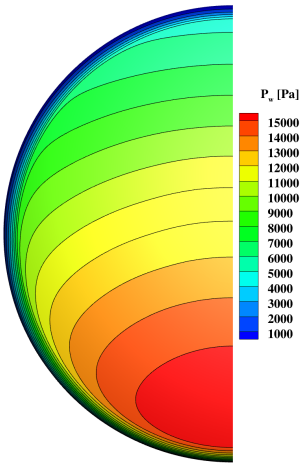

(b) Pressure

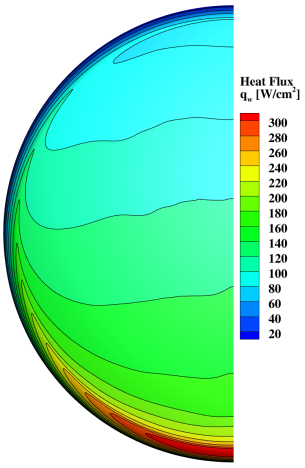

(c) Heat flux

Figure A180. Pressure and heat flux at velocity 10.5 km/s, altitude 65.0 km, and angle-of-attack 154.0 degrees.

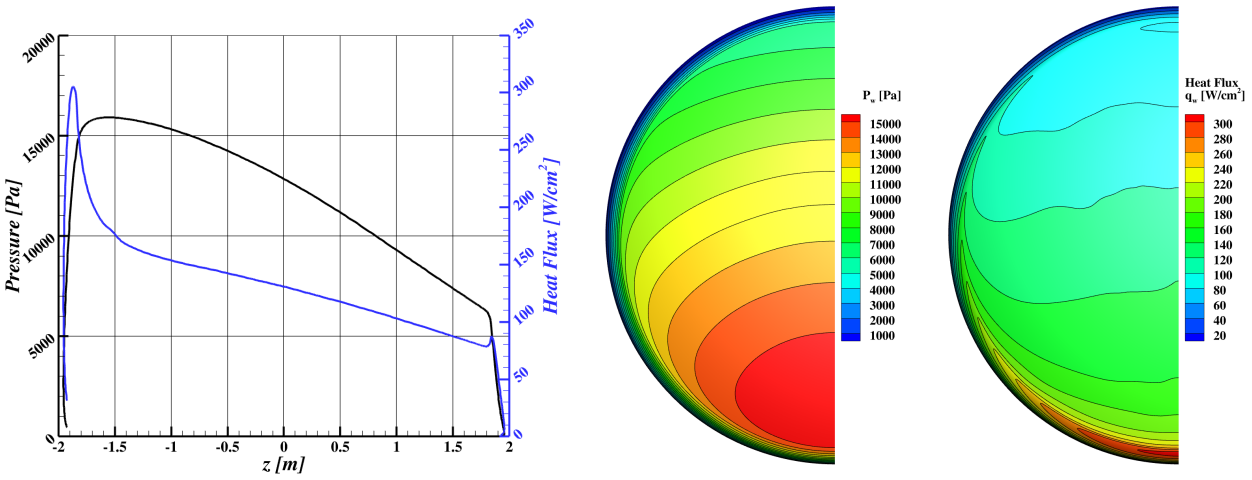

(a) Pitch plane pressure and heat flux (b) Pressure (c) Heat flux

Figure A181. Pressure and heat flux at velocity 10.5 km/s, altitude 65.0 km, and angle-of-attack 156.0 degrees.

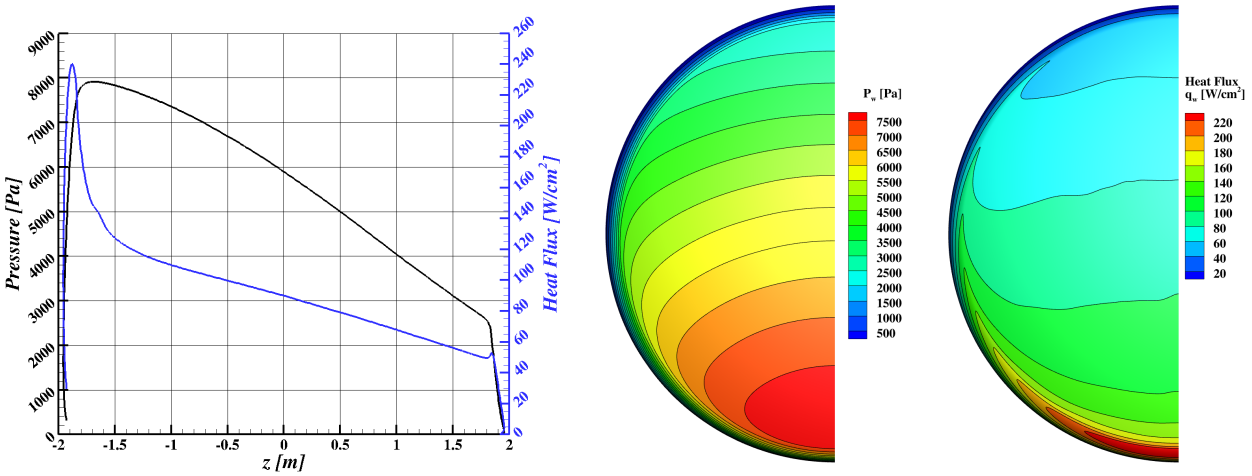

(a) Pitch plane pressure and heat flux (b) Pressure (c) Heat flux

Figure A182. Pressure and heat flux at velocity 10.5 km/s, altitude 70.0 km, and angle-of-attack 152.0 degrees.

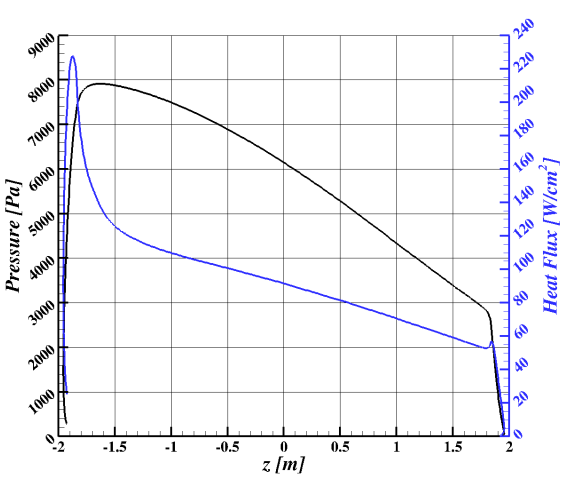

(a) Pitch plane pressure and heat flux

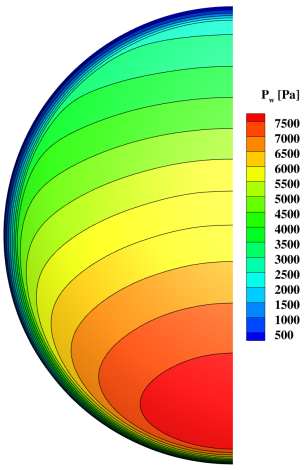

(b) Pressure

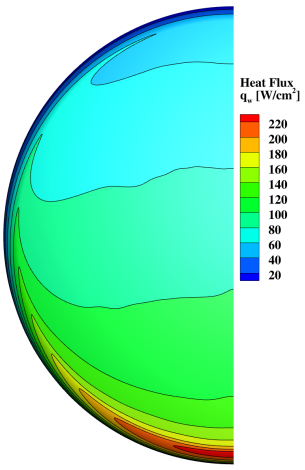

(c) Heat flux

Figure A183. Pressure and heat flux at velocity 10.5 km/s, altitude 70.0 km, and angle-of-attack 154.0 degrees.

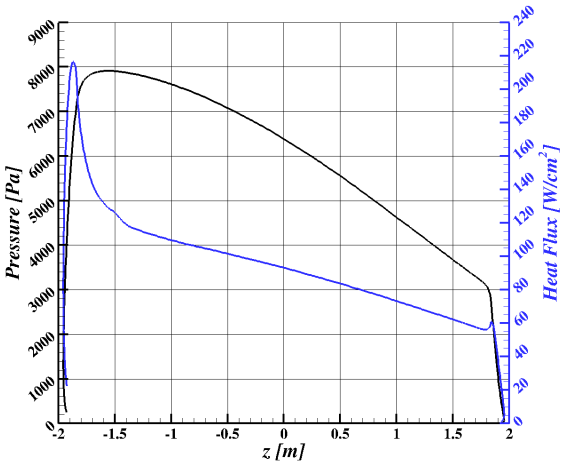

(a) Pitch plane pressure and heat flux

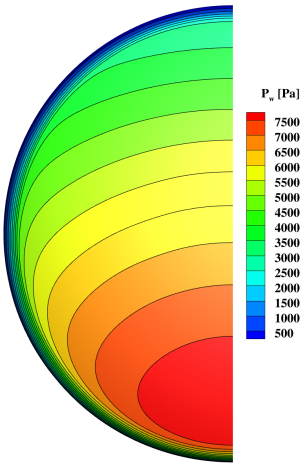

(b) Pressure

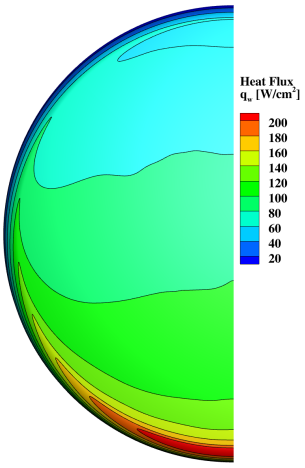

(c) Heat flux

Figure A184. Pressure and heat flux at velocity 10.5 km/s, altitude 70.0 km, and angle-of-attack 156.0 degrees.

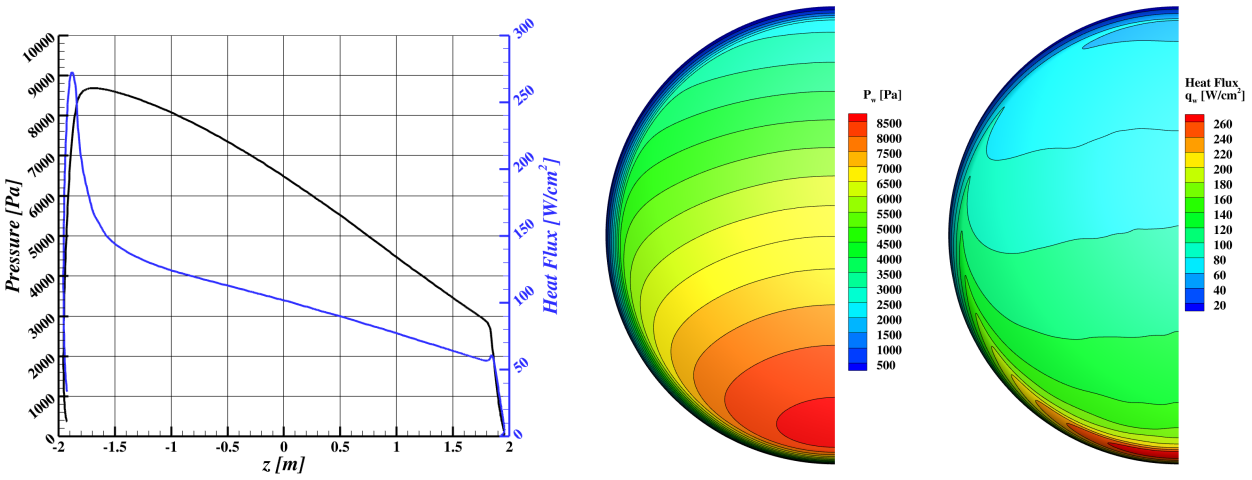

(a) Pitch plane pressure and heat flux (b) Pressure (c) Heat flux

Figure A185. Pressure and heat flux at velocity 11.0 km/s, altitude 70.0 km, and angle-of-attack 152.0 degrees.

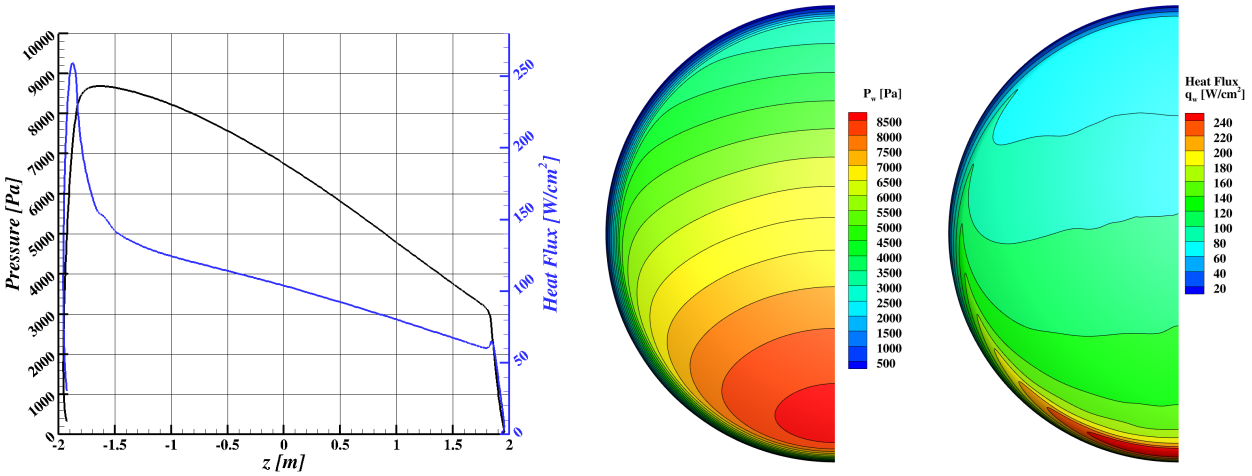

(a) Pitch plane pressure and heat flux (b) Pressure (c) Heat flux

Figure A186. Pressure and heat flux at velocity 11.0 km/s, altitude 70.0 km, and angle-of-attack 154.0 degrees.

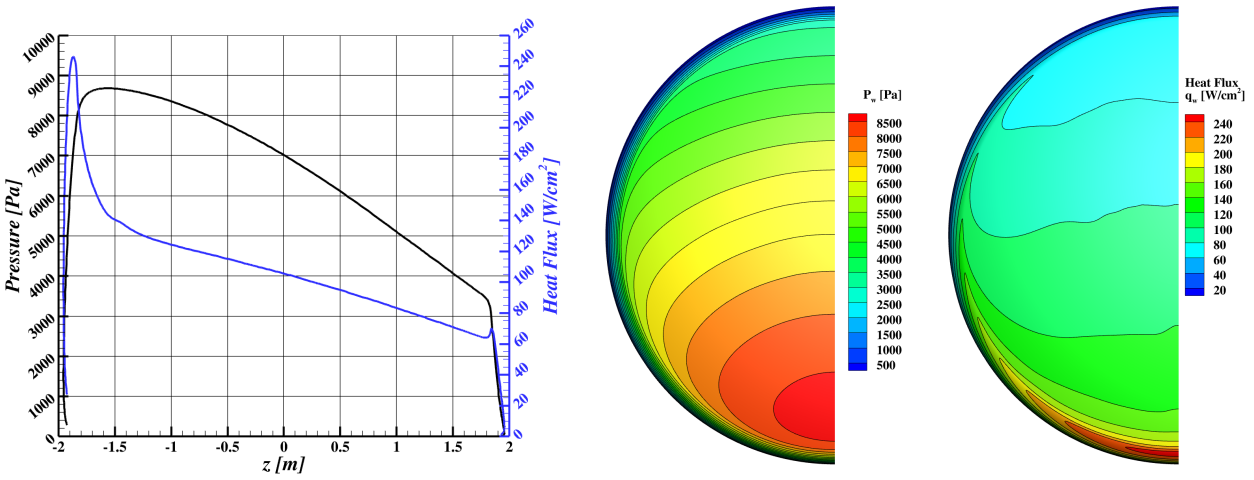

(a) Pitch plane pressure and heat flux (b) Pressure (c) Heat flux

Figure A187. Pressure and heat flux at velocity 11.0 km/s, altitude 70.0 km, and angle-of-attack 156.0 degrees.

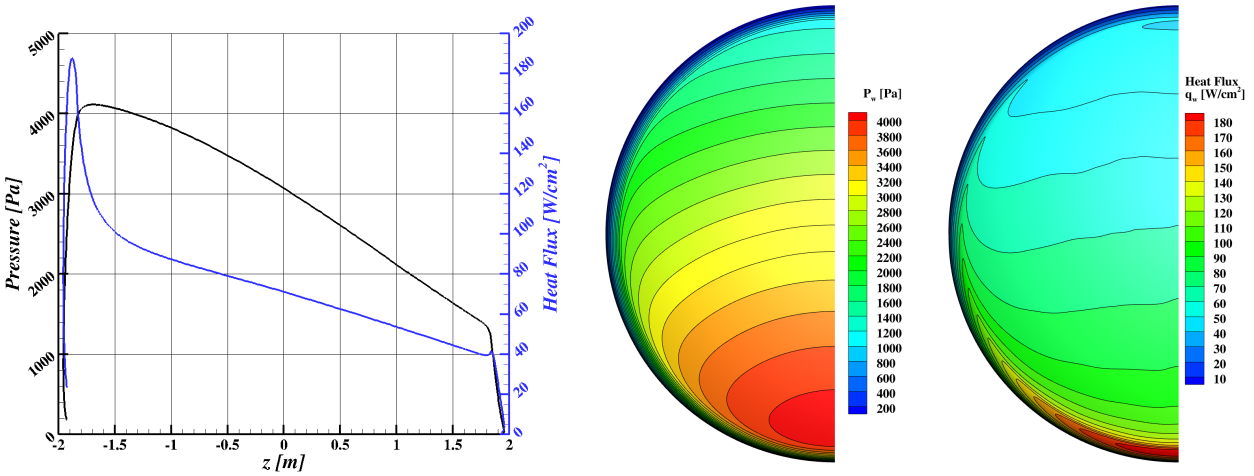

(a) Pitch plane pressure and heat flux (b) Pressure (c) Heat flux

Figure A188. Pressure and heat flux at velocity 11.0 km/s, altitude 75.0 km, and angle-of-attack 152.0 degrees.

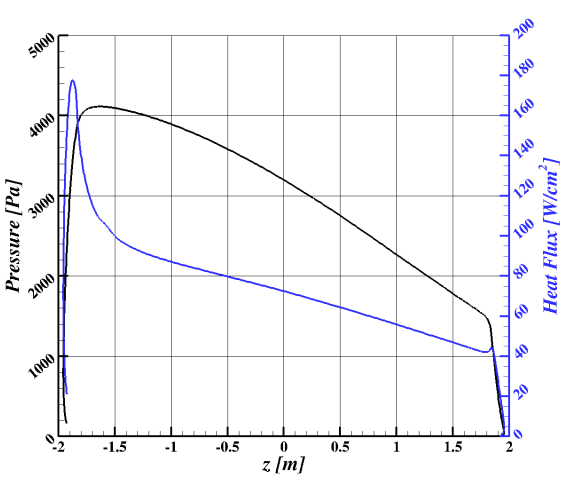

(a) Pitch plane pressure and heat flux

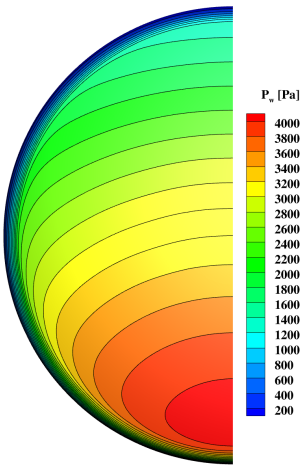

(b) Pressure

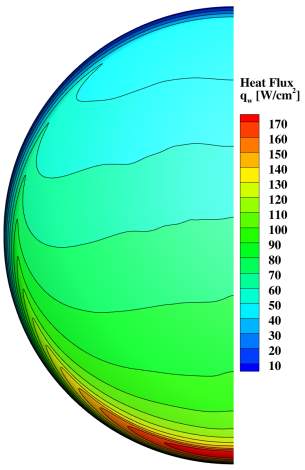

(c) Heat flux

Figure A189. Pressure and heat flux at velocity 11.0 km/s, altitude 75.0 km, and angle-of-attack 154.0 degrees.

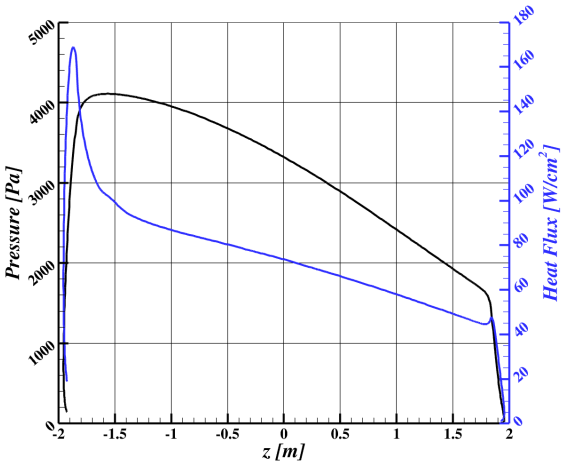

(a) Pitch plane pressure and heat flux

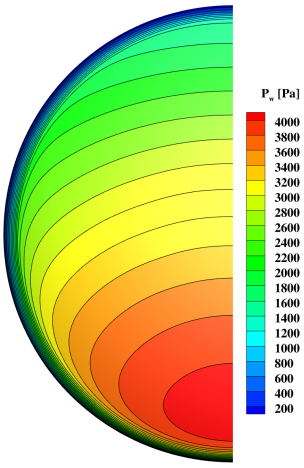

(b) Pressure

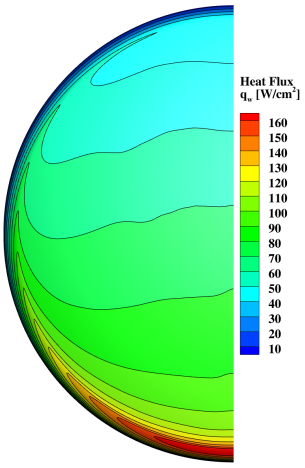

(c) Heat flux

Figure A190. Pressure and heat flux at velocity 11.0 km/s, altitude 75.0 km, and angle-of-attack 156.0 degrees.

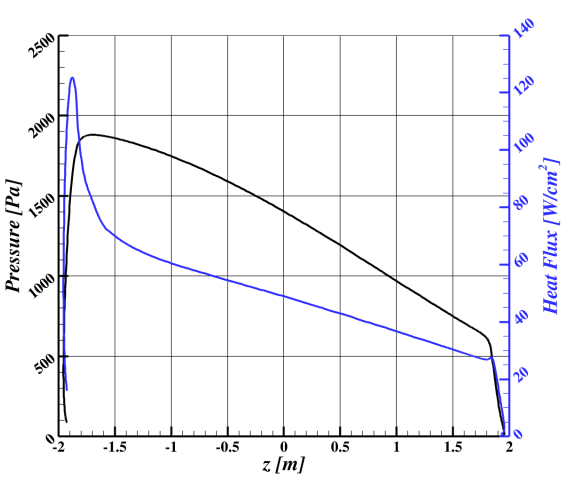

(a) Pitch plane pressure and heat flux

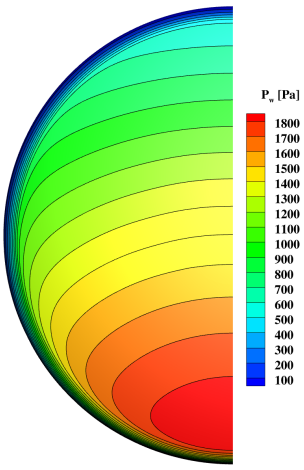

(b) Pressure

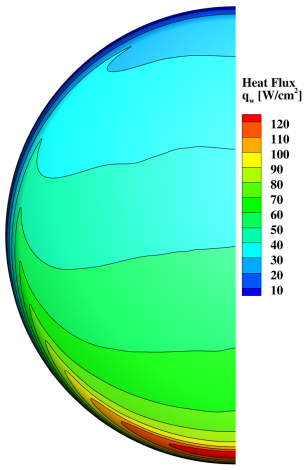

(c) Heat flux

Figure A191. Pressure and heat flux at velocity 11.0 km/s, altitude 80.0 km, and angle-of-attack 152.0 degrees.

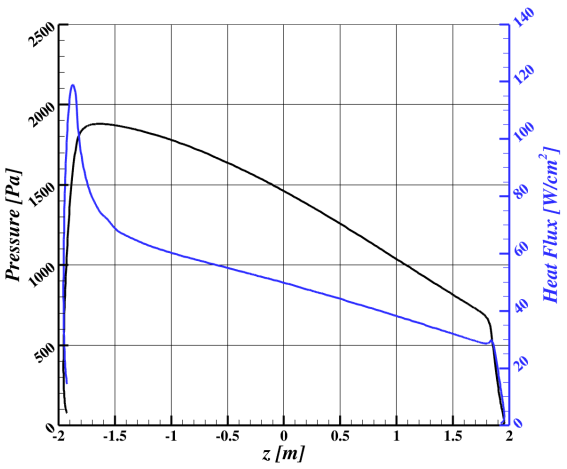

(a) Pitch plane pressure and heat flux

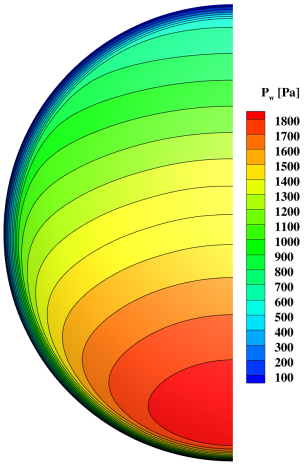

(b) Pressure

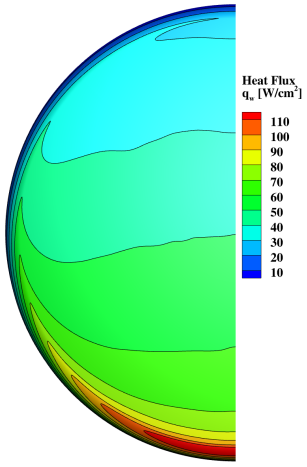

(c) Heat flux

Figure A192. Pressure and heat flux at velocity 11.0 km/s, altitude 80.0 km, and angle-of-attack 154.0 degrees.

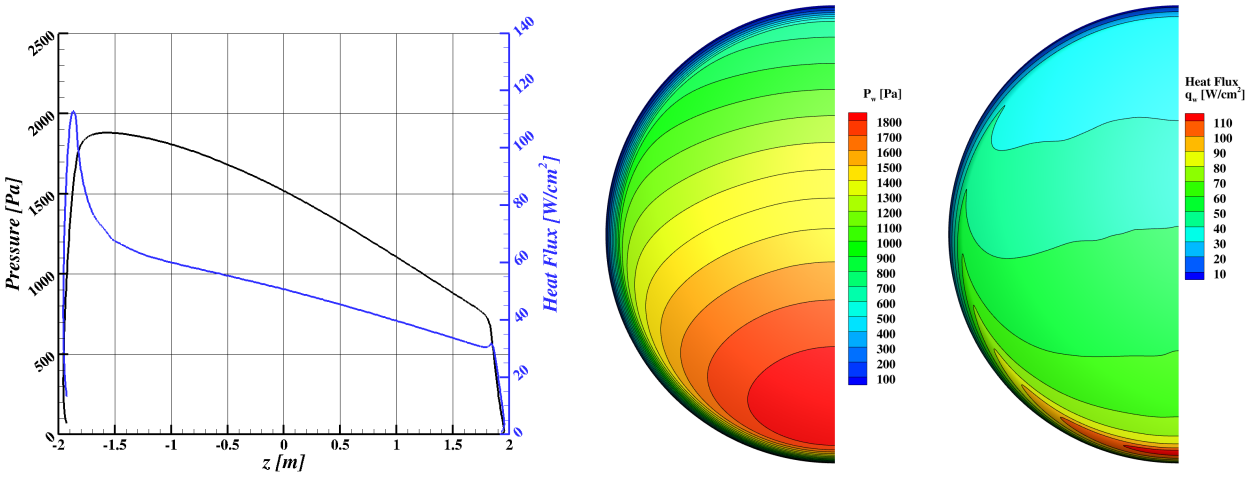

(a) Pitch plane pressure and heat flux

(b) Pressure

(c) Heat flux

Figure A193. Pressure and heat flux at velocity 11.0 km/s, altitude 80.0 km, and angle-of-attack 156.0 degrees.

REPORT DOCUMENTATION PAGE

Form Approved
OMB No. 0704–0188

1. REPORT DATE *(DD-MM-YYYY)*	2. REPORT TYPE	3. DATES COVERED *(From - To)*
01-08-2025	Technical Memorandum	

4. TITLE AND SUBTITLE
Apollo Heat-Shield Half Body Laminar Computational Fluid Dynamics Database

5a. CONTRACT NUMBER

5b. GRANT NUMBER

5c. PROGRAM ELEMENT NUMBER

6. AUTHOR(S)
A. J. Hyatt

5d. PROJECT NUMBER

5e. TASK NUMBER

5f. WORK UNIT NUMBER

7. PERFORMING ORGANIZATION NAME(S) AND ADDRESS(ES)
NASA Johnson Space Center
Houston, TX

8. PERFORMING ORGANIZATION REPORT NUMBER
L–

9. SPONSORING/MONITORING AGENCY NAME(S) AND ADDRESS(ES)
National Aeronautics and Space Administration
Washington, DC 20546-0001

10. SPONSOR/MONITOR'S ACRONYM(S)
NASA

11. SPONSOR/MONITOR'S REPORT NUMBER(S)
NASA/TM–2025–0001451

12. DISTRIBUTION/AVAILABILITY STATEMENT
Unclassified-Unlimited
Subject Category 64
Availability: NASA CASI (443) 757-5802

13. SUPPLEMENTARY NOTES
An electronic version can be found at http://ntrs.nasa.gov.

14. ABSTRACT

A series of Computational Fluid Dynamics solutions have been computed on the Apollo heat-shield geometry for the evaluation of different interpolation approaches within the database of solutions. In addition, given the rise of Artificial Intelligence, this dataset could also be used to develop or evalate the application of Artifical Intelligence methods for the estimation of aerodynamic and aerothermodynamic environments during atmospheric entry. Each of the 185 heat-shield only (no backshell) half body solutions have been computed using standard best practice with NASA's Data Parallel Line Relaxation solver and post processed to calculate quantities of interest at both the surface and boundary layer edge.

15. SUBJECT TERMS
Hypersonic, Heatshield, Aerothermodynamic, CFD

16. SECURITY CLASSIFICATION OF:			17. LIMITATION OF ABSTRACT	18. NUMBER OF PAGES	19a. NAME OF RESPONSIBLE PERSON
a. REPORT	b. ABSTRACT	c. THIS PAGE			STI Help Desk (email: help@sti.nasa.gov)
U	U	U	UU	114	19b. TELEPHONE NUMBER *(Include area code)* (443) 757-5802